International Scientific-Technical and Production Journal

The Paton WELDING JOURNAL

August 2007 # 8

English translation of the monthly «Avtomaticheskaya Svarka» (Automatic Welding) journal published in Russian since 1948

Founders: *E.O. Paton Electric Welding Institute of the NAS of Ukraine International Association «Welding»*

Publisher: *International Association «Welding»*

Address:
E.O. Paton Electric Welding Institute,
International Association «Welding»,
11, Bozhenko str., 03680, Kyiv, Ukraine
Tel.: (38044) 287 67 57
Fax: (38044) 528 04 86
E-mail: journal@paton.kiev.ua
http://www.nas.gov.ua/pwj

State Registration Certificate
KV 4790 of 09.01.2001

Subscriptions:
$324, 12 issues per year,
postage and packaging included.
Back issues available.

CONTENTS

NUMERICAL STUDY OF RISK OF LAMELLAR CRACKS FORMATION IN WELDING OF SHELLS OF MANHOLES INTO BODY OF 75,000 m^3 RESERVOIR

O.V. MAKHNENKO, E.A. VELIKOIVANENKO and **N.I. PIVTORAK**
E.O. Paton Electric Welding Institute, NASU, Kiev, Ukraine

The characteristic case of computational estimation of the risk of lamellar cracks formation is considered in welding of shells of manholes into body of 75,000 m^3 reservoir (town of Brody). On the basis of the analysis of stressed state in the zone of welded joints of oval manholes and resistibility of the material of branch pipe from steel 09G2S to formation and propagation of lamellar cracks, it was found that probability of occurrence in the branch pipes of through lamellar crack type defects is very insignificant. Revealed at hydrostatic tests of the reservoir leakiness of welded joints is due to poor design and the technology applied in performing the welded assembly.

Keywords: *welded structures, girth welds, lamellar-type ruptures, lamellar cracks, hot straightening, numerical study, calculation*

Lamellar failures in modern welded steel structures are quite a rare phenomenon, although yet 40–50 years ago such defects in thick-walled structures in the area of tee and especially cruciform joints were encountered quite often. Studies conducted in the 1970–1980s of the last century stimulated tightening of the requirements to heavy gage steel rolled stock in respect of impurities content (particularly sulfur) and material viscosity in z-direction, which promoted successful prevention of lamellar failures in structures made of such materials. Nevertheless, to fully exclude appearance of lamellar defects is evidently difficult, therefore such a danger must be taken account of. In a number of cases purely technological or design errors are attributed to insufficiently high stability of the material to the formation of said defects.

In this connection quite illustrative is the considered below a quite typical case with welding of shells of manholes into body of reservoir of 75,000 m^3 in town of Brody.

Figure 1, *a* shows a schematic diagram of cross-section of the weld metal where the branch pipe *1* is connected with the reservoir wall *2* and the overlay sheet *3*. This diagram corresponds to the most conservative conditions of welding the branch pipe by one-sided welds to the wall and the overlay sheet. Along the manhole contour the curvature radius varies. In hydraulic tests variant 1 (Figure 1, *a*) provided poor tightness of the joint, which caused appearance of lamellar cracks (Figure 2).

Variant 2 (Figure 1, *b*) shows a variant of a later development of the branch pipe *1* welding technology. In this case the shell wall *2* is first welded to the branch pipe *1* with a two-sided multipass weld, and then the overlay sheet *3* is mounted in place and welded to the branch pipe *1* with a one-sided multilayer weld. Before mounting of the overlay sheet *3*, the weld between the branch pipe and the wall is checked for tightness. Such a variant of the joint has successfully passed hydrostatic testing.

Below is considered the zone of minimal overlay sheet bending radius R, as this zone experiences the highest normal stresses σ_{rr}, responsible for eventual occurrence of lamellar cracks (Figure 2).

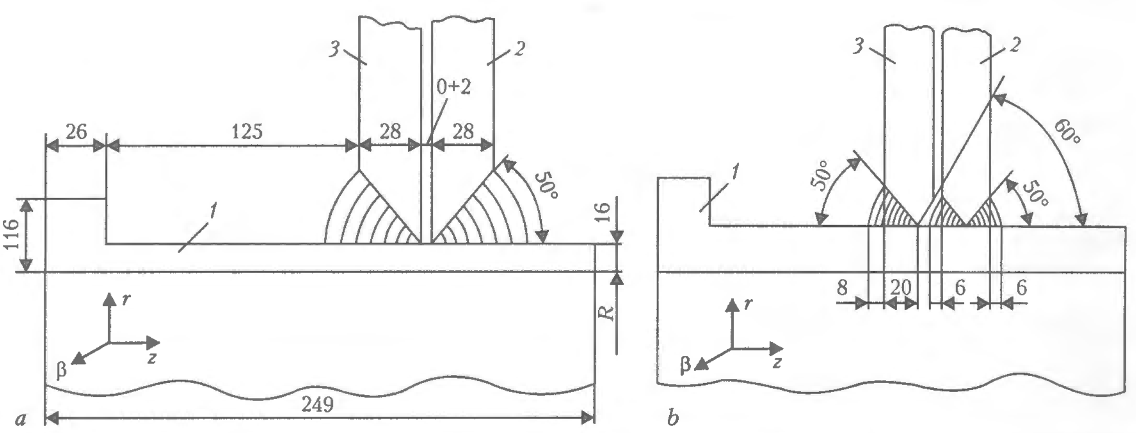

Figure 1. Schematic diagram of welded joint (weld cross-section) of branch pipe *1* with wall *2* and overlay sheet *3* of cleaning manhole of reservoir: *a*, *b* — variant 1 and 2, respectively

The material of branch pipes is low-alloy steels 09G2S (GOST 19281–89) and 06G2B (TU 14-16-150–99). Some branch pipes (approximately 25) were made from steel 09G2S, while others (approximately 70), were made, as well as the reservoir wall, from steel 06G2B. Chemical composition of the material, revealed by the spectral analysis, is shown in Table 1. This Table does not contain such an important, in the context of resistance to formation of lamellar cracks, material characteristic as sulfur content. Steel 06G2B shows a good isotropy of mechanical properties in all directions, therefore with branch pipes from that steel, there are no problems with lamellar rupture. Steel 09G2S produced in compliance with GOST, may contain up to 0.045 % S, and thus possess a quite noticeable anisotropy of mechanical properties. Table 2 contains data from [1] on mechanical properties of steel 09G2S having the following chemical composition, wt.%: 0.05 C; 0.67 Si; 1.3 Mn; 0.1 Cr; 0.02 Ni; 0.02 V; 0.05 Cu; 0.017 P; 0.045 S. It is seen from Table 2 that in steel 09G2S anisotropy of properties is quite noticeable. Therefore a degree of caution in its application in heavy-gauge structures and sustaining loads normal to rolling direction (in r direction, as in Figure 1) is required.

Thickness of branch pipes of 16 mm, is not considered great, however this is the limit value, at which lamellar cracks at higher stresses may occur (see Figure 2).

Lamellar cracks, as it follows from [2], belong to the type of defects in the welded joint zone, which can occur when during welding, the HAZ is loaded inward, in r direction, towards sheet thickness. Such a loading can be due either to the welding process itself (i.e. by welding stresses), or the external loading experienced during testing or operation of the welded joint.

The principal factor affecting plastic properties of the steel sheet throughout its thickness are non-metallic inclusions. Such sulfide or oxide inclusions, during sheet manufacture (rolling) get elongated, whereby films parallel to the rolling direction are formed. Under the action of high normal stresses arising in the plane of such a film, depending on the properties of the base material, brittle or viscous-brittle lamellar fractures (lamellar cracks) may occur.

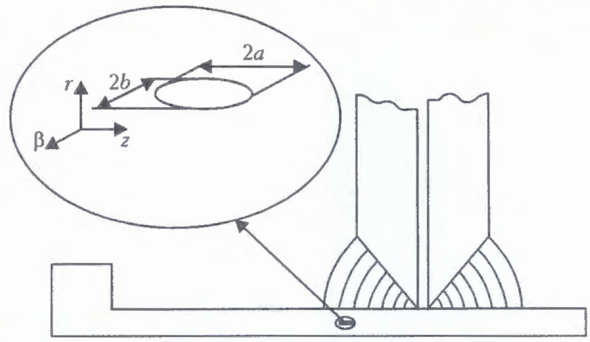

Figure 2. Diagram of lamellar crack in welded joint zone: a, b – dimensions of lamellar crack

Thus, resistance to lamellar failure of rolled steel sheets is controlled by the quantity of sulfide or oxide inclusions, i.e. by the weight fraction of sulfur in steel, as well as by the properties of the matrix to resist both origination and propagation of lamellar cracks. It is natural that with the same quantity of sulfide films, resistance to origination of lamellar cracks will be higher with a more plastic matrix, therefore reduction in area at testing of samples, is to a certain degree a characteristic of said resistance.

Based on the results of multiple tests, the Japanese researchers [2] suggested to refer structural steels, by their resistance to lamellar cracks formation, to one of the 3 classes:

A – high-resistant steels (S < 0.007 wt.%; reduction in area of sheet $\psi_r \geq 25$ %);

B – resistant steels (S < 0.01 wt.%; $\psi_r \geq 15$ %);

C – low-resistant steels (S ≥ 0.02 %, $\psi_r \leq 8$ %).

Said classification provides for quite stringent requirements in respect of stressed state, i.e. corresponds

Table 1. Chemical composition (wt.%) of branch pipes from steel 09G2S (600 × 900 mm) and steel 06G2B (900 × 1500 mm)

Steel	C	Si	Mn	Cr	Ni	Cu	Nb	Mo	Al	Ti
09G2S	0.08–0.12	0.50–0.74	1.25–1.70	0.002–0.092	0.05–0.12	0.011–0.310	0.001–0.012	–	–	–
06G2B	0.04–0.08	0.27–0.32	1.28–1.36	0.004–0.110	0.04–0.07	0.210–0.230	0.028–0.031	0.062–0.078	0.027–0.037	0.011–0.017

Table 2. Mechanical properties of specimen from steel 09G2S 35 mm thick

Sample positioning	Tests								δ_c, mm
	Tensile test at T = 20 °C				Impact bending test, KCV, J/cm^2, at temperatures, °C				
	σ_y, MPa	σ_t, MPa	δ, %	ψ, %	–70	–40	0	+20	
Standard	405	493.6	31.75	76.3	54.5	72.5	174.0	134.0	0.24
Across rolling direction (GOST 28870–90)	349	476.3	27.45	32.0	8.5	12.0	27.5	28.0	0.02

Note. σ_y – yield limit; σ_t – tensile strength; δ – relative elongation; ψ – reduction in area; δ_c – critical crack opening.

to welding of rather fairly loaded weldments of very thick elements.

Following from data of Table 1, it is difficult to assign steel 09G2S to a concrete above class. It can however be assumed that with regard for sulfur content, it is susceptible to lamellar cracks formation, under rather significant stresses applied in r direction (see Figure 2).

Stressed state in branch pipes in welded joint zone was determined under the effect of welding thermal deformation cycle, as well as external loading (for instance, hydrostatic pressure), for this purpose a method of consecutive monitoring of temperature fields, stresses and deformations development in welds, was used. A computer FEM-based software package «Weldpredictions» developed at the E.O. Paton Electric Welding Institute, was used.

Manual arc welding was simulated in filling the groove (see Figure 1) in 10–12 passes, both in welding to the wall and to the overlay sheet. Accordingly, were applied the following welding modes: I_w = 170–300 A, U_a = 25–26 V, $v_w \approx$ 0.15–0.20 cm/s for variant 1 (see Figure 1, a), and I_w = 170 A, U_a = 25 V at various v_w values and the following design values of welding heat input q_h for variant 2 (see Figure 1, b):

Pass No	q_h, J/cm
1	15937
2	15937
3	23906
4	23906
5	15937
6	15937
7	23906
8	23906
9	15937
10	15937
11–17	23906

Necessary for the calculation thermophysical properties and viscosity characteristics depending on the temperature for low-alloy steels of the type considered are available in the database of the package used (Table 3).

Below are presented the results of calculation for cross-sections with respect to weld axis (z = 0 in Figure 1), for acting along the axis of the weld normal stresses $\sigma_{\beta\beta}$, for acting in the plane of branch pipe generatrix transverse stresses σ_{zz}, for through branch pipe thickness stresses σ_{rr} and for tangential stresses σ_{rz}.

Figure 3 demonstrates general picture of distribution of residual stresses over the weld cross-section, after completing the welding procedure by variant 1 (see Figure 1, a) at R = 362.5 mm. It is seen from the Figure that the largest area of high tensile residual stresses is connected with longitudinal stresses $\sigma_{\beta\beta}$, while the smallest one with through thickness stresses σ_{rr}.

For our further consideration are important numerical values of stresses σ_{rr}. Figure 4 shows in more detail distribution of such stresses in the branch pipe in the weld zone -38 mm $< z <$ 38 mm (variant 1). The solid line marks penetration and recrystallization zones ($T >$ 1300 °C), where lamellar cracks are not formed, as typical lamellar structure produced in rolling steel 09G2S, is not present there.

Higher residual stresses σ_{rr} below the mentioned penetration line are observed at R = 362.5 mm, and do not exceed 203 MPa (Figure 4, a), while at R = = 503.5 mm it is 192 MPa (Figure 4, c).

The applied method of consecutive monitoring of stressed state development, enables taking into account as one of the monitoring phases, loading of the considered zone with hydrostatic pressure in testing the reservoir by water filling, after obtaining data on residual stresses.

Figure 4, b, d shows similar results obtained for stress σ_{rr}. It is seen that such a loading partially

Table 3. Mechanical and thermophysical properties of steel 09G2S

Test temperature T_{test}, °C	Young's modulus E, MPa	Yield point σ_y, MPa	Temperature linear expansion coefficient α, 1/°C	Thermal conductivity coefficient λ, J/(cm·s·°C)	Specific heat conductivity $c\gamma$, J/(cm^3·s·°C)
20	208000	400	0.0000120	0.520	3.76
100	203000	367	0.0000120	0.508	3.80
200	199000	347	0.0000130	0.479	3.88
300	195000	335	0.0000137	0.442	4.01
400	188000	310	0.0000142	0.425	4.15
500	172000	282	0.0000147	0.400	4.33
600	153000	220	0.0000150	0.360	4.55
700	143000	114	0.0000152	0.325	4.96
800	130000	53	0.0000153	0.280	5.48
900	108000	37	0.0000190	0.260	5.48
1000	82000	25	0.0000194	0.270	5.42
1100	32000	16	0.0000194	0.290	5.38
1200	7000	8	0.0000195	0.300	5.36

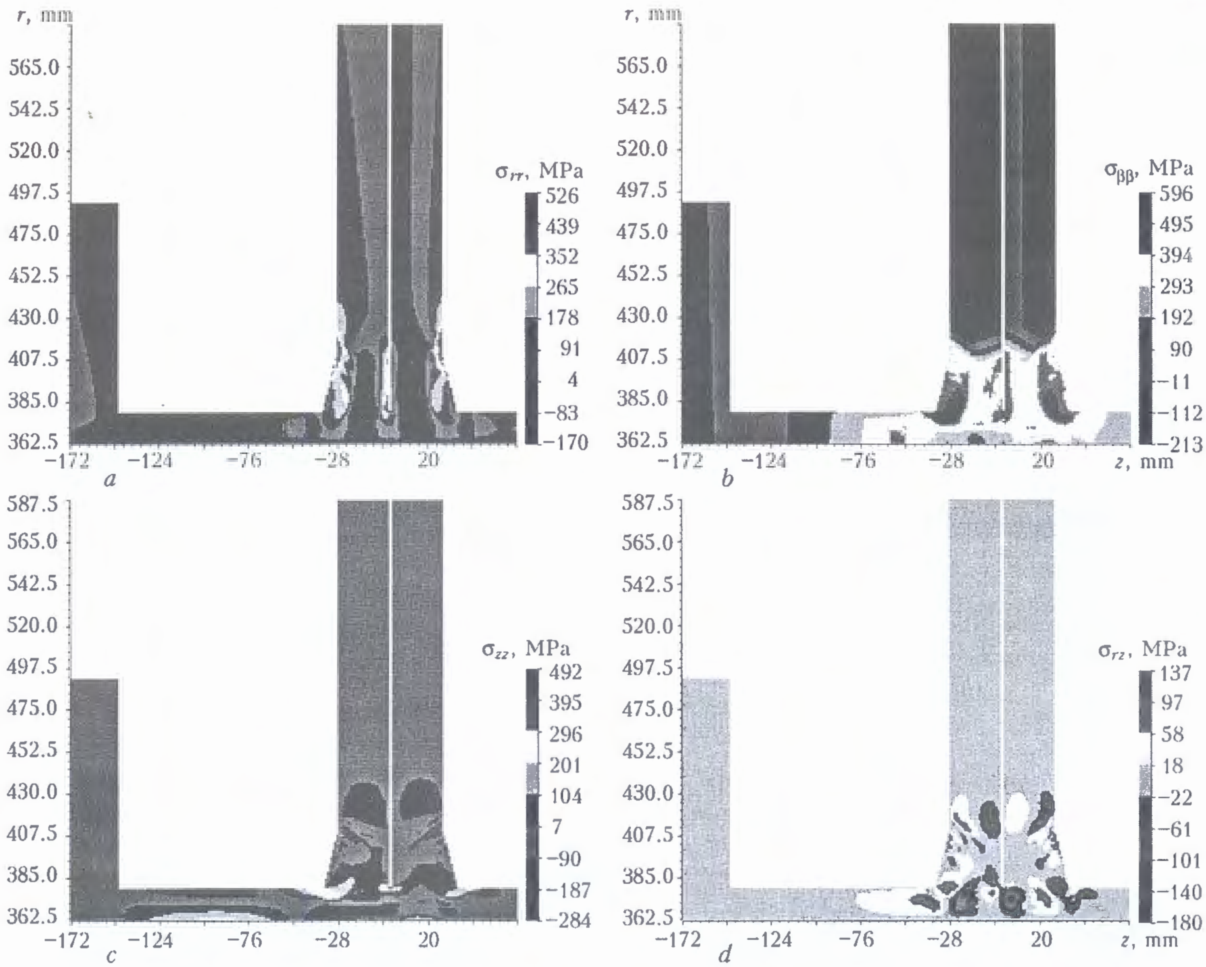

Figure 3. Distribution of the σ_{rr}, $\sigma_{\beta\beta}$, σ_{zz}, σ_{rz} residual stresses over weld axis cross-section at R = 362.5 mm

changes the through thickness stresses distribution pattern and their magnitudes. Characteristically, σ_{rr} maximum values of markedly grow only in the concentrator zone, between the wall and the overlay sheet (zone $z = 0$), where their magnitudes reach approximately 216 (Figure 4, *b*) and 206 MPa (Figure 4, *d*).

Similar picture is observed for other R values too; thus the above regularity remains in force: increasing R reduces σ_{rr}.

Considered also was a variant 2 of a welded joint of Figure 1, *b*. Respective calculations data have shown that at lower welding heat inputs, for this case stresses σ_{rr} somewhat increase in the near-weld zone below penetration border, however such stresses do not exceed 250 MPa.

Since steel 09G2S features reduction in area at tention in r direction of beyond 25 % (ψ = 32 % as in Table 2), the process of nucleation of lamellar type cracks involves tensile normal stresses σ_{rr} of a magnitude exceeding the yield point of the material at respective testing. Proceeding from the data of Table 2, it is more than 350 MPa. This is an average level across specimen section in such testing. True local stresses of incipience will evidently be higher: $\sigma_t/(1 - \psi/100)$ = 726 MPa.

Hence, presence of normal stresses $\sigma_{rr} < 350$ MPa can be easily considered as a quite conservative condition, under which incipience of lamellar cracks does not occur. This condition is fully matched by stressed state in Figures 3 and 4.

It should however be understood that cracks nuclei, on one or other reason, can already exist in the branch pipe material of the considered joint zone, irrespective of residual and total stresses σ_{rr}.

It is necessary to evaluate the potential of such defects growth in the σ_{rr} stress field discussed before.

As a pre-condition of such a growth, it is possible with a certain degree of conservatism, to apply the condition of brittle initiation of a plane crack with a normal r and dimensions $2a \times 2b$ (see Figure 2).

The condition can be written as

$$\bar{\sigma}_{rr}\sqrt{\pi a}\, f_r = K_c,$$

where $\bar{\sigma}_{rr}$ is the mean stress in the area $z \pm a$ (as in Figure 4); f_r is the factor depending on a/b relation and distance between neighboring cracks; K_c is the coefficient of material fracture toughness.

In a specific case, for a system of disc-like cracks of circular form, having a period of $2h$ (Figure 5), under tensile stresses σ normal to x, y plane, factor f_r in point A is determined after [3] by the dependence

σ_{rr}^{res} / r, mm \ z, mm	-37	-35	-33	-31	-29	-27	-25	-23	-21	-19	-17	-15	-13	-11	-9	-7	-5	-3	-1	0	1	3	5	7	9	11	13	15	17	18	19	21	23	25	27	29	31	33	35	
382	0	33	103	158	200	230	248	203	40	-94	-164	-158	-123	-117	-84	-2	128	403	374	0	63	56	-29	-109	-140	-158	-144	-162	-137	-118	-83	12	158	202	185	155	115	48	-22	0
381	0	101	106	157	196	225	237	169	19	-101	-153	-156	-111	-119	-88	-13	107	365	483	0	79	48	-44	-114	-140	-153	-141	-153	-128	-121	-86	-4	129	197	181	152	116	57	3	0
380	0	84	107	152	192	220	230	134	-3	-106	-130	-138	-111	-114	-88	-15	107	318	460	153	12	26	-52	-109	-135	-142	-140	-130	-124	-116	-94	-19	97	189	175	149	114	62	17	0
379	29	110	114	150	188	213	206	96	-24	-121	-133	-99	-119	-98	-84	-10	109	279	365	189	75	70	-57	-104	-130	-133	-138	-101	-131	-98	-100	-32	70	174	170	146	114	74	41	11
378	54	112	124	153	185	201	169	64	-40	-98	-110	-92	-108	-95	-74	-2	105	242	285	174	95	92	-66	-97	-121	-126	-123	-91	-117	-101	-88	-39	48	138	165	143	116	86	58	31
377	75	116	134	155	180	190	132	37	-48	-85	-84	-91	-84	-92	-58	2	99	209	215	152	115	96	-62	-89	-108	-121	-97	-103	-84	-93	-84	-50	26	105	157	141	120	96	75	43
376	85	123	140	156	173	158	98	20	-44	-68	-80	-75	-80	-77	-49	4	92	170	167	141	123	87	-52	-81	-99	-104	-88	-89	-63	-68	-73	-49	6	81	128	139	125	105	85	39
375	73	133	145	155	154	129	77	12	-42	-57	-67	-65	-67	-66	-44	12	78	131	138	127	123	74	-46	-71	-86	-85	-80	-66	-59	-55	-55	-45	-12	60	106	127	125	110	84	21
374	44	123	144	146	134	107	63	9	-32	-53	-57	-56	-58	-53	-30	10	63	102	117	114	112	60	-39	-61	-73	-73	-68	-54	-46	-48	-44	-39	-16	40	87	109	118	105	76	6
373	17	102	132	135	119	92	54	8	-27	-52	-47	-51	-49	-43	-21	9	50	83	98	96	96	48	-29	-49	-61	-61	-55	-46	-34	-36	-39	-39	-15	28	71	92	103	96	66	2
372	4	78	115	119	104	78	45	9	-23	-41	-46	-45	-41	-34	-18	7	43	67	78	79	76	40	-18	-39	-48	-50	-45	-39	-33	-30	-31	-32	-14	23	57	79	86	82	56	0
371	-2	62	94	100	88	65	37	10	-18	-34	-38	-38	-35	-28	-14	6	34	53	61	62	61	35	-7	-27	-38	-41	-39	-35	-29	-26	-25	-24	-11	18	45	64	72	69	46	-3
370	-2	44	73	82	71	52	28	9	-13	-24	-29	-32	-28	-22	-9	4	24	41	47	46	46	33	2	-19	-27	-33	-34	-32	-23	-21	-18	-18	-8	13	38	51	59	56	34	1
369	1	29	54	63	55	40	23	4	-6	-13	-20	-25	-24	-18	-5	2	14	33	36	34	34	32	5	-10	-18	-27	-31	-30	-17	-15	-12	-10	-4	8	26	41	46	42	26	2
368	5	19	37	45	40	28	18	2	-4	-5	-14	-19	-21	-13	-4	0	9	27	26	24	21	31	7	-4	-9	-24	-27	-24	-8	-8	-7	-3	-2	7	16	28	34	29	19	3
367	5	12	23	29	25	19	10	0	-4	2	-9	-16	-15	-8	-4	2	5	18	18	12	13	25	7	0	-2	-23	-17	-14	-6	-4	-2	-1	-1	5	11	19	21	18	14	5
366	6	6	13	17	13	12	6	0	-2	-1	-4	-13	-7	-7	-4	3	0	10	12	5	6	19	5	0	2	-15	-8	-6	-3	-5	-1	1	2	5	7	12	13	10	8	7
365	4	1	5	7	5	5	4	2	2	-1	-1	-5	-2	-3	-2	3	1	3	9	2	0	8	3	0	-2	-7	0	-1	2	-3	2	2	2	2	4	5	6	5	3	4
364	1	1	1	1	1	1	1	1	1	1	0	0	0	0	1	1	1	1	1	1	1	1	1	1	1	1	1	1	1	1	1	1	1	1	1	1	1	1	1	1
363	0	0	0	0	0	0	0	0	0	0	0	0	0	0	0	0	0	0	0	0	0	0	0	0	0	0	0	0	0	0	0	0	0	0	0	0	0	0	0	0

a

σ_{pr}^{res} / r, mm \ z, mm	-37	-35	-33	-31	-29	-27	-25	-23	-21	-19	-17	-15	-13	-11	-9	-7	-5	-3	-1	0	1	3	5	7	9	11	13	15	17	18	19	21	23	25	27	29	31	33	35	
382	0	-183	-90	28	109	168	209	184	38	-79	-132	-110	-55	-28	32	153	346	556	447	0	-214	-160	-165	-200	-204	-199	-168	-164	-125	-100	-61	36	178	224	219	199	179	144	95	0
381	0	-272	-52	47	120	173	208	156	21	-84	-120	-107	-44	-32	26	137	308	575	547	0	-281	-141	-169	-199	-201	-191	-164	-154	-117	-104	-64	20	151	215	210	191	171	135	177	0
380	0	-152	-30	62	127	176	204	125	3	-87	-97	-90	-46	-29	23	128	289	497	524	67	-179	-163	-174	-192	-194	-182	-162	-132	-112	-98	-72	4	121	205	201	183	162	132	130	0
379	-39	-109	-15	71	132	178	189	92	-16	-100	-99	-52	-56	-16	21	123	268	421	468	108	-72	-132	-176	-186	-186	-174	-158	-106	-119	-83	-77	-8	95	189	192	176	158	137	128	42
378	-42	-74	-2	78	136	174	158	63	-30	-76	-76	-46	-47	-17	24	118	240	360	391	127	-21	-102	-179	-177	-175	-167	-143	-96	-107	-85	-68	-17	72	155	185	172	156	142	129	69
377	-25	-40	17	85	139	166	122	39	-36	-64	-52	-47	-27	-19	32	109	214	310	309	131	18	-71	-172	-168	-163	-160	-118	-105	-77	-79	-65	-24	49	124	178	168	155	145	132	79
376	-10	-7	34	90	133	136	91	23	-32	-47	-50	-34	-27	-11	32	98	191	257	244	129	43	-47	-155	-157	-153	-140	-107	-93	-58	-58	-56	-24	28	99	154	164	154	146	130	75
375	-13	24	51	92	116	110	71	17	-29	-37	-39	-27	-19	-6	29	94	162	209	197	122	61	-34	-138	-144	-141	-121	-99	-74	-54	-47	-41	-22	14	79	123	148	150	142	121	56
374	-33	33	62	90	101	90	59	14	-20	-34	-30	-22	-15	0	33	81	134	170	163	111	66	-27	-118	-130	-125	-107	-85	-61	-42	-39	-34	-19	7	60	101	126	137	132	107	39
373	-49	26	63	86	89	77	51	13	-16	-35	-24	-21	-11	4	33	69	111	140	133	97	63	-20	-98	-112	-106	-93	-72	-52	-32	-28	-31	-19	6	47	83	106	119	117	93	31
372	-52	15	57	77	78	65	42	14	-13	-26	-26	-19	-9	5	27	57	94	114	105	81	53	-13	-78	-95	-88	-78	-61	-42	-31	-24	-23	-16	5	39	67	88	100	99	78	25
371	-48	10	47	65	66	54	35	13	-10	-21	-21	-16	-8	5	24	47	76	90	82	65	46	-7	-57	-75	-72	-64	-51	-38	-27	-21	-18	-11	6	32	54	72	83	82	63	19
370	-38	4	36	54	54	43	26	12	-6	-14	-15	-15	-7	3	21	36	57	70	62	50	36	0	-39	-58	-55	-52	-44	-35	-21	-16	-14	-6	8	24	44	59	67	65	48	18
369	-26	-1	27	42	41	33	21	6	-1	-6	-10	-12	-8	1	18	27	40	54	47	37	27	8	-26	-40	-40	-42	-39	-31	-16	-12	-8	0	9	18	32	45	51	49	35	15
368	-15	-3	18	29	30	23	16	3	-1	0	-7	-10	-9	1	12	17	27	43	33	26	16	14	-14	-25	-26	-34	-30	-26	-11	-8	-3	4	9	14	21	31	37	33	25	13
367	-8	-2	10	19	19	16	9	1	-2	5	-4	-10	-8	0	6	13	16	28	23	14	10	15	-7	-13	-12	-30	-19	-13	-5	-7	-3	5	7	10	12	21	23	21	17	11
366	-2	-2	6	11	10	10	5	0	-1	0	-2	-10	-4	-2	1	9	6	15	15	6	5	13	-2	-7	-4	-18	-9	-6	-3	-9	-1	5	4	7	6	12	13	12	10	7
365	1	-2	2	5	3	4	4	2	2	-1	0	-4	-1	-2	0	5	3	5	10	2	0	6	0	-2	-4	-8	-1	-1	2	-5	0	3	2	4	3	5	6	5	4	3
364	0	0	0	0	0	0	0	0	0	0	0	0	0	0	0	0	0	1	0	0	0	1	1	1	1	1	1	1	1	1	1	1	1	1	1	1	1	1	1	1
363	0	0	0	0	0	0	0	0	0	0	0	0	0	0	0	0	0	0	0	0	0	0	0	0	0	0	0	0	0	0	0	0	0	0	0	0	0	0	0	0

b

σ_{rr}^{res} / r, mm \ z, mm	-37	-35	-33	-31	-29	-27	-25	-23	-21	-19	-17	-15	-13	-11	-9	-7	-5	-3	-1	0	1	3	5	7	9	11	13	15	17	19	21	23	25	27	29	31	33	35	
523	0	8	84	142	186	217	237	195	32	-94	-177	-185	-152	-147	-108	-22	114	390	366	0	100	101	7	-99	-149	-171	-171	-173	-141	-81	8	154	188	171	140	101	37	-26	0
522	0	60	90	142	184	212	229	162	14	-97	-165	-179	-144	-145	-113	-31	93	355	471	0	115	95	-11	-106	-147	-167	-167	-161	-137	-84	-6	127	183	166	137	103	47	-2	0
521	0	54	92	140	180	209	221	128	-6	-102	-147	-159	-143	-137	-109	-30	94	308	438	162	43	74	-16	-99	-141	-159	-164	-140	-137	-92	-20	97	177	159	135	103	53	13	0
520	26	82	100	141	177	202	198	92	-26	-117	-148	-118	-147	-124	-104	-25	97	270	354	193	95	118	-26	-88	-131	-148	-158	-122	-143	-96	-29	72	164	154	132	104	64	37	15
519	49	92	108	142	174	192	163	61	-39	-95	-122	-115	-131	-120	-94	-17	93	231	277	176	115	132	-41	-77	-120	-139	-139	-124	-128	-86	-34	48	130	149	130	107	77	58	35
518	71	102	119	145	171	179	127	35	-45	-88	-95	-107	-109	-114	-75	-13	90	201	209	156	135	128	-44	-70	-106	-130	-116	-129	-92	-86	-45	25	98	142	129	111	88	72	45
517	80	113	128	147	164	147	95	18	-41	-72	-89	-95	-100	-95	-65	-8	84	161	164	148	142	111	-37	-63	-93	-109	-109	-109	-85	-80	-46	6	77	114	127	115	98	82	41
516	65	125	135	145	145	122	75	12	-38	-62	-74	-85	-86	-85	-56	2	68	124	140	137	143	92	-33	-53	-80	-92	-97	-88	-77	-69	-40	-8	57	91	116	117	104	80	17
515	33	117	135	138	128	101	60	9	-30	-57	-64	-74	-72	-69	-41	1	52	99	120	125	126	73	-26	-43	-68	-80	-83	-73	-65	-55	-34	-15	37	77	101	108	99	72	1
514	15	96	125	126	112	87	49	6	-28	-51	-55	-63	-58	-56	-34	1	42	81	100	106	107	59	-17	-35	-56	-67	-69	-59	-53	-49	-33	-16	23	60	86	95	90	61	-3
513	7	74	108	112	97	74	42	4	-24	-43	-52	-51	-48	-44	-27	1	34	65	80	86	89	48	-7	-29	-45	-54	-56	-47	-44	-39	-29	-12	15	48	68	80	76	51	-5
512	1	58	90	94	84	60	32	2	-20	-35	-42	-42	-41	-37	-24	1	27	52	62	68	68	41	-1	-23	-35	-43	-46	-40	-36	-32	-23	-10	11	37	56	66	64	41	-4
511	2	43	71	75	68	49	25	2	-14	-26	-32	-35	-35	-29	-18	0	21	41	51	51	51	37	5	-18	-25	-34	-41	-34	-27	-22	-16	-8	6	28	44	53	51	29	-1
510	4	30	53	57	51	38	20	-1	-8	-15	-22	-27	-30	-24	-14	-2	15	32	37	39	40	33	7	-12	-17	-27	-36	-28	-18	-13	-8	-6	4	20	32	40	38	21	-1
509	6	20	38	42	36	27	12	-4	-5	-6	-13	-23	-23	-17	-10	-2	9	26	26	27	27	31	7	-7	-10	-22	-30	-19	-10	-4	-8	-3	2	13	22	29	27	16	1
508	6	12	24	27	24	18	7	-4	-3	2	-7	-15	-18	-10	-6	-2	3	20	15	17	18	24	6	-3	-6	-19	-20	-11	-2	1	-4	-2	1	8	13	19	17	12	3
507	5	8	11	14	13	10	5	-2	0	1	-1	-8	-11	-6	-4	-2	1	11	10	8	6	19	4	-1	-1	-10	-10	-3	-2	1	-1	1	1	4	6	12	9	7	6
506	2	3	4	4	4	3	3	1	0	-1	-1	-2	-5	-4	-1	0	2	4	5	4	0	10	3	0	-1	-2	-3	-1	-1	3	2	1	-1	2	1	5	3	3	4
505	1	0	0	0	0	0	1	1	0	0	0	0	0	0	0	0	0	1	0	0	0	1	1	1	1	1	1	1	1	1	1	1	1	1	1	1	1	1	1
504	0	0	0	0	0	0	0	0	0	0	0	0	0	0	0	0	0	0	0	0	0	0	0	0	0	0	0	0	0	0	0	0	0	0	0	0	0	0	0

c

σ_{rr}^{pr} / r, mm \ z, mm	-37	-35	-33	-31	-29	-27	-25	-23	-21	-19	-17	-15	-13	-11	-9	-7	-5	-3	-1	0	1	3	5	7	9	11	13	15	17	19	21	23	25	27	29	31	33	35	
523	0	-213	-136	-9	87	155	201	180	38	-70	-136	-125	-74	-48	14	130	314	556	448	0	-212	-130	-135	-184	-204	-206	-183	-170	-125	-54	42	173	209	201	180	155	117	67	0
522	0	-319	-102	19	102	163	203	155	25	-70	-122	-119	-67	-49	7	119	282	547	538	0	-306	-105	-138	-183	-200	-197	-178	-157	-121	-58	27	147	202	193	173	150	112	127	0
521	0	-208	-72	37	114	170	200	127	10	-72	-102	-99	-67	-43	7	113	267	473	489	67	-189	-130	-141	-176	-190	-187	-175	-136	-120	-65	14	120	193	185	166	144	111	97	0
520	-44	-178	-55	50	122	172	186	97	-8	-85	-103	-59	-73	-32	7	108	247	398	421	100	-77	-101	-146	-165	-180	-175	-168	-119	-123	-69	4	96	179	177	160	141	116	100	31
519	-55	-131	-39	59	126	168	159	70	-18	-62	-77	-57	-60	-34	10	104	222	337	337	114	-24	-72	-153	-154	-167	-168	-150	-119	-109	-60	-3	73	147	170	156	140	121	106	55
518	-44	-87	-20	67	128	160	126	46	-22	-54	-51	-52	-41	-32	20	94	199	291	262	114	17	-47	-150	-146	-154	-159	-128	-122	-78	-61	-13	51	118	164	153	139	124	110	63
517	-31	-46	2	75	123	133	96	31	-17	-39	-47	-43	-37	-20	22	86	177	238	206	112	46	-32	-136	-137	-142	-138	-119	-104	-71	-54	-15	33	95	142	149	138	127	111	59
516	-35	-9	22	76	107	109	78	26	-15	-30	-35	-36	-28	-17	21	84	147	190	168	109	63	-21	-121	-125	-129	-120	-107	-86	-64	-44	-12	19	75	112	135	135	125	102	42
515	-59	4	36	74	93	89	64	23	-8	-28	-27	-30	-20	-9	26	71	118	154	138	102	66	-16	-105	-111	-113	-105	-92	-72	-52	-35	-11	12	57	92	115	123	116	91	27
514	-65	2	42	70	81	77	53	19	-7	-25	-23	-24	-12	-3	24	61	98	124	113	88	62	-12	-87	-96	-97	-91	-77	-60	-44	-31	-11	10	42	74	97	106	102	77	21
513	-60	-3	39	63	71	64	45	16	-6	-20	-23	-18	-9	0	22	52	80	99	89	73	54	-10	-67	-81	-82	-76	-65	-48	-39	-22	-9	9	33	57	79	89	86	65	17
512	-54	-4	34	54	61	52	34	12	-4	-15	-19	-14	-8	0	17	42	65	80	68	58	42	-5	-52	-66	-67	-63	-54	-41	-31	-16	-5	7	27	44	62	72	71	53	15
511	-42	-6	26	43	50	42	27	10	-1	-10	-13	-12	-9	0	14	32	51	62	54	43	31	2	-35	-52	-52	-51	-46	-35	-23	-13	0	8	20	35	47	57	56	40	15
510	-29	-6	20	33	36	32	21	5	2	-3	-7	-10	-10	-1	11	22	37	48	40	32	25	6	-23	-38	-39	-42	-39	-28	-14	-8	5	7	15	25	36	42	42	29	13
509	-17	-6	15	25	25	23	13	0	2	3	-2	-11	-9	-1	7	15	25	37	27	22	17	13	-14	-25	-26	-34	-30	-20	-8	-2	4	8	10	16	25	30	29	21	11
508	-10	-4	9	16	17	15	8	-1	2	7	-1	-8	-10	0	5	9	13	27	16	14	11	13	-8	-15	-15	-28	-23	-12	-4	-1	3	7	7	9	15	19	19	14	8
507	-4	-2	3	8	9	9	5	-1	3	4	3	-4	-6	-1	2	4	7	14	11	7	2	13	-3	-8	-6	-14	-11	-4	-2	0	2	6	4	4	7	11	10	8	6
506	-1	0	1	2	3	2	2	-1	0	0	0	0	-4	-2	1	2	3	5	5	3	-2	8	0	-2	-3	-3	-4	-1	0	1	3	4	2	2	3	4	4	3	2
505	0	0	0	0	0	0	0	0	0	0	0	0	0	0	0	0	0	0	0	0	0	1	1	1	1	1	1	1	1	1	1	1	1	1	1	1	1	1	1
504	0	0	0	0	0	0	0	0	0	0	0	0	0	0	0	0	0	0	0	0	0	0	0	0	0	0	0	0	0	0	0	0	0	0	0	0	0	0	0

d

Figure 4. Residual stresses σ_{rr} across weld axis cross-section (*a, c*) and total σ_{rr} in hydrostatic pressure testing of reservoir (*b, d*) at R = = 362.5; (*a, b*) and 503.5 (*c, d*) mm: solid line is penetration line dividing the weld zone and the base metal

$$f_r = \frac{2}{\pi}\,[1 + 0.2393\varepsilon^3 + 0.0810\varepsilon^5 + 0.0574\varepsilon^6 + \varepsilon^7\,(0.0035 + 0.0537\,(\cos^4\theta + \sin^4\theta) + 0.0147\cos^2\theta\,\sin^2\theta)], \quad \varepsilon = a/h. \qquad (1)$$

At $a/h = 0.8$, $f_r = 0.744$; at $a/h = 0.9$, $f_r \approx 1.162$. With a certain degree of conservatism, it can be accepted that in reality $f_r < 1.4$.

K_c value in r direction can be determined through values δ_c, σ_y and modulus of elasticity $E = 2\cdot10^5$ MPa:

Table 4. Determination of a_{cr} depending on $\bar{\sigma}_{rr}$

$\bar{\sigma}_{rr}$, MPa	$2a_{cr}$, mm	$2a$, mm (as in Figure 4)
300	10.0	0
250	14.4	0
200	22.6	~3.0
150	40.2	~10.0

$$K_c = \sqrt{2\delta_c E\sigma_y} = \sqrt{2\cdot 0.02\cdot 2\cdot 10^5\cdot 350} = 1673 \text{ MPa}\cdot\text{mm}^{1/2}.$$

Accordingly we find that critical crack size $2a_{cr}$, depending on stresses $\bar{\sigma}_{rr}$ is described as

$$2a_{cr} = 2\left(\frac{1673}{\bar{\sigma}_{rr}}\right)^2 \frac{1}{\pi f_r^2} = 0.324\left(\frac{1673}{\bar{\sigma}_{rr}}\right)^2.$$

Table 4 shows the results of calculation for different $\bar{\sigma}_{rr}$.

Here too are specified values characterizing dimensions of the zone lying in the cross-section across the weld a (see Figure 4, *a, b*) within which range the level of stresses is not below $\bar{\sigma}_{rr}$. It is seen that values of a are significantly lower than values of a_{cr}, i.e. feasibility of growth of hardly possible hypothetical discontinuities having a_{cr} dimensions in the obtained σ_{rr} stress field (see Figure 4, *a, b*) is rather small. Similar phenomenon is observed for the case of Figure 4, *c, d*, as well as for other manhole sizes at $R > 362.5$ mm.

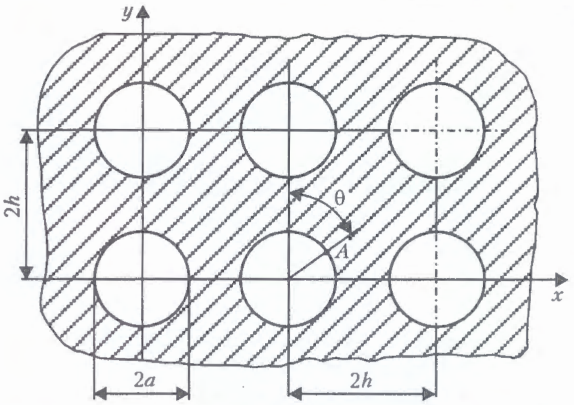

Figure 5. Section of infinite body with double-periodic system of disc-like cracks in plane $r = 0$

CONCLUSIONS

1. Feasibility of occurrence of through lamellar crack type defects in branch pipes from steel 09G2S in welded joints with reservoir wall is small. It can be explained by relatively small thickness of branch pipe walls (16 mm) and rather high (over 25 %) values of the material reduction in area in the direction normal to the rolling plane.

2. It can be considered that application of steel 09G2S for branch pipes of oval-shaped manholes of 75,000 m^3 reservoir is quite acceptable.

3. Leakiness of welded joints observed in hydrostatic tests of the reservoir is due to poor design and technological solution of the welded assembly.

1. Bernatsky, A.V. (2000) Influence of anisotropy of the rolled stock mechanical properties on initiation and development of tough and lamellar-tough fractures. *The Paton Welding J.*, 7, 31–37.
2. Hrivnyak, I. (1984) *Weldability of steels*. Ed. by E.L. Makarov. Moscow: Mashinostroenie.
3. (1988) *Fracture mechanics and strength of materials*. Ed. by V.V. Panasyuk. Vol. 2: Stress intensity factors in bodies with cracks. Kiev: Naukova Dumka.

MATHEMATICAL MODEL OF REVERSIBLE HYDROGEN BRITTLENESS*

A.V. IGNATENKO
E.O. Paton Electric Welding Institute, NASU, Kiev, Ukraine

A mathematical model of reversible hydrogen brittleness (RHB) of metals with body-centered cubic lattice is proposed. The model is based on classical Siener-Stroh model of microcrack formation in the metal grain by dislocation mechanism, and includes the model of hydrogen transfer by edge dislocations. A programme enabling estimation of the effect of hydrogen on metal grain failure stress was created. In simulating RHB, concentration of free hydrogen in metal, speed of movement of edge dislocations, metal temperature and grain size were taken into account. Calculation-based curves are compared with experimental ones. The dependencies obtained accord well with experimental evidence on RHB.

Keywords: *welded structures, reversible hydrogen brittleness, mathematical model, hydrogen transfer, edge dislocations, submicrocrack, degree of embrittlement*

Now in wide use in the world are metal welded structures from high-strength low-alloy steels. Hydrogen presence in metal often makes a strong negative impact on strength and durability of such structures. Thus, among various kinds of hydrogen embrittlement of structural steels, reversible hydrogen brittleness (RHB) [1] merits special attention, as it can arise even at rather small concentration of hydrogen in metal (about 10 $cm^3/100$ g and less). Quite often preheating of the structures is applied for prevention of RHB, as well as heating of welded joints in the course of welding, which markedly raises the cost of manufacturing of the entire welded structure. Therefore, application of cheaper technologies for elimination of negative influence of hydrogen is topical. For working out of such technologies, it is necessary to have a good understanding of those mechanisms by which hydrogen decreases metal strength characteristics. Modern physical methods do not allow yet, using direct experiments, studying, for example, kinetics of hydrogen distribution in welded joints, mechanism of pores and cracks formation in welds, and a number of other processes [2]. In this connection, there arises a necessity of construction of adequate physical model of RHB, calculation on its basis of reduction of metal strength under the influence of hydrogen, and comparison of the obtained results with experimental data.

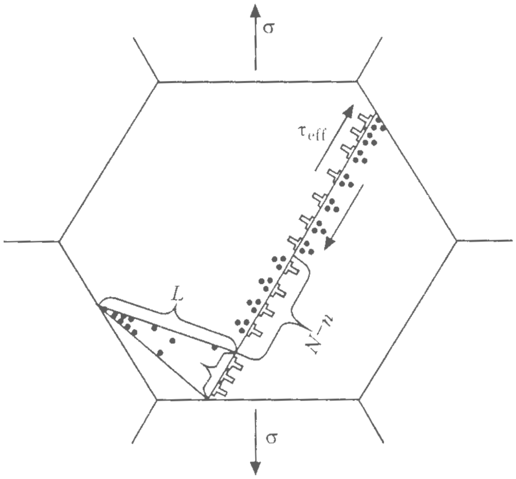

Figure 1. Scheme of hydrogen submicrocrack development within metal grain

In [3], a mathematical model of hydrogen transfer by edge dislocations in metal with BCC lattice is proposed. The program for calculation of the quantity of hydrogen transported by an edge dislocation is created. On the basis of this model and an improved Siener–Stroh model of submicrocrack formation by the dislocation mechanism, a mathematical model of brittle failure of the metal, caused by hydrogen, is developed. The essence of the model consists in the following. During action of stresses leading to plastic deformation, in metal grain plain congestion of edge dislocations is formed. Under the influence of tangential stresses, dislocations start to move, thus entraining free hydrogen being on their way (Figure 1). On grain border or on any other obstacle, moving edge dislocations are blocked (in the literature it is accepted to write that the top of dislocation congestion is blocked). If the applied external (in relation to grain) stresses are high enough, so in the top of the congestion the dislocations start to merge, forming a submicrocrack. Hydrogen, transferred by dislocations, getting into the volume of submicrocrack, reduces its surface energy. Thereby hydrogen facilitates submicrocrack growth, thus it loses its stability at lower stress. At macrolevel, it manifests itself as hydrogen metal embrittlement.

Physical essence of the term «hydrogen transfer by edge dislocation» consists in the following. Around the edge dislocation, the crystalline lattice of metal is distorted and is in the deformed state. Near the edge dislocation there is an area Ω of tensile stresses, featuring raised solubility of hydrogen. Therefore at dislocation occurrence there begins a diffusion of hydrogen from the area of metal with normal solubility into

*This work was executed under the guidance of academician of the NAS of Ukraine I.K. Pokhodnya.

the area Ω. In the case when the dislocation does not move, hydrogen diffusion proceeds until the equilibrium is established. If under the influence of external stresses the edge dislocation moves, so together with it the area Ω also moves. The hydrogen, trying to fill the formed potential well, begins diffusing, following the dislocation. The diffusion of hydrogen atoms arises, directed towards movement of the edge dislocation. In other words, it can be stated that edge dislocation transfers hydrogen.

Hydrogen redistribution in metal at macrolevel is influenced by stresses, concentration and temperature gradients. For calculations, a certain mean concentration of hydrogen in metal grain is used. In the given model it is assumed that edge dislocations transfer the hydrogen only within the metal grain. Thus, dislocations influence hydrogen redistributions in metal at microlevel, raising concentration of hydrogen in certain areas of grain.

The following assumptions were used as the basis of mathematical model of brittle failure of metal with hydrogen participation:

- submicrocracks arise according to the mechanism of Siener–Stroh model;
- speed of deformation of metal is constant;
- temperature of metal during deformation is considered constant;
- all dislocations in the plain congestion are identical and transfer equal quantities of hydrogen;
- all the hydrogen, transferred by edge dislocations, gets into submicrocrack;
- in the submicrocrack, equilibrium distribution of hydrogen according to the adsorption isotherm is established;
- in submicrocrack volume, the hydrogen is molized, while on the surface it is dissociated.

According to [4–7], energy of the system «congestion of edge dislocations–submicrocrack» can be presented as

$$W = \frac{(nb)^2G}{4\pi(1-\nu)} \ln \frac{4d}{L} + \frac{(N-n)^2b^2G}{4\pi(1-\nu)} \ln \frac{4\pi\sqrt{e}(1-\nu)d}{(N-n)Gb} \times \tau_{eff} + 2\gamma L - \frac{\pi(1-\nu)L^2}{8G}\sigma^2 - \frac{nbL}{2}\sigma \sin 45°, \quad (1)$$

where L is the submicrocrack length; n is the quantity of dislocations which have formed it; σ is the main normal stress; γ is the specific surface energy of metal changing under hydrogen influence; G is the shear modulus; ν is Poisson's ratio; d is the size of metal grain; b is the Burgers vector modulus; e is the base of the natural logarithm; τ_{eff} is the effective tangential stress a little exceeding the yield strength.

Various modifications of equation (1) are used for determination of critical stress σ_c at which the submicrocrack loses stability and, as a consequence, destroys metal grain [4–7]. For this purpose the equation (1) is differentiated separately with respect to L and n, from the obtained equations the point of unstable equilibrium of the system «congestion of edge dislocations–submicrocrack» is found, and critical values of L_c, n_c and σ_c are defined. Thus calculated value of σ_c is considered as the minimum tensile stress which is necessary to apply to the metal to perform its brittle failure.

Equation (1) is true only when specific surface energy γ remains invariable during submicrocrack growth. However, in the presence of hydrogen in the metal, this condition is not fulfilled, as in this case γ is a complex function of metal temperature, submicrocrack length, quantity of edge dislocations which have joined it, and quantity of the hydrogen brought by dislocations. Therefore, in equation (1) it is necessary to substitute summand $2\gamma L$ with integral $2\int \gamma dL$:

$$W = \frac{(nb)^2G}{4\pi(1-\nu)} \ln \frac{4d}{L} + \frac{(N-n)^2b^2G}{4\pi(1-\nu)} \ln \frac{4\pi\sqrt{e}(1-\nu)d}{(N-n)Gb} \times \tau_{eff} + 2\int \gamma dL - \frac{\pi(1-\nu)L^2}{8G}\sigma^2 - \frac{nbL}{2}\sigma \sin 45°. \quad (2)$$

For exact calculation of σ_c using equation (2), it is necessary to consider the dynamics of submicrocrack growth, which complicates the calculation.

Value τ_{eff} is estimated by means of Hall–Petch relation [8, 9] $\sigma_y = \sigma_0 + K_y/\sqrt{d}$ for the metal yield limit σ_y:

$$\tau_{eff} = \frac{(\sigma_y - \sigma_0)}{2} = \frac{K_y}{2\sqrt{d}}, \quad (3)$$

where K_y is the factor of inclination of straight line in co-ordinates σ, $\sqrt{d}$.

The quantity of edge dislocations of the same sign N is considered invariable after reaching a maximum under the influence of external stress. If it is accepted that sliding length is equal to the grain size, then maximum quantity of dislocations N in the congestion can be estimated by the formula [10]

$$N = \frac{(1-\nu)d\tau_{eff}}{Gb} = \frac{(1-\nu)\sqrt{d}K_y}{2Gb}. \quad (4)$$

In calculating the influence of hydrogen on surface energy of the submicrocrack, it was considered that hydrogen adheres to the Langmuir equation of adsorption isotherm for diatomic gases which dissociate at adsorption [11]:

$$\theta = \frac{\sqrt{ap}}{1 + \sqrt{ap}}, \quad (5)$$

where θ is the degree of coverage of submicrocrack surface with hydrogen; p is the hydrogen pressure; a is the adsorption constant.

According to the Gibbs adsorption equation, change of surface energy of the metal at adsorption on it of hydrogen, equals [11]

$$\gamma = \gamma_0 - 2\frac{kT}{b^2} \ln (1 + \sqrt{ap}) = \gamma_0 + 2\frac{kT}{b^2} \ln (1 - \theta), \quad (6)$$

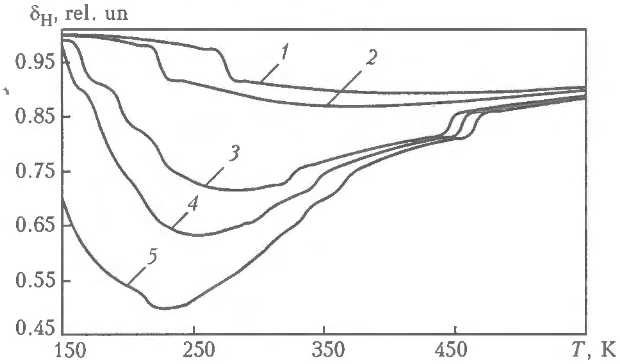

Figure 2. Degree of hydrogen embrittlement δ_H of iron with hydrogen depending on temperature T at different speeds of movement of edge dislocations (factor of diffusion of hydrogen $D = 1 \cdot 10^{-7}$ exp $[-10880/(RT)]$, mean concentration of hydrogen C_0 = = 6 cm^3/100 g): *1* — $V_0 = 1$; *2* — $5 \cdot 10^{-1}$; *3* — 10^{-1}; *4* — $5 \cdot 10^{-2}$; *5* — 10^{-2} m/s

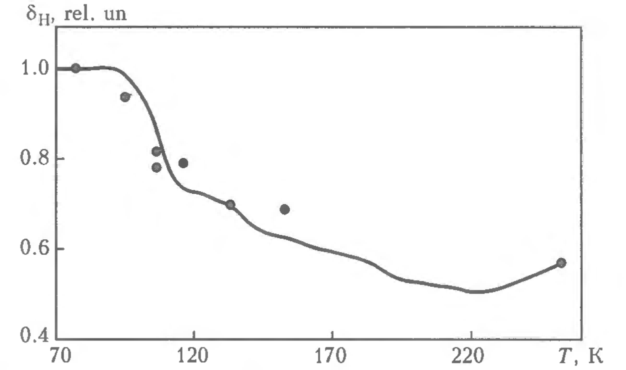

Figure 4. Comparison of experimental (dots) [15] and calculated (curve) data of the degree of hydrogen embrittlement δ_H for steel 09G2S (C_0 = 6.3 cm^3/100 g, $V_0 = 8 \cdot 10^{-4}$ m/s)

where γ_0 is the specific surface energy at metal–absolute vacuum border; T is the metal temperature; k is Boltzmann's constant.

Connection between quantity of hydrogen N_H, which is delivered by dislocations into the submicrocrack volume, and values L, θ, p, is established by means of the equilibrium equation:

$$\frac{N_H n}{b} = \frac{2\theta L}{b^2} + \frac{nbLp}{kT}. \tag{7}$$

Influence of hydrogen on the degree of reduction of metal brittle strength δ_H was calculated proceeding from the criterion of hydrogen brittleness suggested in [12]:

$$\delta_H = \frac{R_{ms}^H}{R_{ms}} \approx \frac{\sigma_H}{\sigma_0}, \tag{8}$$

where R_{ms} is the resistance to microspalling; σ_0 is the value of tensile stress in the neck of the specimen; R_{ms}^H is the characteristic of hydrogenized metal.

On the basis of the reported mathematical model, the program of calculation of behaviour of system «plain congestion of edge dislocations–submicrocrack» is developed. Degree of hydrogen embrittlement δ_H of the metal was calculated on the basis of the system of equations (2)–(8) and mathematical model of hydrogen transfer by edge dislocations. In calculations the data typical for low-alloy steels [4, 8] were used: G = 80 GPa; v = 0.25; $b = 2.56 \cdot 10^{-10}$ m; γ_0 = = 2 J/m^2; K_y = 0.6 MPa/m$^{1/2}$, as well as constants of adsorption of hydrogen on iron surface a = 37.5 Pa^{-1} [11]. It was also taken into account that the quantity of dislocations n merged in congestion top into a submicrocrack, can be only integral positive number. Therefore, periodic jumps of the obtained curves are explained by discreteness of n values.

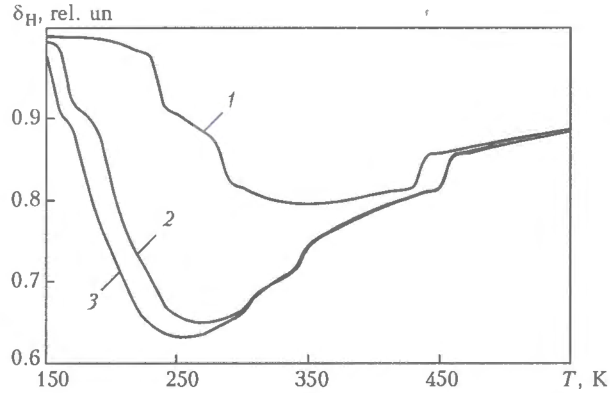

Figure 3. Degree of hydrogen embrittlement δ_H of iron with hydrogen depending on temperature T for different diffusion factors of hydrogen in metal (speed of movement of edge dislocation $V_0 = 5 \cdot 10^{-2}$ m/c, C_0 = 6 cm^3/100 g): *1* — $D = 1.76 \cdot 10^{-7}$ exp $[-6651/(RT)]$; *2* — $D = 2.2 \cdot 10^{-7}$ exp $[-12970/(RT)]$; *3* — $D = 10^{-7}$ exp $[-10880/(RT)]$

Results of the calculations are presented in Figures 2–4. Figure 2 shows dependencies of $\delta_H = \sigma_H/\sigma_0$ on metal temperature T for different speeds of movement of edge dislocations V_0. It is seen that in a certain interval of speeds V_0, maximal embrittling effect the hydrogen exerts at temperatures close to normal (curve minimum $\delta_H(T)$). Deviation from this temperature in one or another direction leads to the reduction of negative effect of the hydrogen on metal strength. With increasing V_0, reduction of brittle strength of metal decreases, while the dependence minimum $\delta_H(T)$ shifts into the area of higher temperatures. Speed of movement of edge dislocations V_0 is proportional to relative speed of metal deformation $\dot{\varepsilon}$ [6, 13]. Therefore, the results of calculation, presented in Figure 2, agree well with experimentally established temperature-speed peculiarities of RHB [12, 13]. Figure 3 shows comparison of the results for different factors of diffusion of hydrogen D in metal [14], which characterize mobility of hydrogen in metal. Hence, the higher is D, the more hydrogen is transported by dislocations to the place of submicrocrack formation. The calculation shows that increase in the factor of diffusion D, with other conditions being equal, raises sensitivity of iron to hydrogen. Figure 4 presents comparison of experimental data [15] and calculated curve of the degree of hydrogen embrittlement δ_H for steel 09G2S. From the above results it is seen that suggested mathematical model of RHB of alloys of iron with BCC lattice, i.e. structural steels, agrees well with experimental data, and can be applied for estimation of the influence of hydrogen on physical and mechanical properties of metals.

1. Pokhodnya, I.K., Shvachko, V.I. (1997) Physical nature of hydrogen induced cold cracks in structural steel welded joints. *Avtomatich. Svarka*, **5**, 3–12.
2. Pokhodnya, I.K. (2004) Control of hydrogen in weld metal. In: *Proc. of Int. VOM-2004 Conf.* (Donetsk, 2004), 449–453.
3. Shvachko, V.I., Ignatenko, A.V. (2007) Model of transportation of hydrogen with dislocations. *The Paton Welding J.*, **2**, 24–26.
4. Kotrechko, S.A., Meshkov, Yu.Ya., Mettus, G.S. (1988) Brittle fracture of polycrystalline metals under complex stress state. *Metallofizika*, **6**, 46–55.
5. Garofalo, F., Chou, Y.T. (1960) Effect of hydrogen on stability of microcracks in iron and steel. *Acta Metallurgica*, 8(**8**), 504–512.
6. Vladimirov, V.I. (1984) *Physical nature of fracture of metals*. Moscow: Metallurgiya.
7. Pokhodnya, I.K., Shvachko, V.I., Utkin, S.V. (2002) Effect of hydrogen on equilibrium of dislocation submicrocrack in α-iron. *Fiz.-Khimich. Mekhanika Materialiv*, **1**, 1–8.
8. Meshkov, Yu.Ya., Pakharenko, G.A. (1985) *Structure of metals and brittleness of steel products*. Kiev: Naukova Dumka.
9. Meshkov, Yu.Ya., Serditova, T.N. (1989) *Fracture of wrought steel*. Kiev: Naukova Dumka.
10. Hirt, J., Lote, I. (1972) *Theory of dislocations*. Moscow: Atomizdat.
11. Petch, N.J. (1956) The lowering of fracture stress due to surface adsorption. *Philosophical Magazine*, 1(**4**), 331–337.
12. Pokhodnya, I.K., Yavdoshchin, I.R., Shvachko, V.I. et. al. (2004) *Metallurgy of arc welding. Interaction of gases with metals*. Ed. by I.K. Pokhodnya. Kiev: Naukova Dumka.
13. Kolachev, B.A. (1985) *Hydrogen brittleness of metals*. Moscow: Metallurgiya.
14. Spivak, L.V., Skryabina, N.E., Kats, M.Ya. (1993) *Hydrogen and mechanical posteffect in metals and alloys*. Perm: PGU.
15. Pokhodnya, I.K., Shvachko, V.I., Kotrechko, S.A. et al. (1999) A new method for quantitative determination of sensitivity of steels to hydrogen embrittlement. *Mater. Sci.*, 34(**4**), 538–543.

LASER CUTTING OF METALLIC AND NON-METALLIC MATERIAL SHEETS AND PLATES

The offered process of laser cutting is based on location and spacing of blanks of any contour using laser radiation with a power of up to 1 kW. In this case the erosion products are removed from the radiation-affected zone with an air-oxygen mixture jet.

The hardware system comprises a fast-flowing technological CO_2-laser, three-axis manipulator, optical section mirrors and cutter with a focusing lens.

Length of a sheet or plate to be cut depends upon the size of the manipulator and usually amounts to 1–2 m. One of the cutting systems available at the Department is shown in the Figure.

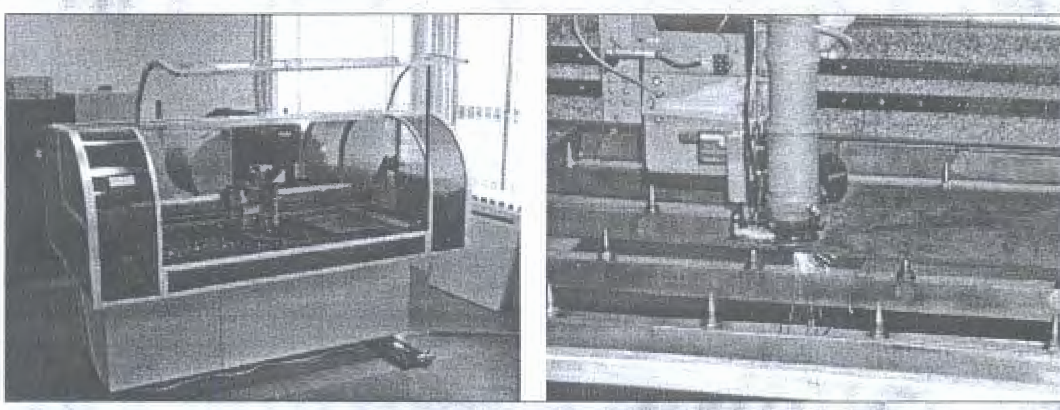

General view of the computer-controlled laser cutting system and process of cutting of steel sheets

Compared with the microplasma technology, the laser cutting is characterised by a substantial increase in accuracy (±0.01 mm), and the resulting cuts are free from tapering. Width of the cuts is up to 0.7 mm, which considerably reduces the amount of wastes, makes the technology environmentally friendly and improves labour conditions. This technology is free from such harmful factors characteristic of plasma cutting as noise and light of the electric arc. Emission of harmful fumes is substantially lower in this case. The technology can be used to cut non-conducting materials of large thickness.

Productivity of the process is up to 500 mm/min in cutting ferrous steel 6 mm thick, and up to 2000 mm/min in cutting stainless steel 1 mm thick.

Application. Cutting of ferrous and stainless steels up to 6 mm thick, wood, cardboard, plywood up to 20–30 mm thick, plastics and organic glass up to 40 mm thick, rubber, hard-alloy compounds and other materials.

Dr. Shelyagin V.D.
E-mail: shelyagin@paton.kiev.ua, laser77@online.com.ua

INFLUENCE OF THE METHOD OF MELTING TITANIUM ALLOYS ON THEIR WELDABILITY AND SERVICE CHARACTERISTICS

S.V. AKHONIN, V.F. TOPOLSKY, I.K. PETRICHENKO, E.L. VRZHIZHEVSKY and **R.N. MISHCHENKO**
E.O. Paton Electric Welding Institute, NASU, Kiev, Ukraine

The influence of the method of titanium alloy production by the process of vacuum-arc remelting or electron beam cold hearth melting on the metal performance and its weldability is considered in the case of medium-alloyed titanium alloy VT6. It is shown that the difference in the strength and ductility properties is negligible. It is established that irrespective of the production process, the fracture toughness K_{Ic} of the base metal is on the same level, and fracture toughness of the metal of EB welds is higher than that of the base metal in both cases. The characteristic of cyclic crack resistance of both the base metal of VT6 titanium alloy produced by different melting processes and of its welded joints is shown to be on the same level.

Keywords: *arc welding, titanium alloys, vacuum-arc remelting, electron beam melting, weldability, welding modes, structure, mechanical properties, crack resistance*

Traditional method of manufacture of ingots of titanium alloys, including VT6, is vacuum-arc remelting (VAR) [1, 2]. In recent years, in melting of ingots and slabs of non-alloyed titanium and titanium alloys, has gained wide acceptance the technology of electron beam cold hearth melting (EBCHM) [3, 4]. For the last ten years, in the USA and in the CIS countries, new electron beam plants with total capacity of 26,000 t of titanium ingots a year are put in operation [5].

Determination of the influence of the method of melting of metal (VAR or EBM) on service characteristics and weldability of titanium alloys was carried out by the example of medium-alloy titanium alloy VT6 belonging to alloys with Ti–6Al–4V alloying system, whose share in the world market makes more than 70 % [1, 2].

The purpose of the present work consists in the establishment of the influence of the method of melting of ingots of titanium alloys on their weldability, weld formation, structure, mechanical and service characteristics of the welded joints performed by fusion welding.

For carrying out the research, from the melted at SE «SPC «Titan» of the E.O. Paton Electric Welding Institute of NASU by the technology of EBM of ingots of titanium alloy VT6, by method of hot rolling on two-roll reversing rolling mill, were obtained sheets in the thickness of 3, 5 and 12 mm. The metal used for the research, melted by VAR method, had the form of finished sheets VT6 12 mm in thickness, which were then rolled untill their thickness became 3 and 5 mm. Thus for obtaining of fine-grained homogeneous structure, 60 % of deformation was carried out in β-domain (at temperature above 980 °C), and the remaining 40 % in (α + β)-domain (950–860 °C).

Table 1. Chemical composition of titanium alloy VT6 of different melting methods (base — titanium)

Melting method	Content of alloying elements and impurities, wt.%						
	Al	V	Fe	C	O	N	H
VAR	5.5	4.00	0.25	0.100	0.096	0.05	0.015
EBM	5.8	3.95	0.26	0.015	0.130	0.02	0.003

Analysis of chemical composition of the used rolled stock has shown (Table 1) that the content of alloying elements in metal of both methods of melting is very similar.

Welding of test specimens was carried out using the most widely applied to titanium argon-arc (ACW) and electron beam welding (EBW) methods.

ACW was performed using non-consumable tungsten electrode in argon over flux layer, and also using penetrating arc with the use of OB-2146 unit with welding torch A-1272 and power source VSVU-630. In welding over flux layer, ANT-25A and experimental flux OB-3, welding wire VT6sv 1.2 mm in diameter and SP15 2 mm in diameter, were used.

EBW was carried out in UL-144 unit equipped with power source ELA-60/60, welding gun TsF-4 and beam control device SU-220.

For revealing of internal defects, was applied X-ray inspection of welded specimens on RAPS/300-70 apparatus using film T-4, which enabled detecting defects which sizes made not less than 2–3 % of the metal thickness. For detection of the defects which sizes were not resolved by X-ray method, metallographic analysis of transverse and longitudinal sections with microscope «Neophot» was conducted. Sections were prepared by common for titanium alloys technique [6].

At all methods, welding of specimens was carried out under the scheme shown in Figure 1, optimum mode providing absence of defects in welded joint, satisfactory formation of weld face and root was developed on an alloy specimen of the same thickness,

Table 2. Parameters of butt welded joints of alloy VT6 performed by different welding methods

Welding method	Metal thickness, mm	Melting method	Welding mode paremeters			Welded joint paremeters				
			I_w, A	U, V	v_w, m/h	Weld width at top, mm	Weld width at root, mm	Weld root height, mm	HAZ width, mm: At top	HAZ width, mm: At root
AAW	3	VAR	180	12	12	10.5	3.0	0.25	4.2	7.8
		EBM	180	12	12	11.0	2.5	0.20	4.4	8.1
	5	VAR	385	14	30	7.5	4.0	0.30	2.0	3.2
		EBM	385	14	30	8.5	3.0	0.25	1.5	4.0
AAW over flux layer	3	VAR	135	9	12	5.5	5.5	0.30	3.3	3.0
		EBM	135	9	12	5.8	5.2	0.20	3.2	3.4
	5	VAR	250	11	12	8.5	8.0	0.50	4.0	5.0
		EBM	250	11	12	9.0	6.0	0.40	3.5	4.5
EBW	5	VAR	I_b = 38 mA	U_{acc} = 60 kV	25	5.2	2.1	0.16	2.1	3.1
		EBM			25	6.0	1.3	0.10	1.4	3.8
	12	VAR	I_b = 75 mA	U_{acc} = 60 kV	25	3.8	3.5	2.00	1.5	1.0
		EBM			25	4.0	2.9	1.60	1.5	1.0
AAW in groove with wire VT6sv	12	VAR EBM	110 180 230	15 9 9	15	11.0	4.0	1.40	4.0	4.0
AAW of edges with wire CG15cd	12	VAR EBM	110 180 230	15 9 9	20	10.0	4.0	1.30	4.0	4.0

obtained using VAR (Table 2). For elimination of residual stresses, after welding all welded joints were subjected to annealing at temperature 750 °C for 1 h and to cooling on air.

Analysis of welded joints parametres (see Table 2) has shown the obvious tendency to welding current increase in welding the alloys melted by EBM method, irrespective of the method of welding. Hence, for achievement of optimum parametres of the welded joints of alloys melted by VAR method, it is necessary for the alloys melted by EBM method, to increase welding current in welding by all methods, by 10–12 %, which is probably caused by higher density of metal melted by EBM method, in comparison with the metal obtained by VAR method [7].

Thus manufactured plates and their welded joints, for quality estimation, were subjected to static tensile stress and impact bending. Fracture toughness K_{1c} and fatigue crack growth rate (FCGR) were determined.

Use of special halogenide fluxes (ANT-25A, OB-3) allows performing welding of titanium sheets having up to 6 mm thickness, in one pass. Application of flux OB-3 allows reducing welding current by 25 A, in comparison with flux ANT-25A. Feeding of filler wire in welding of metal 5 mm thick during the first pass is conditioned by the necessity of undercuts exclusion. In welding of heavy-gauge metal, the method with groove preparation is applied. In this case the share of filler metal makes approximately 70–80 % of the weld metal volume. For performance of the welded joint close in strength to the base metal (BM), a more alloyed filler wire should be applied. Such properties in welding with groove preparation are provided by welding wire SP15sv developed earlier at the E.O. Paton Electric Welding Institute. For comparison, welding with groove preparation was conducted using filler wire VT6sv (Table 3).

Investigation of microstructure of welded joints of alloy VT6 5 mm thick conducted using AAW (penetrating arc) over flux layer on EBM metal, has shown (Figure 2, *a*–*c*) that the BM has mainly globular structure, though areas with lamellar structure are also observed, while the metal of the weld and near-weld zone of HAZ is characterised by presence of coarse needle-like martensite α′-phase.

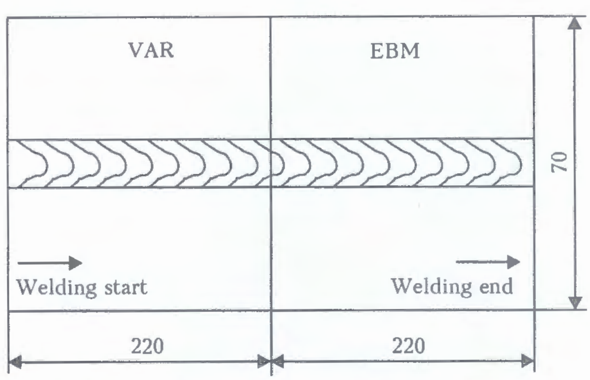

Figure 1. Scheme of welding of specimens by AAW, AAW over flux and EBW methods

Table 3. Mechanical properties of alloy VT6 and its welded joints

Method of welding and welding wire brand	Metal thickness, mm	Melting method	Base metal		Welded joint			Failure site
			σ_t, MPa	*KCV*, J/cm^2	σ_t, MPa	*KCV*, J/cm^2		
						Weld	HAZ	
AAW over flux layer	5	VAR	970	42	950	30	32	Weld
		EBM	980	36	970	27	30	Same
AAW over flux layer with welding wire: VT6sv	5	VAR	970	42	955	32	38	»
SP15sv	5				968	32	38	HAZ
VT6sv	5	EBM	980	36	975	27	38	Weld
SP15cv	5				980	32	38	HAZ
AAW in groove: VT6sv	12	VAR	950	40	940	30	34	Weld
SP15sv	12				952	33	34	HAZ
VT6sv	12	EBM	1000	35	950	27	32	Weld
SP15cv	12				998	30	32	HAZ
EBW	12	VAR	960	45	960	40	37	BM
		EBM	1010	37	1020	30	28	Same

Note. Mean values based on the results of five specimens testing are cited.

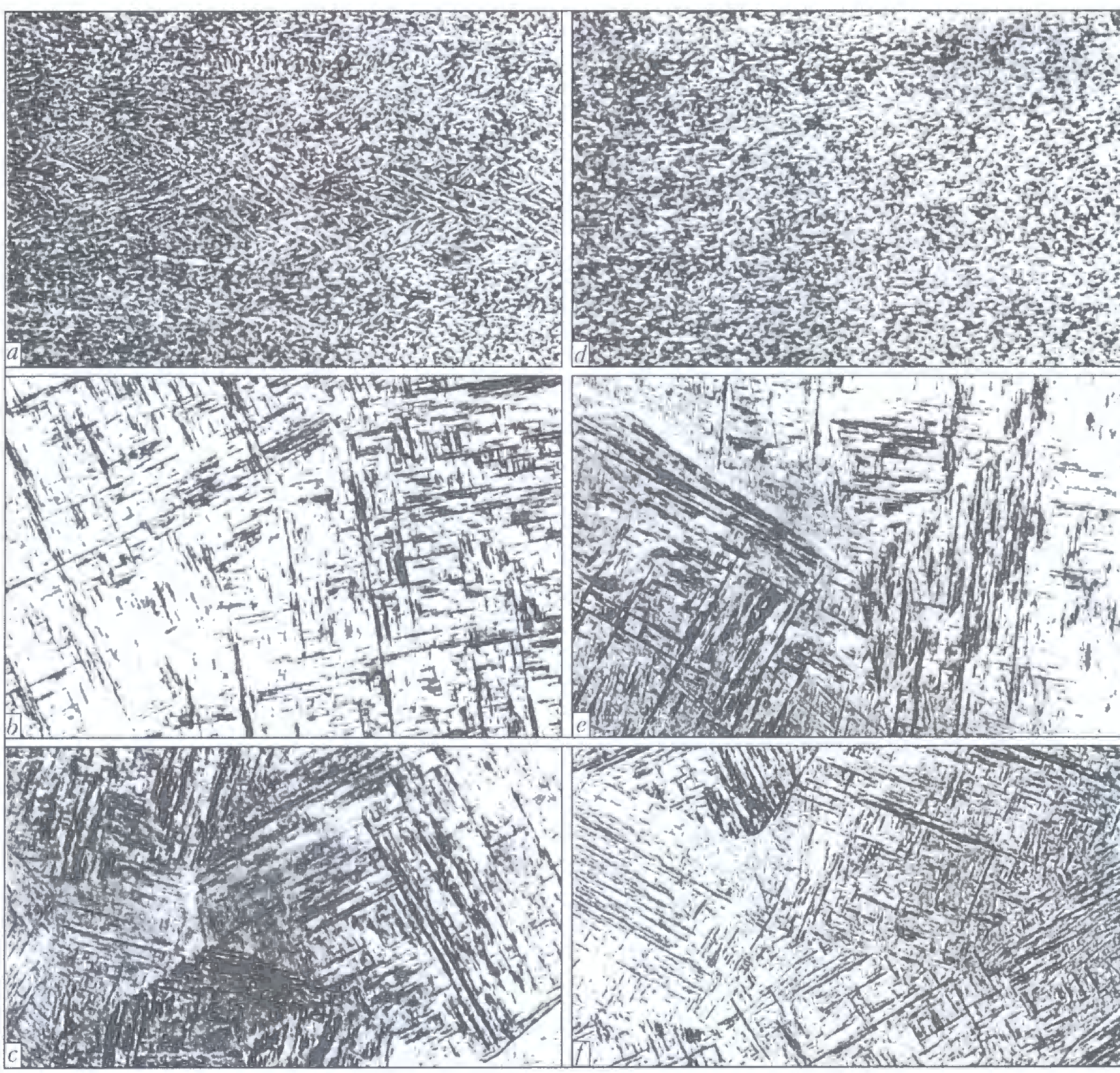

Figure 2. Microstructure of welded joint metal of alloy VT6 obtained by EBM (*a*–*c*) and VAR (*e*–*f*) 5 mm thick, performed by AAW with penetrating arc: *a, d* — BM; *b, e* — weld; *c, f* — HAZ metal (×200)

Corresponding zones of the welded joint of alloy VT6, obtained using VAR method, have similar structures (Figure 2, *d, e*).

The BM obtained by EBM method, after rolling down to 5 mm thickness, has smaller degree of α-phase globularization in its structure than the metal melted by VAR method. Noted features are connected with some differences in modes of rolling of the alloys melted by different methods. However structures of the weld metal and the HAZ are identical and similar to the structure of corresponding areas of the welded joint performed by AAW method on metal 3 and 12 mm in thickness, although structures of BM differ (metal melted by VAR method has globular-lamellar, while that by EBM method has globular structure).

Application of flux in welding (AAW over flux) has not brought essential changes in the structure of welded joint.

Mechanical properties of BM and welded joints performed using AAW over the flux layer, AAW in groove and EBW, after annealing at temperature 750 °C for elimination of residual stresses, are entered in Table 3. Analysis of the obtained results shows that the welded joints performed by through penetration with simultaneous feeding of filler wire SP15sv, and also in groove by this wire, have strength and plasticity practically the same as BM. The same joints performed using filler wire VT6sv, have a little bit inferior properties, both in respect of strength and plasticity. As to EBW, irrespective of the method of melting of the alloy, strength of welded joints is at the level of BM, impact toughness of the weld metal and HAZ make nearly 80–85 % of that of BM, which corresponds to technological recommendations and also requirements of domestic and foreign standards on welded joints of alloy VT6 or its analogue Grade 5.

The difference in strength characteristics of the welded joints performed on metal obtained by VAR and EBM methods, is insignificant, while impact toughness of the weld and HAZ metal depends not so much on the method of welded metal melting, but on the welding method. Impact toughness in HAZ metal after AAW is higher than in the weld, while in EBW the reverse tendency is observed.

To the most important characteristics defining serviceability of welded joints from high-strength titanium alloys, belong also fracture toughness K_{1c} and FCGR. Fracture toughness on air K_{1c} defines resistibility of a material to failure at static or fatigue loading in the presence in it of cracks. Estimation of K_{1c} of the BM and the metal of welded joints of titanium alloys melted by VAR and EBM methods, was carried out according to normative document ASTM1 E 399–90.

Tests of welded joints of the titanium alloy VT6, conducted according to the above technique, allowed defining fracture toughness K_{1c} for the metal melted by EBM and VAR methods, having 12 mm thickness (Table 4). Analysis of the obtained results has shown that titanium alloys melted by VAR and EBM methods, as well as their welded joints, are very close in terms fracture toughness (K_{1c} of the BM are accordingly 61.3 and 60.8 MPa√m, wlile K_{1c} of the welded joint are 78.5 and 72.5 MPa√m).

Table 4. Values of fracture toughness of BM and welded joints performed by EBW

Specimen #	Method of alloy melting (joint site)	K_{1c}, MPa√m
1	EBM (BM)	65.9
2		54.0
3		62.6
4	EBM (HAZ metal in EBW)	73.9
5		69.4
6		74.2
7	VAR (BM)	62.2
8		61.9
9		54.4
10		66.8
11	VAR (HAZ metal in EBW)	78.3
12		77.9
13		79.3

It is significat that fracture toughness of the welded joints metal is higher than that of BM. According to authors of [8], the latter is connected with different structures of BM (globular prevails) and welded joint (lamellar coarse-grained structure). Lamellar structure features sharper changes in cracks propagation direction than globular one, sometimes also their branching with formation of secondary cracks is observed. Increment of total crack length occurring as a result of these processes, requires higher energy, and involves large volumes of metal into plastic deformation work.

After the tests, fractures of the failed specimens were investigated. Figure 3, *a* shows general view of the BM fracture surface. In its top, where the fatigue crack developed from a notch, three steps of its spasmodic growth are observed, the failure mechanism is quasispalling with elements of tough failure (Figure 3, *b*). Transition from the zone of fatigue crack propagation to the zone of crack propagation at static loading of the specimen is presented in Figure 4, *c*. In this section of the specimen prevails ductile character of failure with stratification areas which, apparently, arise at crack propagation along persistant strips of sliding. While in the initial zone of propagation of the main crack under static loading against the background of pit fracture, individual facets of quasispalling occur, so in the process of its further advancement, elements of quasibrittle failure disappear, and the fracture structure becomes exclusively pit one (Figure 3, *d*).

Surface of the fracture of BM specimen of alloy VT6 melted by VAR method, has a similar structure.

Despite difference in structure of fine-grained BM and coarse-grained weld metal, microstructure of fractures of specimens of the welded joints performed by EBW, is similar to the structure of similar fracture

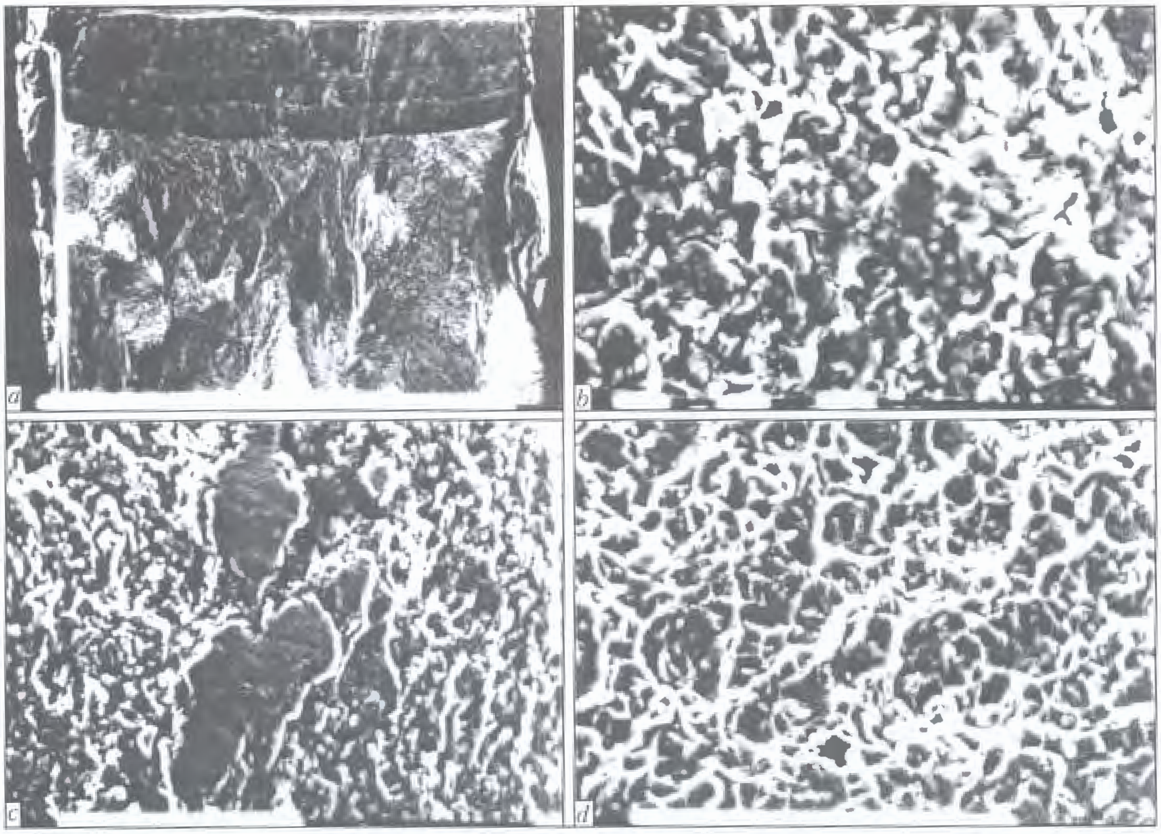

Figure 3. Fracture (a — ×10) and fractographic picture of the surface of titanium alloy specimen obtained by EBM for (explanations see the text)

sites of BM samples. On the site of fatigue crack development, the prevailing mechanism of failure is quasispalling, while transition to crack propagation under static loading is accompanied by increasing quantity of ductile elements in the fracture structure.

Thus, having analyzed results of comparative tests of fracture toughness of BM of alloy VT6 melted by VAR and EBM methods, and its welded joints performed by EBW, it is possible to draw a conclusion that for fractures of samples of BM and welds, the basic mechanism of failure in the zone of fatigue crack development is quasispalling. At further crack advancement under the influence of static loading in fractures of BM samples is observed transition to tough failure, while in fractures of samples of weld metal mainly to intergranular tough failure.

Fatigue tests for cyclic crack resistance [8, 9] of BM samples of alloy VT6 melted by VAR and EBM method, and metal of the welds performed by EBW, were conducted according to the requirements of standard ASTM-E647–93. Flat specimens having 60 × × 4 mm section with central located crack-like defect were tested. In welded specimens were defined regularities of fatigue cracks growth at their development in weld metal.

Central located crack-like defect was performed in the shape of a circular aperture 1.5 mm in radius and mechanical cuts of 1.5 mm. Then at cyclic loading, with amplitude of loads smaller than the amplitude at testing, were grown cracks in both sides of cuts, untill one of them reached 1 mm length. The obtained central located defect was taken as a fatigue crack for further investigation of specimens fatigue failure kinetics.

Growth rate of the fatigue crack as defined as a relation of crack length increments to the corresponding increment of quantity of cycles of stress variations, the scope of stress intensity factor calculated for mean value of crack length. As a result of processing of experimental data were constructed kinetic diagrams of fatigue failure both for BM melted by VAR and EBM, and for its welded joints performed by EBW (Figure 4). On the obtained kinetic diagrams of fatigue failure, experimental data cover the range of rate variation from $0.5 \cdot 10^{-8}$ to 10^{-5} m/cycle and a range of change of scope of corresponding to these rates scope of stress intensity factor from 15 to 75 MPa$\sqrt{m}$, which corresponds to linear (Paris's) section of kinetic fatigue failure diagrams.

Fractographic investigation of fractures of the failed specimens after fatigue tests have shown that in a zone of slow crack development, both in the BM and in the weld metal, quasibrittle failure is prevailing. At transition to the zone of accelerated crack development, character of BM and welds failure becomes mixed one. Along with elements of quasibrittle failure, arise elements of tough failure, in particular, in welds elements of intergranular tough fracture are mainly observed. In the zone of final spalling mainly intergranular tough failure is observed.

Analysis of the results of cyclic crack resistance tests has shown that FCGR in BM of the titanium

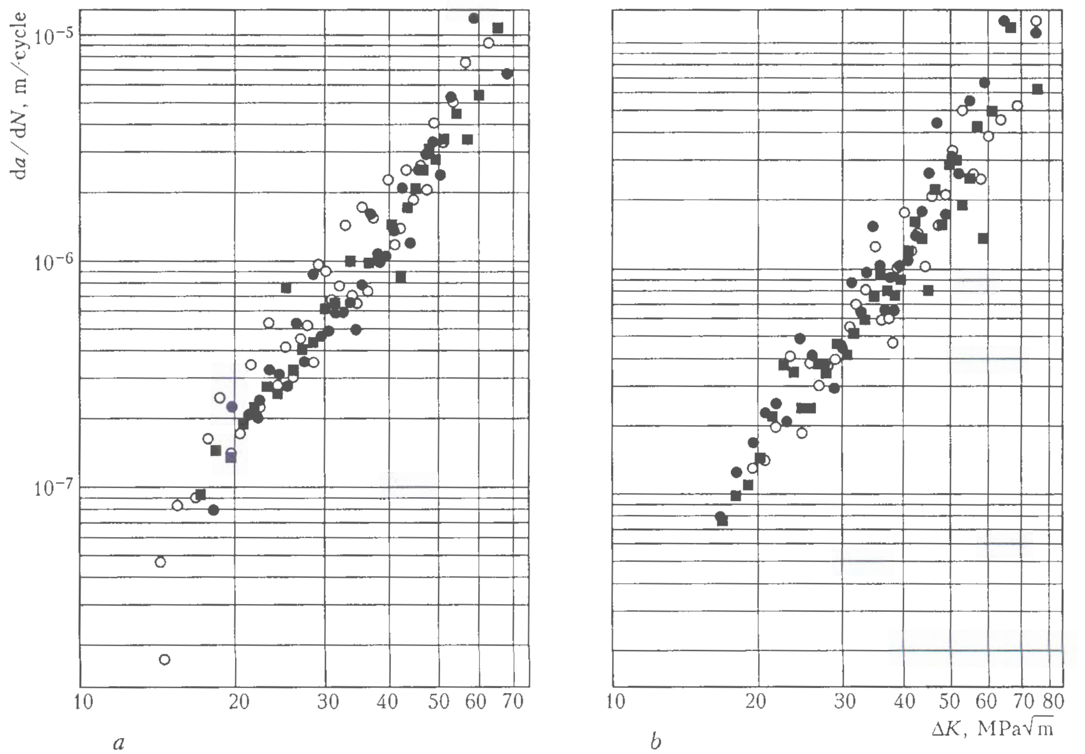

Figure 4. Kinetic diagram of fatigue failure of welded joints of titanium alloy VT6 performed by EBW: *a* — EBM; *b* — VAR

alloy VT6 obtained by different melting methods (VAR or EBM), and also weld metal of their butt joints perform by EBW, is practically identical. It follows from the fact that all experimental data of corresponding kinetic diagrams of fatigue failure, taking into account the zone of their dispersion, practically coincide, forming a uniform zone of dispersion.

Thus, the conducted complex of investigations has shown that weldability and service properties of the titanium alloy VT6 performed by different methods (VAR or EBM), and also its welded joints, are practically coincident. The obtained results confirm that use of the advanced EBM technology for making titanium alloys has good prospects.

CONCLUSIONS

1. For obtaining of fine-grained homogeneous structure in the deformed high-strength titanium alloy (VT6) melted by EBM, it is necessary to carry out rolling in β-domain untill deformation of 55–60 % and 40–45 % in diphasic (α + β)-domain.

2. For obtaining of optimum equivalent parametres of joints in welding of the alloys obtained by EBM, it is necessary to increase welding current by 10–12 % in comparison with welding of alloys obtained by VAR method.

3. It is shown that irrespective of the method of melting of alloy VT6, strength of welded joints performed by EBW is at the level of BM, while impact toughness of weld and HAZ metals correspond to 80–85 % of that of BM. Similar characteristics are provided by AAW using welding wire SP15sv.

4. It is established that irrespective of the method of melting of alloy VT6, fructure toughness K_{1c} is at the same level, while fructure toughness of welds perform by EBW, in both cases is higher than that of BM.

5. Titanium alloys obtained by EBM, and their welded joints fully meet the requirements of standards and ASTM, and compare well with alloys melted by VAR, and corresponding welded joints.

6. It is established that cyclic crack resistance of BM of titanium alloy VT6 obtained by various melting methods (VAR, EBM), and also weld metal of butt joints performed by EBW, is practically identical.

7. Alloys melted by EBM, can be recommended for application in various branches of national economy at manufacturing of vital welded structures.

1. Mitchel, A. (1987) The production of high-quality materials by special process. *J. Vac. Technol.*, **4**, 2672–2677.
2. Seagle, S.R. (1990) New titanium developments in products, processes and applications in the USA. In: *Proc. of Int. Conf. on Titanium* (Dayton, USA, 1990), Vol. 1, 66–73.
3. Poulsen, E., Chinnis, W., Mede, M. (1999) Status of titanium cold hearth melting. In: *Proc. of 9th World Conf. on Titanium* (St.-Petersburg, June 7–11, 1999), 1541–1544.
4. Paton, B.E., Trigub, N.P., Akhonin, S.V. et al. (1996) Some tendencies of development of metallurgical refining of titanium. *Problemy Spets. Elektrometallurgii*, **1**, 25–31.
5. Paton, B.E., Trigub, N.P., Akhonin, S.V. et al. (2006) *Electron beam melting of titanium*. Kiev: Naukova Dumka.
6. Borisova, E.A., Bochvar, G.A., Brun, M.Ya. et al. (1980) *Metallography of titanium alloys*. Moscow: Metallurgiya.
7. Paton, B.E., Trigub, N.P., Kozlitin, D.A. et al. (1997) *Electron beam melting*. Kiev: Naukova Dumka.
8. Boek, D. (1980) *Principles of fracture mechanics*. Moscow: Vysshaya Shkola.
9. Troshchenko, V.G., Pokrovsky, V.V., Prokopenko, D.V. (1987) *Crack resistance of metals under cyclic loading*. Kiev: Naukova Dumka.

HEATING BY PLASMA ARC OF FLAT ELECTRODE AXIALLY FED INTO PLASMATRON

V.V. CHIGAREV, K.A. KONDRASHOV, N.A. MAKARENKO and **N.A. GRANOVSKY**
Priazovsky State Technical University, Mariupol, Ukraine

The paper presents the data on heating of a flat electrode (flattened flux-cored wire) inside the plasmatron by the plasma arcs during plasma surfacing by the combined method. It is established that application of the pulsed mode of plasma arc running, in which the flat electrode periodically becomes the cathode relative to the plasmatron nonconsumable electrode, improves its heating efficiency, while the proneness of the process to shunting of plasma arcs by the flat electrode is enhanced.

Keywords: *plasma surfacing, combined method, plasma arc, heat input into flat electrode, pulsed mode, double arc formation, shunting of plasma arc, active cathodic spots of arc*

Plasma surfacing by the combined method, having a number of advantages before other methods of surfacing (possibility of visual supervision of the process; high efficiency of metal deposition [1]; small depth of penetration of the base metal, allowing obtaining metal of preset chemical composition already in the first deposited layer and, in so doing, save expensive alloy steels, alloys and nonferrous metals; rather low heat input [2]) causes insignificant thermal strains in the surfaced workpiece, reduces the risk of structural changes in the base metal and reduces residual stresses therein.

The carried out investigations [3] have allowed developing a series of flux-cored wires [4] for application in plasma surfacing by the combined method. At the same time, the process of plasma surfacing by the combined method with application of flattened flux-cored wire as a consumable electrode, has not been sufficiently studied by now, which prevents its introduction despite of a number of its advantages: higher efficiency; possibility of regulation of geometrical dimensions of the deposited bead and penetration of the base metal due to the change in placement of planes of flattened flux-cored wire with respect to the surfacing rate vector; possibility of surfacing aluminium and its alloys workpieces, for which manufacturing of flux-cored wire having a soft fragile aluminium shell, is problematic.

One of the major research problems in this direction is studying of processes of heating [5] of flattened flux-cored wire with heat of plasma arc. Heating by plasma arc of the shell of flattened flux-cored wire changes its resistivity, which increases its emission of heat due to passing current of its own arc. In turn, increasing temperature of the shell of flattened flux-cored wire increases rate of its melting, changes mass transfer character, influences the processes occurring in the core of flattened flux-cored wire.

Establishment of the mechanisms of heating of flat consumable electrode (flattened flux-cored wire) by plasma arc using combined method of plasma surfacing (with consumable and nonconsumable electrodes), was the purpose of the research conducted at the Chair of Metallurgy and Technology of Welding Engineering of Priazovsky State Technical University.

In [6], a method of estimation of heating of consumable electrode by the heat of plasma arc in consumable electrode plasma-arc welding is presented, however this method is suitable only for the estimational characterization of the heating process, and is rather inexact, which the authors admit.

The method of estimation of heating of consumable electrode suggested before [7], allows estimation of heating at various sections of running plasma arc: before the nozzle, inside plasma-shaping nozzle channel, at the section of visible extension from the plasmatron, and also definion the beginning of the process of shunting of plasma arc with consumable electrode. Despite sufficient accuracy of this method, it is suitable only for the case of application of circular-section consumable electrode, i.e. of a wire. Application as consumable electrode of flattened flux-cored wire having close to rectangular section, changes conditions of plasma arc running [8], character of electrode melting, which makes the method of [7] unsuitable for the research of heating of flat electrode by plasma arc heat.

It should be noted that application for surfacing of pulse modes of consumable electrode arc running, wherein it periodically becomes the cathode in relation to nonconsumable electrodes of the plasmatron [8], leads to occurrence on the surface of consumable electrode of additional heating sources: cathodic spots of arcs «consumable electrode–nonconsumable electrodes».

In this connection, there appeared a necessity of developing a new technique of investigation of heating of flat consumable electrode in plasma surfacing by the combined method, considering the factors listed above and allowing studying the process of heating of flat consumable electrode in plasma surfacing by the combined method.

Research was conducted on the installation which function diagram is presented in Figure 1, using the method of measuring the quantity of heat getting into the flat specimen-simulator having O-like 3 × 6 mm section, at its heating, in various sections of plasma arc. The simulator could be translated in axial direction (in Figure 1 it is shown by arrow).

Flattened flux-cored wire is heated up by plasma arc heat in the following sections: before the nozzle («nonconsumable electrodes–nozzle») $l_{n.e.n}$; in plasma-shaping nozzle channel of plasmatron $l_{n.ch}$, and in the section of visible extension (outside plasmatron) $l_{v.e}$.

Heat power released in the simulator was defined by the formula

$$P = C(T_2 - T_1)q, \quad (1)$$

where P is the heat power; C is the specific heat capacity of water; q is the per second water flow rate.

Measurements were conducted by consecutive immersing of the simulator into various zones of the arc. Thus, first was defined heat power in section $l_{n.e.n}$, then the simulator was immersed into the channel of plasma-shaping nozzle (*PN*), and again heat power inputted into the simulator was defined, then was calculated heat power inputted into the simulator in *PN* channel by the formula

$$P_{n.ch} = P_{01} - P_{n.e.c}, \quad (2)$$

where $P_{n.ch}$ is the heat power inputted into the simulator in *PN* channel $l_{n.ch}$; P_{01} is the total heat power in sections $l_{n.e.n}$ and $l_{n.ch}$; $P_{n.e.n}$ is the measured (in the previous experiment) power inputted into the simulator in pre-nozzle section $l_{n.e.n}$.

Similarly was calculated the heat power inputted into the simulator in the section of visible extension:

$$P_{v.e} = P_{02} - P_{01}, \quad (3)$$

where $P_{v.e}$ is the power inputted into the simulator in the section of visible extension; P_{02} is total heat power inputted into the simulator in the presence of a visible extension.

Research conducted both in the continuous, and in the pulsed mode of plasma arcs running. In pulsed mode the simulator through a load rheostat was periodically connected to the workpiece. Thus at each pulse it became the cathode in relation to nonconsumable plasmatron electrodes, and on its lateral surface appeared active cathodic spots [8].

The pulsed mode was provided by means of periodically rendered conducting power transistor *VT1*. Duration of current pulse was 3 ms, pause — 7 ms, pulse repetition frequency was 100 Hz.

As is seen in Figure 2, current pulse has close to rectangular shape. Leading edge of the pulse is more flat than the falling one, which is due to inductance of welding circuits and power source. The rectangular shape of the current pulse is indicative of fast spontaneous start of arcs «nonconsumable electrodes of plasmatron–consumable electrode» and of stability of

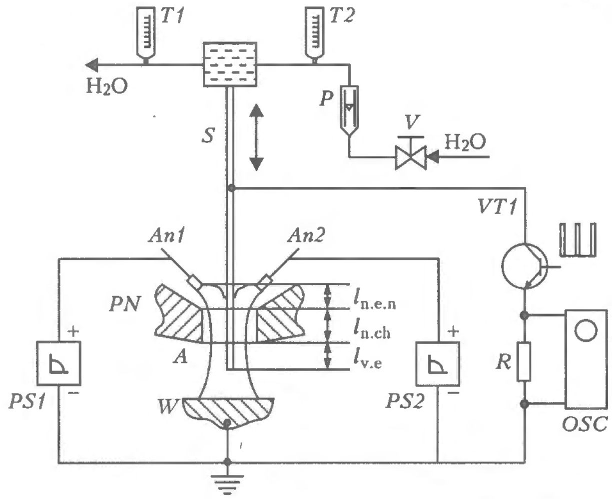

Figure 1. Schematic of the installation for definition of consumable electrode heating by heat of plasma arcs: *T1*, *T2* — thermometers; *P* — rotameter; *V* — valve; *W* — workpiece; *A* — plasma arc; *An1*, *An2* — plasmatron anodes; *PS1*, *PS2* — plasma arcs power sources; *R* — resistor; *OSC* — oscillograph

the process of running of these arcs, which allows drawing a conclusion on constancy of thermal energy inputted into the flat consumable electrode by cathodic spots of arcs during the entire time of current pulse passage.

Studied was also the process of shunting of plasma arc by the flat copper specimen. It was established that shunting process in the continuous mode began at a visible extension more often than in the pulsed mode. Shunting process was accompanied by increased heat input into the specimen *S* and fusing of specimen end face. The latter is more intensive at a pulsed mode, which testifies that imposition of pulses forms active cathodic zones on the surface of the specimen, which continue to exist also after the pulse termination, thus facilitating the process of plasma arcs shunting.

For the pre-nozzle section, a dependence presented in Figure 3, *a*, has been obtained from which it follows that in the pulsed mode efficiency of heating of the flat electrode is higher than in the continuous mode (curves *2* and *1*, accordingly), which is due to periodic occurrence on the surface of the electrode of active cathodic spots.

By and large increase of the current of plasma arcs causes augmentation of heat flow into the flattened flux-cored wire in the pre-nozzle section of its heating.

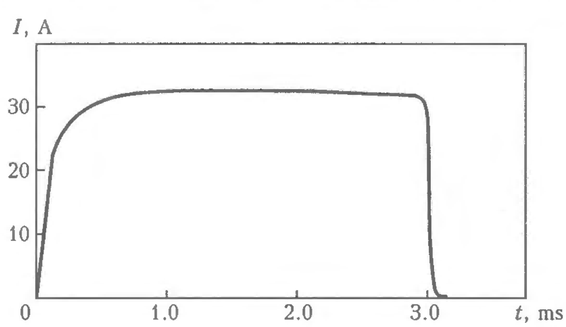

Figure 2. Shape of the current pulse passing through resistor *R*: $I_{pl1} = I_{pl2}$ = 90 A; diameter of plasma-shaping nozzle d_n = 10 mm; Q_{Ar} = 5.2 l/min; distance «nozzle–workpiece» is 14 mm; specimen extension outside the nozzle is 3 mm

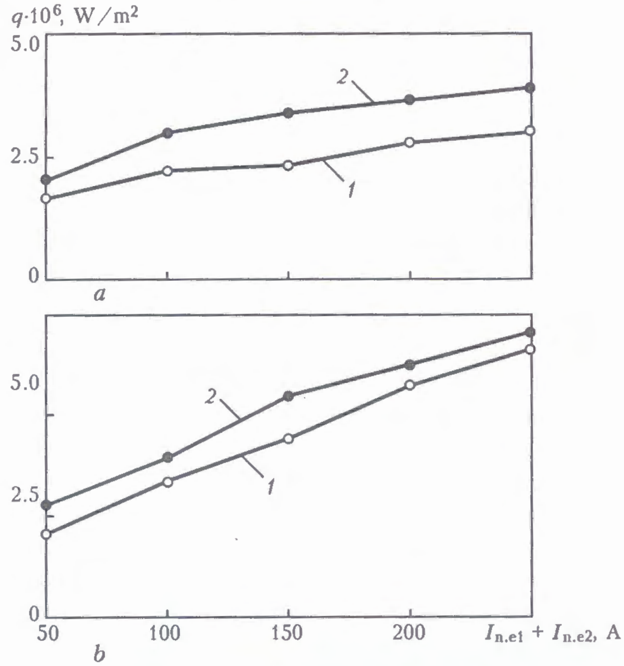

Figure 3. Dependence of heat flow into the simulator in section «nonconsumable electrodes–nozzle» (*a*) and plasma-shaping nozzle channel (*b*) on total current of nonconsumable electrodes at continuous (*1*) and pulsed (*2*) mode: d_n = 10 mm; Q_{Ar} = 5.6 l/min; $l_{n.e.n}$ = 5 mm; $l_{n.ch}$ = 4 mm

These data are consistent with those described in [7], typical for round-section consumable electrode. It should be noted that efficiency of heating of flattened flux-cored wire even in the continuous mode has appeared to be a little higher than efficiency of heating of the wire investigated in [7], which is due to asymmetry of flattened flux-cored wire and disturbance of laminarity of the gas flow at its edges (such a disturbance of flow laminarity leads to more intensive heat exchange between the plasma arc and the flattened flux-cored wire [9]).

Dependences of heat flows into the flattened flux-cored wire in «nozzle channel» section of also agree with the data of [7] (Figure 3, *b*).

Again, as for pre-nozzle section, efficiency of heating of the flat specimen appeared to be higher than for the round-section specimen. Increase in heat flow into the specimen in the section of the nozzle channel at increase of plasma arcs current is greater than in pre-nozzle section, which is due to the arc contraction in the plasmatron nozzle channel.

In the pulsed mode of arc running, heat input into the flattened flux-cored wire in section $l_{n.ch}$, appears to be higher than in the continuous one, which can not result from its heating by active cathodic spots during the pulses, as this heating has already been taken into consideration in the research of heating of flattened flux-cored wire in the pre-nozzle section.

Inspection of the specimen-simulator after the tests has shown presence of traces of erosion on its end face, and also local fusions of the end face, which is indicative of arc occurrence between the specimen-simulator and the workpiece. Thus, shunting of plasma arc takes place in the pulsed mode even in the case of absence of extension of the specimen-simulator out of the plasmatron.

The process of arc shunting is accompanied by double arc formation. In this case the probability of occurrence of double arc is described by the Steenbeck minimum principle, which for the given case is of the form

$$U_{n.e.n} + U_{n.ch} > U_{a.c} + U_{c.c} + IR_m, \qquad (4)$$

where $U_{n.e.n}$ is the voltage in arc section $l_{n.e.n}$, V; $U_{n.ch}$ is the voltage in the arc section inside the channel of plasma-shaping nozzle, V; I is the current in the simulator, A; $U_{a.c}$ is the anodic voltage drop on the copper simulator, V; $U_{c.c}$ is the cathodic voltage drop on copper simulator, V.

Considering, that $R_m \to 0$, it is possible to consider that

$$U_{n.e.n} + U_{n.ch} > U_{a.c} + U_{c.c}. \qquad (5)$$

It is known [10, 11] that for copper $U_c + U_a$ = = 22–26 V.

Performing measurements of voltages $U_{n.e.n}$ and $U_{n.ch}$ is rather difficult, as these arc sections are inside the plasmatron. In this connection were measured voltages between nonconsumable electrodes and a probe located at the exit of plasma arc from plasmatron nozzle. As the probe was used a tungsten wire 0.5 mm in diameter, continuously fed into the plasma arc. The voltage was followed with the cathodic voltmeter. Results of measurements have shown that voltage between anodes of plasmatron and the probe was 6–9 V. It is necessary to subtract from this voltage 2–3 V of near-anode voltage drop on nonconsumable electrode of the plasmatron. Thus, according to the Steenbeck minimum principle, occurrence double arc formation on the copper specimen-simulator is impossible.

At the same time, it is known [10, 12] that in combined plasma processes, between the workpiece and the consumable electrode a weak current arc at electrically neutral consumable electrode is observed. Occurrence of this arc is, obviously, connected with a spontaneous discharge of the charge carriers in the plasma arc onto the surface of consumable electrode, owing to this between the consumable electrode and the workpiece there appears an electrical potential leading to occurrence of weak current arc.

It should be noted that occurrence of such an arc is essentially facilitated by that it runs inside the plasma arc having the temperature 2–3 times higher than the arc of the consumable electrode [12], i.e. it exists in conditions of outer forced ionization. Thus with increase of the surface area of the consumable electrode, the contact area of the consumable electrode with plasma arc will grow, that will lead to increased quantity of charge carriers discharging on the surface of the consumable electrode, and will cause increase of the current of the arc between the workpiece and the elctrically neutral consumable electrode. It is should be underlined that at such mechanism of consumable electrode arc running, only one active spot on electrode end face will be formed, the role of the second spot will be performed by the surface of the electrode plunged into the plasma arc. Flattened flux-cored wire (unlike round-section electrode) has a much greater surface in relation to the cross-section area; in this connection the effects described above in its application as a consumable electrode manifest themselves much more strongly, which also gives rise to higher efficiency of heating of flat-section specimen-simulator.

However, the specified factors are effective both at continuous, and at pulsed modes of plasma arc running, at the same time, efficiency of heating of the flat simulator in plasma-shaping section of plasmatron nozzle channel at the pulsed mode appears higher, and its end face bears traces of erosion and fusions. Noted features allow drawing a conclusion that active cathodic spots on the surface of the specimen being in the column of the plasma arc continue to exist also after the pulse termination, owing to what the current of the weak current arc increases. Hence, increases also heat input into the simulator. Current pulses passing through the simulator play on its surface the role of active cathodic spots initiators, i.e. they play the role of starting pulses.

It should be noted that only part of plasma arc current is diverted into the simulator, thus double arc formation does not occur to the full, the plasma arc runs steadily between the plasmatron anodes and the workpiece, i.e. only partial shunting of plasma arc is observed.

It is known [10, 11] that near-cathode voltage drop is influenced by a considerable number of factors, including gas composition, anode and cathode materials, presence in the arc of metal vapours.

Considering features of combined plasma arc surfacing (immersing of consumable electrode into the column of plasma arc being a powerful source of external ionization), it is possible to assume that in these conditions near-cathode voltage drop on the copper simulator will appear much lower than reported in [10, 11], characterising the process of argon-arc welding. In this case the processes of arc shunting will proceed more intensively.

Heat input into the copper simulator in the presence of visible (outside plasmatron) extension was studied. Dependence of heat input into the simulator on total current of plasmatron nonconsumable electrodes is presented in Figure 4. As is clear from the Figure, intensive shunting of plasma arc at continuous process and an extension of 8 mm, begins at currents exceeding 120 A (it corresponds to fast increase in heat flow into the simulator). In application of pulsed mode, shunting processes intensively increase at currents of plasma arc of 105 A, thus with current increase, heat input into the simulator increases much faster than in application of the continuous mode. It should be noted that heat flow into the flat simulator in the continuous mode appears greater than into the round-section electrode, and arc shunting begins at smaller currents of plasma arc than as it is described in [7].

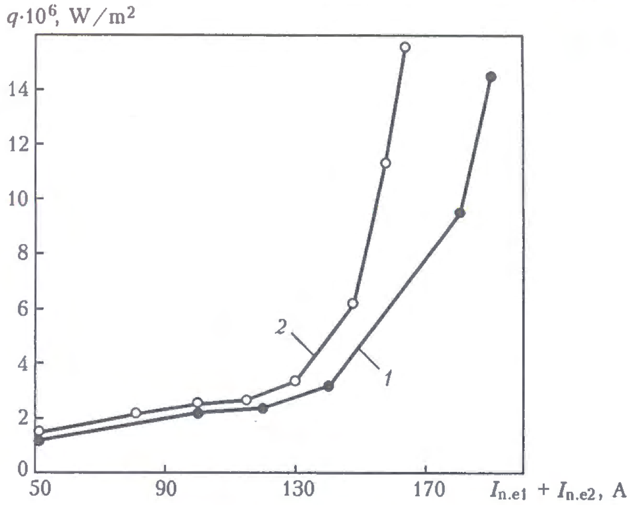

Figure 4. Dependence of heat flow into the simulator in section «nonconsumable electrodes–nozzle» on total current of nonconsumable electrodes at continuous (*1*) and pulsed (*2*) modes: d_n = = 10 mm; Q_{Ar} = 6.2 l/min; $l_{n.e.n}$ = 5 mm; $l_{n.ch}$ = 4 mm; $l_{v.e}$ = 4 mm

The obtained data confirm the assumption stated above of the mechanism of plasma arc shunting in combined plasma surfacing with application as a consumable electrode of flattened flux-cored wire, and also on the role of pulsed mode of plasma arc running in shunting processes.

Influence of the plasma arc current and visible (outside plasmatron) simulator extension on the process of plasma arc shunting (Figure 5) was studied.

As a criterion of shunting of plasma arc, two values were assumed: the first one is the beginning of intensive increase in heat flow into the simulator (Figure 5, bottom curves) and sharp increase in heat flow into the simulator (top curves). Points of bends shown in Figure 4 correspond to these curves.

From Figure 5 it follows that at the modes, corresponding to the points located below the shaded

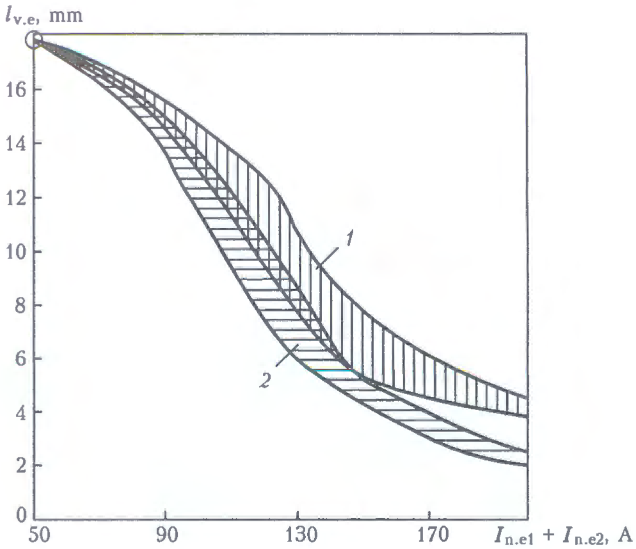

Figure 5. Dependence of length of visible extension of the simulator at which shunting of plasma arc is observed, on total current of nonconsumable electrodes at continuous (*1*) and pulsed (*2*) modes

zones, intensive shunting does not occur. Increasing the plasma arc current produces directly proportional increase of the heat flow into the simulator in the zone located between the curves. Arc shunting quickly increases, also heat flow into the simulator sharply increases. The points of the modes, located above the shaded areas, correspond to unstable modes of surfacing, at which process of surfacing can be disturbed, namely double arc formation is probable.

As is clear from Figure 5, with increase in plasma arc current, the admissible visible extension of the consumable electrode decreases, which should be taken into account in working out technological processes of combined plasma surfacing with application of flattened flux-cored wire. In case of application of pulsed mode, intensive shunting of plasma arc begins at smaller values of the visible extension, which confirms the role of current pulses getting into the simulator as initiating the shunting process.

Pulsed mode of plasma arc running should be recognized as less resistant against double arc formation. Hence, parametres of this mode should be maintained more accurately in conduction of surfacing works. In practical application of surfacing, critical parametres are the current of plasma arc and value of visible outside plasmatron extension of flattened flux-cored wire.

CONCLUSIONS

1. Heating of flat consumable electrode with plasma arc heat is higher than heating of round-section electrode. Thus processes of plasma arc shunting develop more intensively at application of flat consumable electrode. The pulsed mode of plasma arcs running increases heating of the flat electrode and facilitates the beginning of the shunting process.

2. Pulses of the current of arcs «nonconsumable electrodes–flat consumable electrode» initiate the process of the beginning of plasma arcs shunting. Thus from the end face of the flat electrode emerges a low-power arc «flat electrode–workpiece», which fuses the end face of the flat electrode. Its occurrence is established even at the presence of the flat electrode end face inside the plasmatron nozzle.

3. Shunting by the flat electrode of the plasma arc at pulsed mode of its running begins in conditions insufficient for this process occurrence (according to the Steenbeck minimum principle).

1. Sidorov, A.I. (1987) *Recovery of machine parts by spraying and surfacing*. Moscow: Mashinostroenie.
2. Kornienko, A.N., Makarenko, N.A., Kondrashov, K.A. (2000) Study of heating efficiency of parts in plasma-MIG surfacing. In: *Proc. of 5th Int. Sci.-Techn. Conf. on Problems of Welding, Metallurgy and Related Technologies*. Tbilisi: GWA, 104–108.
3. Chigarev, V.V., Makarenko, N.A., Kondrashov, K.A. et al. (2001) Features of electrode wire melting in surfacing by plasma-MIG process. *The Paton Welding J.*, **8**, 10–12.
4. Chigarev, V.V., Makarenko, N.A., Kondrashov, K.A. (2001) Features of flux-cored wire melting in plasma-MIG process. In: *Proc. of 2nd Int. Conf. on Welding Consumables of CIS countries «Arc Welding. Materials and Quality at the Threshold of the 21st Century»* (Oryol, RF), 73.
5. Metcalf, J.C., Quigley, M.B. (1975) Heat transfer in plasma-arc welding. *Welding J.*, **3**, 99–103.
6. Akulov, A.I., Bozhenko, B.L., Ronsky, V.L. (1983) Heating of electrode metal in plasma-argon-arc-MIG welding. *Svarochnoe Proizvodstvo*, **2**, 8–10.
7. Makarenko, N.A. (1999) *Development of plasma process with axial feed of flux-cored wire for surfacing of moulds*: Syn. of Thesis for Cand. of Techn. Sci. Degree. Mariupol.
8. Chigarev, V.V., Kondrashov, K.A., Granovsky, N.A. (2006) Improvement of quality of deposited metal in plasma-MIG cladding of aluminium alloys. *The Paton Welding J.*, **6**, 40–42.
9. Malakhovsky, V.A. (1987) *Plasma welding*. Moscow: Vysshaya Shkola.
10. Lenivkin, V.A., Dyurgerov, N.G., Sagirov, Kh.N. (1989) *Technological properties of shielded-gas welding arc*. Moscow: Mashinostroenie.
11. Leskov, G.I. (1970) *Electric welding arc*. Moscow: Mashinostroenie.
12. Ton, H. (1975) Physical properties of the plasma-MIG welding arc. *Appl. Phys.*, **8**, 922–938.

AUTOMATIC SINGLE-PASS ELECTRIC ARC WELDING OF STEEL CURRENT LEADS OF ELECTROLYZERS FOR ALUMINIUM PRODUCTION

G.V. KUZMENKO[1], V.G. KUZMENKO[1], N.V. BOLOTOV[2] and Yu.V. SHEMET[3]
[1]E.O. Paton Electric Welding Institute, NASU, Kiev, Ukraine
[2]OJSC Shelekhov Specialized Enterprise «Repair of Buildings and Structures», Shelekhov, Russian Federation
[3]OJSC Siberian R&D Institute for Aluminium and Electrode Industry «SibVAMI», Irkutsk, Russian Federation

Technology of automatic arc welding of plate–blooms joint in OA-300M2 electrolyzers of Irkutsk Aluminium Plant is described. The new technology is based on the process of embedded electrode arc welding. The developed technology and equipment can be applied for welding large cross-section parts, also in site conditions.

Keywords: *automatic electric arc welding, movable embedded electrode, flux-cored wire, penetration, electrolysis production, electrolyzer bussing, cathode core*

Development of the technology of aluminium production by electrolytic method is accompanied by growth of current loading of electrolyzers. In recent years were designed and constructed electrolyzers for currents 300 kA and higher. Stringent requirements were thus specified to the system of current supply of electrolyzers, which should provide minimum losses of electricity in the course of its long (five and more years) operation [1, 2]. As a rule, at designing current lead assemblies preference is given to welded joints as being most reliable and providing minimum electric resistance. Considering the necessity of conducting high currents, elements of current leads to electrolyzers for aluminium production have rather large cross-sections, which poses certain problems by the choice of the welding method. Besides, joints are most often located in hard-to-reach places, which complicates welding works even more. Until recently specialized welding technology and equipment providing high-efficiency welding of current leads was unavailable.

Figure 1. Shop No. 9 of Irkutsk Aluminium Plant under construction

Since June 2005, at Irkutsk Aluminium Plant of OJSC SUAL (IrkAZ, town of Shelekhov, Irkutsk oblast), is under way construction of the fifth series of electrolysis production, namely two buildings containing 100 electrolyzers with the working current exceeding 300 kA (Figure 1). According to the design, on each electrolyzer at its installation, it is necessary to weld 80 joints having cross-section 80 × 220 mm (40 on each side). These joints connect steel (St3) cathodic cores (blooms) with steel-aluminium intermediate bosses (plates). The latter are steel cast parts (steel 15L) with aluminium flexible chute welded to it by means of resistance butt welding. In total at installation of electrolyzers in both buildings it is necessary to weld 16,000 joints. Welding works to perform said joints have to be carried out in constrained conditions (Figure 2). Dimensions of the working zone (between frame elements of cathodic casing) are only 550 mm in width, 1200 mm in height and 600 mm in depth. Thus the blooms are installed between frame elements in pairs, the distance between them being 330 mm.

At the stage of studying this matter, experts of IrkAZ, SibVAMI (head design organization) and Shelekhov Specialized Enterprise «Repair of buildings and structures» (ShSP RZS), the general contractor

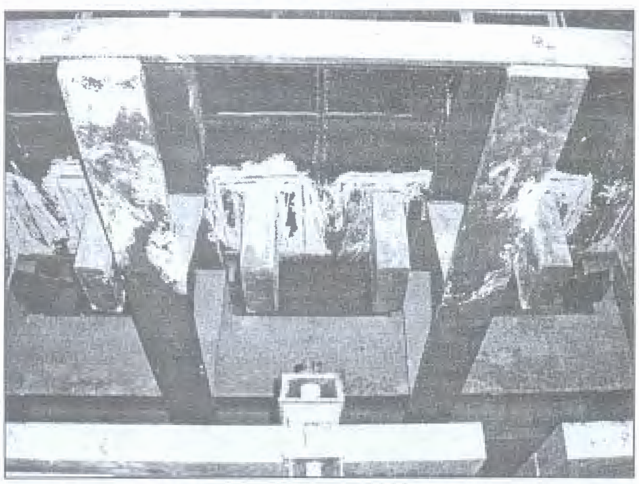

Figure 2. Cathodic cores (blooms) of electrolyzer

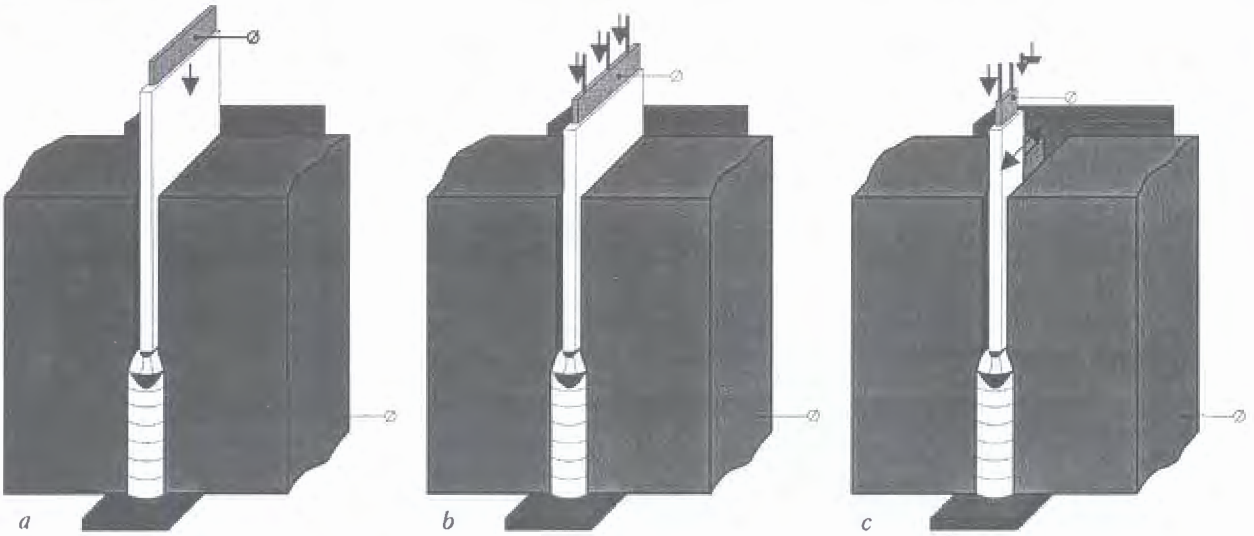

Figure 3. Scheme of single-pass electric arc welding using an embedded large-section electrode (*a*), with stationary consumable nozzle (*b*) and oscillating consumable nozzle (*c*)

for construction of the fifth series electrolysis production of IrkAZ, considered some variants of welding of said joints: semi-automatic electric arc, electroslag, thermit welding and so forth. However neither of them conforms to the specified requirements to quality and productivity.

In recent years, at the E.O. Paton Electric Welding Institute, NASU, Kiev, Ukraine, was developed a new high-efficiency method of electric arc welding using the embedded electrode [3–5] intended for welding of joints of compact sections in narrow gap. The method can be implemented in two variants.

The first one is welding by large cross-section electrode (Figure 3, *a*) provided for the use of the covered plate electrode with the core 4–6 mm thick and having the width equal to the thickness of welded parts. In the course of welding, the electrode is fed in as it is consumed. According to the second variant the embedded electrode in the form of consumable nozzle is used, while additional filler metal in the form of wires is fed through the channels in the electrode core. Thus the electrode can be both stationary (Figure 3, *b*), and moved parallel to edges being welded in the course of welding (Figure 3, *c*).

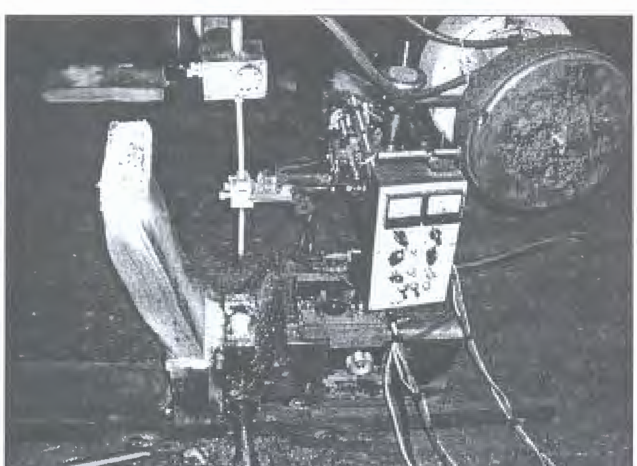

Figure 4. Full-size model of plate–blooms assembly

This method has been proposed to experts of IrkAZ, SibVAMI and ShSP RZS as an alternative for connection of the plate with the bloom in electrolyzers OA-300M2 during construction of the fifth series of electrolysis production at IrkAZ.

At the preliminary stage the agreement on carrying out of demonstration of the method of welding with embedded electrode in one of the operating shops of the enterprise was reached with management of SUAL IrkAZ. To this end, a group of experts of the E.O. Paton Electric Welding Institute with necessary welding equipment and materials was sent to Shelekhov. Using experimental portable welding automatic machine, full-scale models of blooms and plates were welded (Figure 4). In Figure 5 is shown macrosection of the welded joint. It should be noted that welding was carried out in conditions of magnetic field influence, in immediate proximity with current supplying buses conducting the current up to 56 kA.

Figure 5. Macrosection of welded joint (material to be welded is steel St3 80 mm thick)

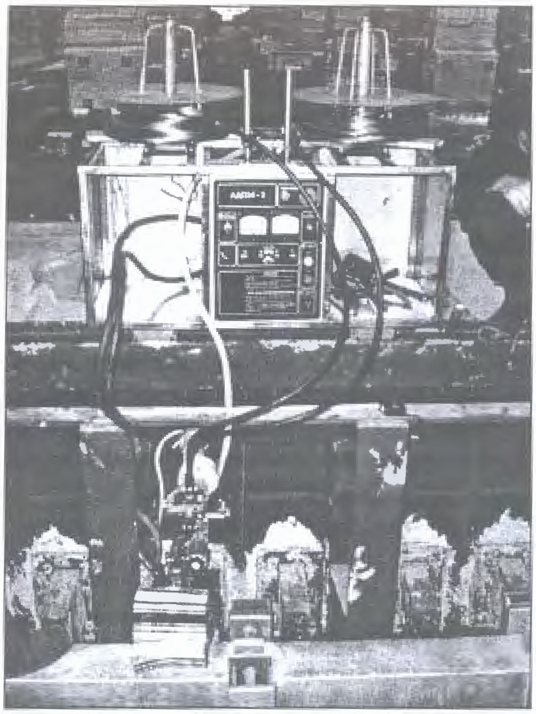

Figure 6. Machine ADPM-2 for welding of plate–blooms joint at electrolyzer installation

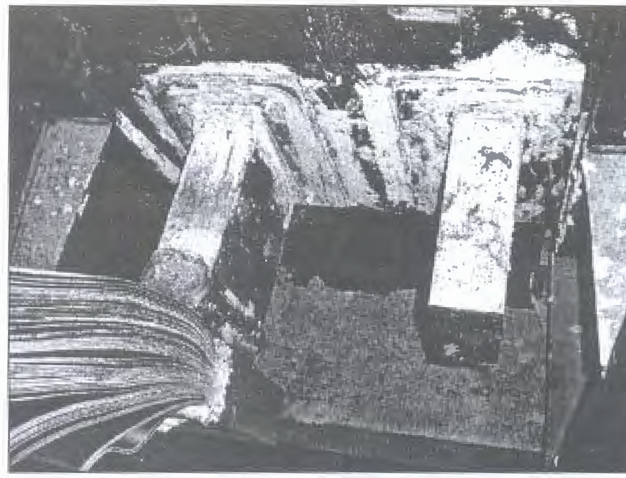

Figure 7. Plate–blooms joint before (*on the right*) and after welding (*on the left*)

Positive results of demonstration of the method of welding with embedded electrode have convinced management of SUAL IrkAZ of the possibility of creation on its basis of industrial technology, therefore at the beginning of 2006 between SUAL IrkAZ, ShSP RZS and PWI, was concluded the contract on the development of technology, equipment and consumable materials for performance of plate–blooms welded joints.

At the first stage of realization of the project were conducted experiments which purpose was the choice of the scheme of plate–blooms joint welding, most suitable in concrete production conditions. It was found out that welding by large cross-section electrode, although enabled obtaining in laboratory conditions of welded joints of satisfactory quality, did not provide sufficient resistance of welds to porosity and required application of special electrodes which mass production is not organized yet.

Welding trials using stationary consumable nozzle have shown that at the given thickness of welded parts (80 mm), for provision of uniform penetration of edges, it is necessary to feed not less than four filler wires, which essentially complicated the equipment operation and made it of little use in assembling site conditions.

As a result, the scheme of welding by two flux-cored self-shielded wires fed through two consumable tubular electrodes-nozzles making reciprocating movements (oscillations) in the gap between welded edges for their full penetration has been chosen. Advantages of the given scheme of welding are the following:

• possibility of active influence on metallurgical processes in the weld pool by means of introduction of alloying additives and deoxidizers into the core of the flux-cored wire;

• relative simplicity and the compactness of the equipment, facilitating its use in constrained assembling site conditions;

• universality, i.e. possibility of welding of parts 10–150 mm thick by changing the quantity of used electrodes (one or two), welding modes (from 250 to 900 A) and amplitude of oscillations;

• possibility of manufacturing of electrodes by industrial methods on extruding machines, which is especially important at the organization of their mass production.

In the course of performance of works under the contract, experts of the E.O. Paton Electric Welding Institute developed a specialized equipment (ADPM-2) and consumables (wire PP ANPM1), and also tubular embedded electrodes (ANPM-8), enabling to provide required productivity and quality of welded joints.

Welding machine ADPM-2 (Figure 6) complete with attachments for assemblage of the joint and formation of the weld features compactness, which is especially important in assembling site conditions. The machine has two modifications: for welding right and left blooms. As a source of welding current was applied welding rectifier VDU-1250 of SELMA company.

Technical characteristics of welding machine ADPM-2

Welding current regulation range, A	250–900
Arc voltage, V	no more than 40
Diameter of electrode wire, mm	2.4
Quantity of electrode wires, pcs	2
Wire feed rate, m/h	50–300
Speed of oscillations, m/h	5–15
Amplitude of oscillations, mm	0–70
Weight, kg:	
welding head	12.8
conductor	10.5
control box (with empty coils for wire)	50

For performance of works on the fifth series electrolysis production of IrkAZ were manufactured and supplied to the customer in total ten machines ADPM-2 (including two trial ones) and a set of consumable materials, training of welding machine operators was carried out. With participation of experts of the E.O. Paton Electric Welding Institute, at the end of 2006–beginning of 2007, directly at construction sites of shops Nos. 9 and 10, more than a thousand plate–blooms joints were welded (Figure 7), including at low temperatures (as low as –25 °C). Then the team of welders of ShSP RZS, having mastered the technology and the equipment in full, has started their industrial use. By present time more than 10,000 joints have been welded.

Results of industrial application of the method of welding using an embedded electrode, corresponding welding equipment and consumables have shown the following:

• machine time of welding of a joint having a section 80 × 220 mm at a nominal gap of 16–18 mm and welding current of 600–800 A, is 10–12 min, therefore productivity of up to 15 joints on one machine in a shift, taking into account labour hours for preparation of joints and installation of fixtures was reached;

• the developed equipment and attachments feature sufficient reliability, and, thanks to the rational design, can be easily repaired in shop conditions;

• operation of the equipment does not require highly skilled personnel, which considerably reduces time of mastering the technology;

• quality of welded joints meets the requirements on electric conductivity.

As a whole, it is possible to conclude that electric arc welding using embedded electrodes has received further development, which enabled to create on its basis a highly effective industrial technology which can be recommended for use at other aluminium plants at capital construction and introduction of powerful electrolyzers, repair of cathodic devices in operating electrolysis shops, where still, up till now, are used demountable (bolt-connected) current leads.

1. Vetyukov, M.M., Tsyplakov, A.M., Shkolnikov, S.I. (1987) *Electrometallurgy of aluminium and magnesium*. Moscow: Metallurgiya.
2. (1971) *Reference book for metal-makers of non-ferrous metallurgy*. Ed. by Yu.V. Bajmakov, Ya.E. Kantorovich. Moscow: Metallurgiya.
3. Kuzmenko, V.G., Kuzmenko, G.V. *Consumable electrode welding process and electrode for its realization*. Pat. 68361 Ukraine. Int. Cl. B 23 K 9/2. Publ. 26.12.2004.
4. Kuzmenko, V.G., Kuzmenko, G.V. *Consumable electrode welding process and electrode for its realization*. Pat. 2219021 RF. Int. Cl. B 23 K 9.14, 35/36. Publ. 29.12.2003.
5. Kuzmenko, V.G., Kuzmenko, G.V., Galinich, V.I. et al. (2006) Single-pass arc welding of thick metal using embedded electrode. *The Paton Welding J.*, **6**, 35–39.

AUTOMATIC ARGON-ARC WELDING FOR SEALING CARTRIDGES WITH WASTE NUCLEAR FUEL

K.A. YUSHCHENKO, G.G. MONKO, D.V. KOVALENKO and **V.A. PESTOV**
E.O. Paton Electric Welding Institute, NASU, Kiev, Ukraine

Technology of automatic argon-arc welding and equipment for sealing P-89 cartridges from steel 08Kh18N10T for Chernobyl NPP nuclear waste disposal have been developed. Development of the technology of automatic argon-arc welding of the cap to the cartridge and technology of test welding of the nozzle tap for helium pumping into the cartridge allowed optimization of technical requirements to welds for performance of welding operations in site.

Keywords: *automatic argon-arc welding, resistance welding, special installation, technique and technology of welding, cartridge P-89, stainless steel, waste nuclear fuel*

Now for storage of waste nuclear fuel (WNF) at GSP Chernobyl Nuclear Power Plant (ChNPP) are used cases with 196 cartridges P-89 (Figure 1). In the future the burial place for cases is provided in the now constructed in the territory of GSP ChNPP storehouse of waste nuclear fuel (SWNF-2).

The cartridge for storage of WNF was designed by Company «Framatome ANP» (France) and produced at OJSC «M.V. Frunze SNPO» (Sumy, Ukraine).

The technology of welding for sealing of cartridges was optimized on the Framatome automated specialized installation in welding (fade-out weld) the cap to the cartridge after loading of WNF with preset non-penetration degree. After pumping helium into the cartridge through the union tap, resistance welding is carried out, which is not recommended for application at NPP by the rules and norms effective in atomic engineering of Ukraine.

In this conection it was necessary to execute the following amount of works:

- develop technology of welding and equipment for welding the cap to the cartridge;
- choose the method of welding and its optimum modes;
- investigate non-destructive and destructive monitoring and testing methods for estimation of the quality of welded joints of the cartridge;
- investigate corrosion resistance of welded joints;
- develop the technology of welding and equipment for welding of the union with the cartridge;
- choose the method of welding and define optimum modes of welding the cap to the cartridge after helium pumping in;
- apply non-destructive and destructive methods of monitoring and testing for estimation of the quality of welded joints of the union and the cartridge;
- develop the technology of elimination of the defects arising in welding.

This work was executed according to the contract with «Framatome ANP» which provided performance of sufficient amount of research necessary for working out of automated technology of welding of the cap with the cartridge and resistance welding of the union tap for helium pumping into the cartridge at the assembling site of GSP ChNPP.

As the basic structural material for the cartridge was used high-alloy corrosion-resistant stainless steel 08Kh18N10T. The cartridge body is a pipe-like cylindrical vessel having the following overall dimensions: total length 3872.5 mm; diameter 89 mm; length of the cap 276.5 mm; length of the union for helium pumping in 21.0 mm. Welded joints operate within temperature range from –40 to 50 °C in the conditions of intensive radiation, vacuum inside the cartridge is 400 Pa.

For automatic argon-arc welding of the cap with the cartridge, resistance welding of the union tap for helium pumping in and quality control of welds of

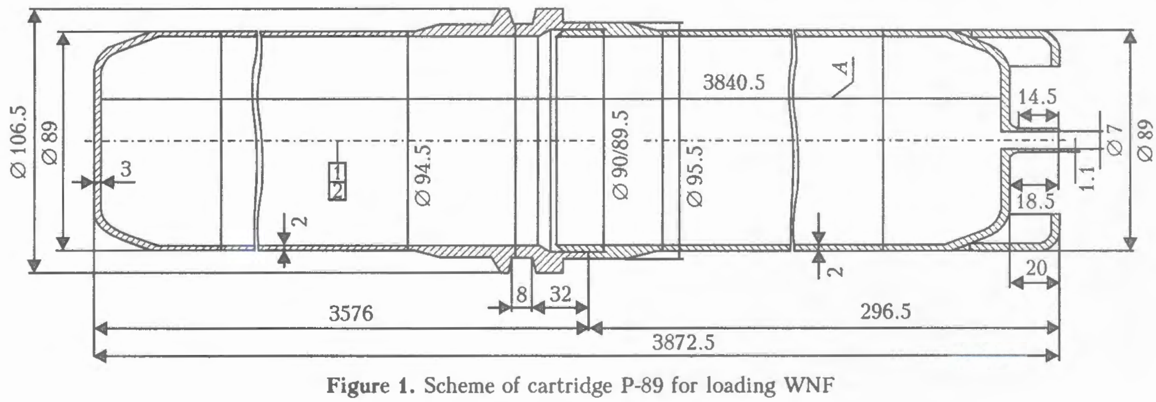

Figure 1. Scheme of cartridge P-89 for loading WNF

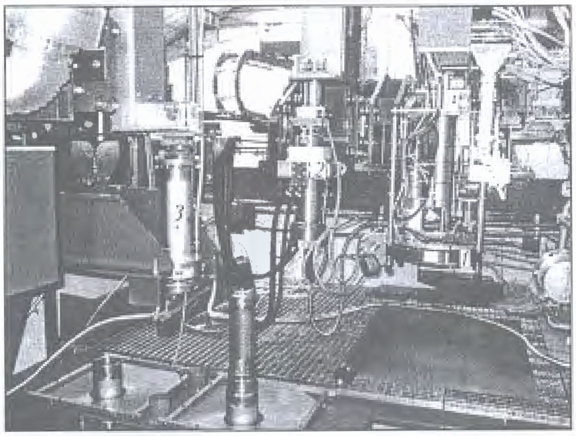

Figure 2. General view of special installation for welding the cap with cartridge P-89 in the chamber: *1* — head for welding the cap to the cartridge; *2* — head for helium pumping in and welding of sealing (welding in) of the union tap; *3* — head for cartridge testing for tightness with helium after completion of the series of sealing works

the cartridge and the union for permeability, «Framatome ANP» has created a special automated installation with the chamber for the entire cycle of manufacturing of two cartridges, consisting of three heads (Figure 2).

For tacking and welding, special programs entered into the memory of the computer for controlling power supply source «Polysoude» and planetary welding head (Figure 3), were developed.

The technology of automatic argon-arc welding of the cap with the cartridge loaded with WNF, is implemented under a certain scheme (Figure 4). The luminescent mark 8 mm wide on the frame is aligned with the mark 0′ on planetary welding head. This operation is carried out by the operator manually; he stays is in a safe premise and supervises its performance on the computer monitor. Then he puts the welding head with the tungsten electrode over the joint and manually performs a test revolution through 360°, the head being on the joint. If position of tungsten electrode–joint coincides, the following operation is carried out. By preparation for tacking the welding torch automatically returns into position 0′. After switching on the program «Tack welding», the welding torch is set into position 0″, then it automatically makes a

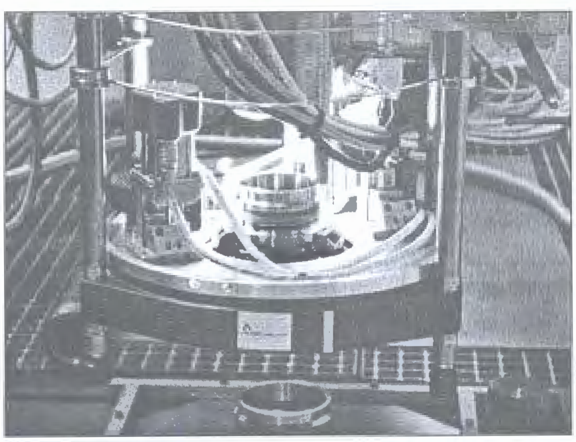

Figure 3. General view of planetary welding head for performance of girth weld in welding of the cap with the cartridge

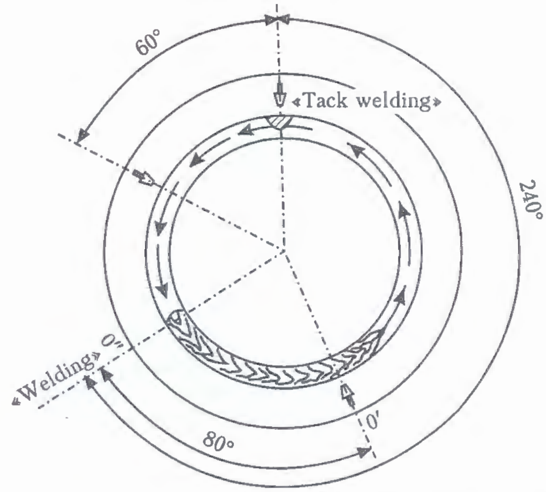

Figure 4. Scheme of welding of the cap with the cartridge

240° revolution, stops and at welding current I_w = = 80 A by contacting the tacking is performed. Figure 5 shows tacking sequence diagram.

After tacking, the welding head automatically deviates through 60° so that on the monitor it is possible to see tack weld quality. This process takes 10 s, then the welding torch returns in position 0′. If tack weld is poor-quality (does not coincide with tungsten electrode–joint position, or any other), the operator carries out tungsten electrode position correction on the joint, and the process is repeated.

Before automatic welding of the cap with the cartridge, during 10–15 s purging of the entire system with argon is carried out.

With «Start» button, under the preset program of welding, the welding head returns into position 0″, and at the preset mode by contacting automatic argon-arc welding of the cap with the cartridge is carried out, after which termination during 10 s argon feeding in goes on. Figure 6 shows the succession of operations during welding the cap with the cartridge.

On special installation, using the head *2* (see Figure 2), after welding the cap with the cartridge, resistance welding of the union tap for helium pumping into the cartridge is carried out.

Technology of resistance welding of union tap for helium pumping into cartridge P-89. After welding the cap to the cartridge, the latter is moved to the head *2* (see Figure 2) of special installation, where automatic pumping of helium into the cartridge through the union tap, then flattening of the tap with

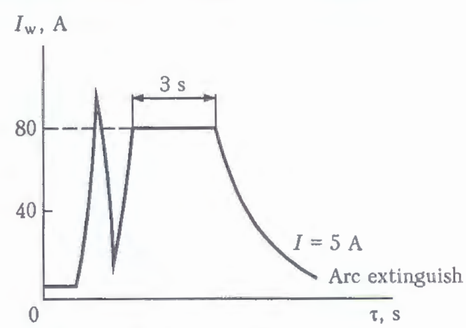

Figure 5. Sequence diagram of tack welding the cap to the cartridge (U_a = 13 V)

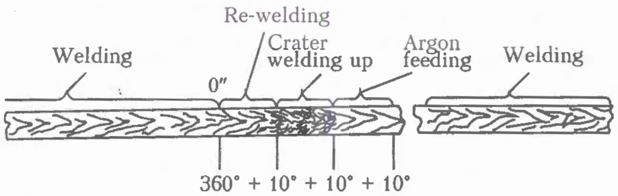

Figure 6. Succession of operations during welding the cap with the cartridge (length of weld L_w = 298.5 mm)

force P and its resistance welding (which technology was tried out by «Framatome ANP»), are carried out.

Sequence diagram of resistance welding of the union tap (Figure 7) includes five stages:

• cramping of electrodes while in cold condition (time τ_0 is cramping of electrodes with force P);

• preliminary heating at gradual temperature increase (linearly accruing function of preliminary heating during τ_1 + preheating heating during τ_2 with intensity I_p);

• transition stage τ_3 in our case is reduced;

• welding with linear increase of I_w (during τ_4 + during τ_5);

• maintaining electrodes cramping and caulking (τ_6 is cramping of electrodes with force P).

Trials conducted by «Framatome ANR», have confirmed serviceability of this special installation for resistance welding of the union tap for sealing of cartridge P-89.

Technology of welding of reference specimens of the cap with the cartridge at the E.O. Paton Electric Welding Institute. At the E.O. Paton Electric Welding Institute, were conducted trials on welding of reference samples of pipes with simulation of technology of welding of cartridges P-89. Welding was conducted on installation ADSV-6 with welding universal manipulator M11010 and power source VSVU-315U. Welding was carried out on samples of pipes from stainless steel 08Kh18N10T 75 mm in diameter with 5.4 mm wall thickness. Butt joints of reference sample were in full correspondence with cartridge drawings. Reference samples were manufactured at the modes of welding specified in Table 1.

Macrosections of the welded reference samples were prepared, their investigation has shown that with increasing pulse current I_p, from 120 to 145 A, at the pause current I_{pause} = 80 A, the width of the weld B_w makes 6.8–7.5 mm, and depth of penetration H_{pn} is 2.2–3.0 mm (Figure 8).

Table 1. Modes of welding of pipe reference specimens

Sample #	I_p/I_{pause}, A	B_w, mm	H_{pn}, mm
1	120/80	6.8–7.0	2.20–2.40
2	125/80	7.4–7.6	2.60–2.75
3	132/80	7.5–7.6	2.80–2.90
4	145/80	7.3–7.5	2.90–3.00

Note. v_w = 6 m/s; U_a = 13 V; pulse duration τ_p = 0.2 s; pause duration τ_{pause} = 0.3 s; argon consumption was 9 l/min.

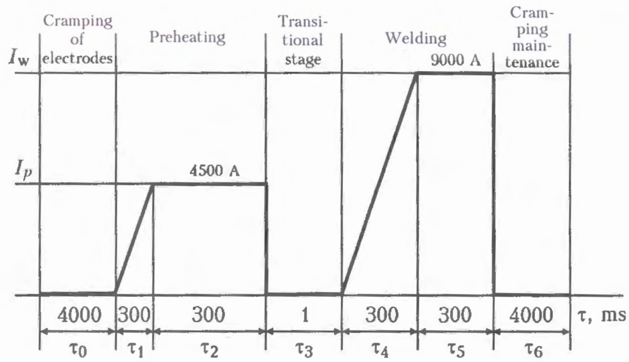

Figure 7. Sequence diagram of resistance welding of union tap for helium pumping into the cartridge

Tensile static tests were conducted at 20 °C (GOST 6996–66, type XIII) of welded joints with various depths of penetration, which results are presented in Table 2.

Analysis of the properties of welded joints performed using automatic argon-arc welding of reference samples on pipes 75 mm in diameter from the steel 08Kh18N10T, as applied to the cartridge, has shown that welds feature fairly high durability at minimum penetration depth H_{pn} = 1.8–2.0 mm. Results of the research testify that the welded joint is characterized by resistance to intercrystalline corrosion at test method AM (GOST 6032–4).

Technology of welding of the cap with cartridge P-89 at «Framatome ANR» Company. Trials on automatic argon-arc welding of the cap with the cartridge on full-scale models with application of the Frama-

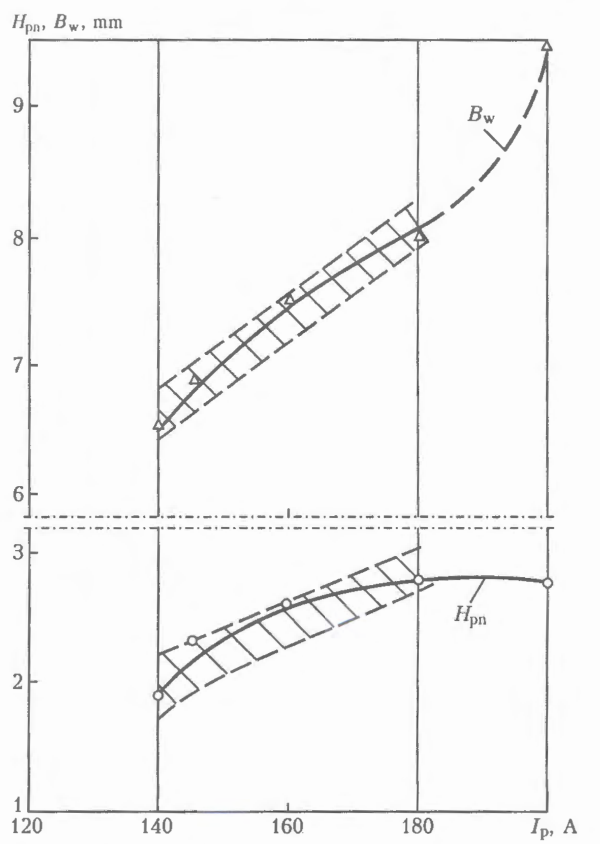

Figure 8. Influence of the pulse current I_p at pause current I_{pause} = = 80 A on penetration H_{pn} and weld width B_w of reference specimens welded at the E.O. Paton Electric Welding Institute

Table 2. Mechanical properties of welded joints of reference specimens of the 08KhN10T steel cartridge cap

Sample #	σ_t, MPa	α-phase content in weld metal, vol.%	B_w, mm	H_{pn}, mm
1	357.5–443.7 / 410.2	1.8–3.0	7.0	1.8–2.0
2	467.7–561.6 / 500.6	1.8–3.5	7.5	2.4–2.6
Note. Results of testing of at least 3 samples are presented.				

Table 3. Modes of welding-in of cap with cartridge on special installation of «Framatome ANP» Company

Sample designation	I_p/I_{pause}, A	B_w, mm	H_{pn}, mm
P1	160/80	7.5	2.4–2.6
P2	160/80	7.5	2.4–2.6
P3	140/80	6.5	1.8–2.0
P4	150/60	6.5	–
P5	140/80	6.5	–
P6	180/80	8.0	2.75
P7	180/80	8.0	–
P8	160/80 (repair welding)	–	–
P9	200/80	9.5	2.60–2.75
Note. v_w = 6 m/h; U_a = 13.5 V; τ_p = 0.2 s; τ_{pause} = 0.3 s; argon consumption was 15 l/min at lengths of welding cables and hoses of 35 m.			

tome special installation at the modes presented in Table 3 have been conducted.

Study of macrosections has shown that with increase of pulse current from 140 to 180 A at pause current of 80 A, depth of penetration changes from 1.80 to 2.75 mm, while width of the weld from 6.5 to 8.0 mm.

It was established that optimum depth of penetration H_{pn} = 2.4–2.6 mm and weld width B_w = 6.5–7.5 mm is obtained at the following mode of welding: I_p = 160–180 A; I_{pause} = 80 A; τ_p = 0.2 s; τ_{pause} = 0.3 s; U_a = 13.5 V; v_w = 6 m/h; argon consumption of 15 l/min.

Further increase of pulse current to 200 A at pause current 80 A increases width of the weld to 9.5 mm, penetrating only thickness of «tongue» of lap joint. It is explained by small (l = 12 mm) length of lap, and also by presence of gap (air space). Therefore increase of the pulse current above 180 A is not expedient.

Quality control of welded joints at cartridge sealing. It is necessary to apply installations and equipment to quality control of welded joints which should meet the requirements of PNAE G7-010–89. Application of installations and equipment, not specified in standards (for example, imported ones) is allowed, on condition that it provides conformity with all requirements of PNAE G7-010–89 and is agreed upon with head materials science organization.

Quality control of the fade-out girth weld in welding the cap to the cartridge is made using developed at the E.O. Paton Electric Welding Institute automatic control system, and testing for helium tightness — using the head *3* (see Figure 2).

Thus operations are carried out in the following sequence:

- vacuum is created inside the cap of the head *3* tightly fitted on the cap of the cartridge with welded-in union tap (vacuum level below 400 Pa);
- vacuum is measured;
- cartridge is filled with helium at pressure $1 \cdot 10^4$ Pa;
- pressure of helium in the cartridge is measured;
- signal informing about presence of leak of helium in the workpiece is given.

At testing of tightness, speed of helium leakage in both welds (automatic arc-welded girth one of cup to cartridge, and resistance-welded one performed in welding union tap), should not exceed $1 \cdot 10^{-5}$ Pa·m^3·s^{-1}.

Technology of elimination of defects after welding. All defects (inadmissible deviations from the established rules of indicators control), revealed in welded joints at their non-destructive testing, should be eliminated. At correction of defects in welding the cap to the cartridge, application of the following technologies is allowed:

- automatic argon-arc re-welding of the butt girth weld in welding the cap to the cartridge;
- complete mechanical removal of the girth weld with mounting of the new cap and performance of welded joint on automated installation according to the accepted technology of welding;
- mechanical removal of the defective weld by means of special device in the cartridge welding chamber.

The following technologies are applied for elimination of defects in resistance welding of the union tap for helium pumping in:

- resistance re-welding;
- complete mechanical removal of the girth weld with mounting of the new cap and performance of welded joint on automated installation according to the newly accepted technology of welding;
- helium pumping in and resistance welding of the union tap.

Thus, the research of the technology of automatic argon-arc welding of the cap with the cartridge and technologies of resistance welding of union tap for helium pumping into cartridge P-89 was carried out, which has allowed optimization of technical requirements to welds for performance of welding works at assembly operations at burying WNF at ChNPP.

DEVELOPMENT OF ELECTRODES FOR WELDING AND DEPOSITION OF ALUMINIUM BRONZES

V.V. KORCHEMNY, N.V. SKORINA and **V.A. ANOSHIN**
E.O. Paton Electric Welding Institute, NASU, Kiev, Ukraine

The paper gives the characteristics and some features of the technology of manufacturing coated electrodes for manual arc welding and deposition of aluminium bronzes developed at the E.O. Paton Electric Welding Institute. The optimum temperature of electrode baking is determined, which guarantees a low susceptibility of the coating to moisture absorption.

Keywords: *arc deposition, aluminium bronze, coated electrodes, coating mass, modes of heat treatment, welding and technological properties, deposited metal, chemical composition, heat input, mechanical properties*

Aluminium bronze is widely applied in different industries thanks to its high mechanical and physical properties (thermal stability, corrosion resistance, low friction coefficient, etc.). For economical use of this scarce and expensive nonferrous metal is applied deposition — an effective method of restoration of the dimensions of the worn out parts and manufacturing of bimetallic items with preset operational characteristics.

The simplest and cheap method is manual arc deposition (welding) with coated electrodes. The analysis of foreign prospectuses shows that in the developed countries many firms-manufacturers of electrodes (Alunox, MTC, UTP, etc.) have in their nomenclature of products some brands of electrodes for welding and deposition of bronzes. At the same time, high cost of imported electrodes limits their use in required volumes at the enterprises of Ukraine.

Considering that in Ukraine there is no production of electrodes for welding and deposition of aluminium bronzes, at the E.O. Paton Electric Welding Institute, NASU, Kiev, Ukraine, was conducted a complex of research works aimed at development of such electrodes. As a result of research, special coated electrodes ANBA-1 with cores from standard wire BrAMts9-2 are proposed.

Usually basic requirements to the electrodes include: necessity of provision of preset operation properties of the deposited metal, required welding and technological characteristics of electrodes and acceptable technological effectiveness of their manufacturing. As a rule, welding and technological properties of electrodes and quality of deposited metal are to an appreciable degree conditioned by the choice of binder and slag-forming systems of the electrode coating, therefore much attention was paid to selection of namely these components of the coating.

At the choice of the basis of slag system, the best results were obtained at the use as components of the coating of electrodes of cryolite and fluorides of alkali-earth metals. Cryolite, being easily fusible and low hygroscopic component, has low density, wets well the surface of surfaced metal and is characterized by low chemical activity with respect to the metal of weld pool, promotes dissolution of aluminium oxide film. Thanks to its ability to interact with water vapour with formation of hydrogen fluoride, fluoric salts of alkali-earth metals reduce propensity of the metal to formation of pores.

As binding agent of electrode coatings was chosen sodium-potassium water glass which is characterized by minimum water retention ability and provides stable arc running process. Optimum parametres of liquid glass and conditions of manufacturing techniques have been defined, which provide a steady process of preparation of coating mass (preventing danger of clodding) and the required stable in time consistency of the coating mass. The latter is characterized by smooth extrusion process at moulding of electrodes (Figure 1) and rather high strength of crude coating on electrodes.

Hygroscopicity of coatings of electrodes was defined based on the increase of their weight ΔW as a result of moisture absorption in the hydrostat at constant humidity of 84 % (saturated solution of bromic potassium at room temperature).

Optimum conditions of heat treatment of electrodes are chosen. As the study has shown that temperature of calcination of electrodes of 300 °C is optimum. In this case minimum hygroscopicity of the coating (Figure 2) is reached and required welding and technological properties of electrodes are provided. Further rise in temperature of calcination only slightly affects hygrosorption capability of coatings,

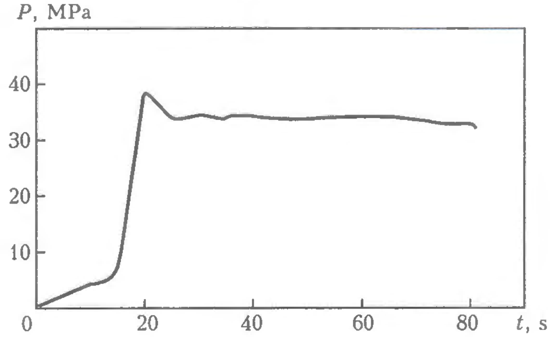

Figure 1. Extrusion curve of coating mass of electrodes AMBA-1 (4.0 mm die diameter at mass consumption $Q = 1$ cm^3/s)

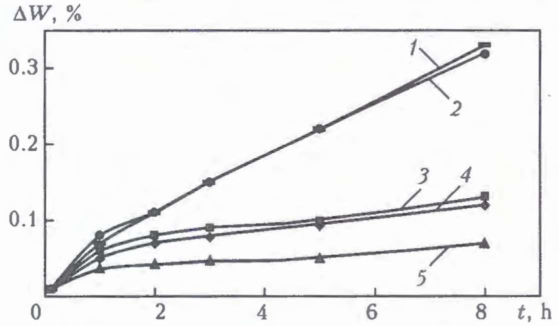

Figure 2. Absorption kinetics of atmospheric moisture by coating of electrodes ANBA-1 calcinated at different temperatures, °C: *1* — 100; *2* — 150; *3* — 200; *4* — 250; *5* — 300

but increases power inputs at manufacturing of electrodes.

The comparative estimation of welding and technological properties of electrodes ANBA-1 with a Russian analogue LPI-73 was conducted. For each electrode brand was carried out one- and three-layer deposition onto the plate from steel 09G2S. Research has shown that at deposition stable process of arc running, fine drop transfer of electrode metal with minimum spattering is observed. A little higher losses of electrode metal for spattering are observed at deposition with electrodes LPI-73. Surface of beads is fine-scaled, with smooth transition to the base metal. At deposition with electrodes LPI-73, slag crust separation was a little bit worse. Visual inspection of beads and macrosections has not revealed pores, only the crater of the first layer at multilayer deposition with electrodes LPI-73, had a crack.

The conducted tests have shown that welding and technological properties of electrodes ANBA-1 are higher than those of electrodes LPI-73. Chemical composition of the metal, deposited using electrodes ANBA-1 and LPI-73, corresponds to composition of low-alloy aluminium bronze (Table 1).

Considering that copper alloys at deposition on steel are inclined to penetration along the boundaries of grains of the base metal [1–3], study of microsections of deposited metal by means of optical microscopy was carried out. The metallographic analysis has shown that at heat input of 29 kJ/cm, in some places intercrystalline penetrations of aluminium bronze into steel were observed (Figure 3, *a*). Depth of penetrations made no more than 0.2 mm. At reduction of heat input, the tendency to decrease in the quantity of penetrations was observed, and at 22 kJ/cm penetrations into steel were already absent (Figure 3, *b*). In [4] it is shown that penetration of copper alloy into steel to the depth of 0.8 mm does not detriment strength of bimetallic joints.

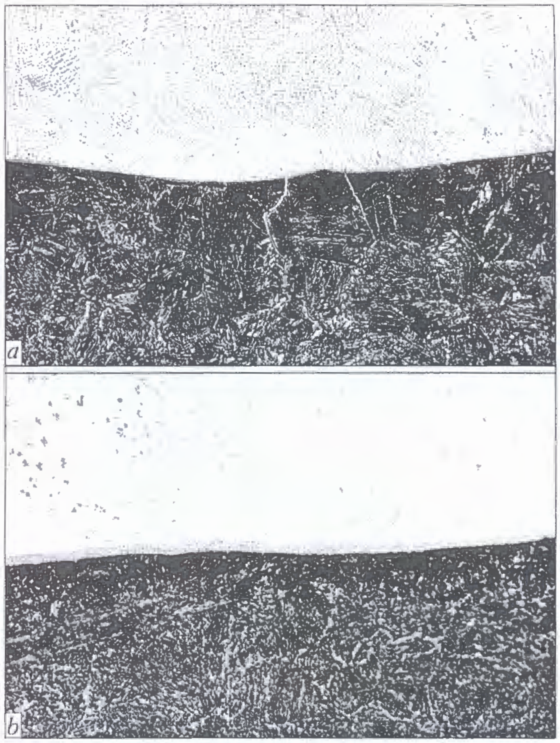

Figure 3. Microstructures of the zone of fusion of aluminium bronze with steel at different values of heat input: *a* — 29; *b* — 22 kJ/cm (×200)

Table 1. Chemical composition of cast bronze metal and of metal deposited using coated electrodes, wt.%

Material	Cu	Al	Mn	Fe	Ni	Si
Bronze casting BrA9Mts2L according to GOST 473–79	Base	8.0–9.5	1.5–2.5	–	–	–
Metal deposited on steel with electrodes:						
ANBA-1	Base	8.0	1.8	3.6	0.7	0.5
LPI-73	Base	6.5	1.6	4.5	2.8	0.8

Table 2. Mechanical properties of cast bronze metal and of metal deposited using coated electrodes ANBA-1

Material	σ_y, MPa	σ_t, MPa	δ, %	ψ, %	*HB* hardness
Bronze casting BrA9Mts2L according to GOST 473–79	150	400	20	–	90–120
Metal deposited with electrodes ANBA-1	$\frac{207.7–216.3}{212.0}$	$\frac{549.8–562.2}{556.0}$	$\frac{37.2–42.0}{39.6}$	$\frac{35.5–45.5}{40.5}$	$\frac{146–162}{154}$

Study of mechanical properties of the metal, deposited using electrodes ANBA-1, was conducted by measurement of strength and Brinell hardness properties. Static tensile tests were conducted on round proportional samples with diameter of working section of 6 mm (GOST 6996–66). Results of the tests are presented in Table 2. Analysis of mechanical properties has shown that the cast bronze BrA9Mts2L strength characteristics are lower than those of deposited aluminium bronze, hardness in deposited metal is higher than in cast, which is due to the presence of iron and nickel in the deposited bronze.

Pilot production of small series of new electrodes is organized at the E.O. Paton Electric Welding Institute, NASU, Kiev, Ukraine.

1. Milichenko, S.L., Gamov, N.S. (1981) Features of formation of structure and properties of aluminium bronze deposited on steel. In: *Theoretical and technological principles of surfacing. Surfacing in machine-building and repair*. Kiev: PWI.
2. Dzhevaga, I.I., Lebedev, Yu.M., Ivashchenko, G.M. (1970) Investigation of fusion zone of welded joint of carbon steel with aluminium bronze. *Avtomatich. Svarka*, **8**, 11–14.
3. Timofeev, V.N., Isaev, N.I. (1965) Surfacing of copper alloys on steel surfaces. *Ibid.*, **4**, 34–37.
4. Vajnerman, A.E. (1970) Influence of copper alloy penetrations on properties of joints made by surfacing of copper alloys on steel. In: *Surfacing of metals*. Part 2. Leningrad: LDNTP.

DEVICE FOR PULSE STABILIZATION OF AC WELDING ARC

AC arc welding has a number of advantages (simplicity and reliability of the applied equipment, economical efficiency as against welding rectifiers and generators, the absence of magnetic blow-outs and others), however a small stability of AC arcing restricts its application.

Device that provides stabilization of the arc discharge in AC welding is developed at the E.O. Paton Electric Welding Institute. The operation of the device consists in pulse introduction of additional energy into the welding arc in the moments of change of its polarity. This is a small-size, light and not expensive device switched to any serial welding transformer without electronic control units making it universal and saving electric energy in operation.

Switching of the device for stabilization of arcing (DSA) to the transformer allows essentially expanding the spheres of its application due to imparting to it the properties of a rectifier for manual consumable-electrode arc welding as well as for unit for nonconsumable-electrode argon-arc welding. The use of DSA essentially simplifies the work of the welder and decreases the requirements for his qualification.

Purpose. Welding transformer in a set with DSA may be used for manual arc welding of carbon steels with widely used electrodes intended for any kind of current (MR-3, ANO-4, UONI-13/45, UONI-13/55 and others), manual consumable-electrode arc welding of some stainless and special steels (OZL-8, OZL-26, TsL-39 and others), manual consumable-electrode arc welding of cast iron (TsCh-4 and others), nonconsumable-electrode argon-arc welding of stainless steels, aluminium and its alloys under contact method of arc initiation.

DSA is manufactured in three modifications, which differ in design, use of different electronic bases and the availability of auxiliary functions (switch of stabilizer, gas feed valve) in argon-arc welding.

For power supply the DSA welding transformer should be furnished with weak-current winding, which is easily located on one of the power coils of the transformer. Power supply voltage is a total voltage of additional and welding windings (practically doubled voltage of the secondary winding of the welding transformer).

DSA is switched on automatically or forced at the beginning of welding and automatically switched off (not later than in 1 s after welding is finished).

A range of stabilized welding current is equal to the range of currents of the transformer itself.

Proposals for co-operation. The potential customers can receive on contractual basis all necessary service forms and records as well as services for putting into operation the first lots of DSA.

Contacts: Dr. Andreev V.V.
E-mail: sheiko@paton.kiev.ua

SPECIALIZED INFORMATION-MEASURING SYSTEM FOR MONITORING THE PROCESS OF ARC WELDING

A.E. PIRUMOV[1], I.O. SKACHKOV[1], S.A. SUPRUN[2] and Yu.S. MAKSIMOV[2]
[1]NTUU «Kiev Polytechnic Institute», Kiev, Ukraine
[2]E.O. Paton Electric Welding Institute, NASU, Kiev, Ukraine

The structure and functionality of the mobile information-measuring system intended for registration of electric and time parametres of process of arc welding with subsequent statistical processing and graphic interpretation of obtained results are considered.

Keywords: *information-measuring system, arc welding, electric and time parametres, registration, statistical processing, graphic interpretation*

Development of information technologies essentially expands the field of application of computerized techniques in welding. Improvement of the equipment applied for controlling of welding processes and measurement of energy parametres of welding arc, is accompanied by search of the tools, capable of ensuring the predicted estimation of the quality of manufactured products.

One of such tools is the information-measuring system (IMS) developed together by the Chair of Electric Welding Devices of NTUU «Kiev Polytechnic Institute» and E.O. Paton Electric Welding Institute, NASU, Kiev, Ukraine. It is designed for registration of electric and time parametres of the process of arc welding with subsequent statistical processing and graphic interpretation of the obtained results.

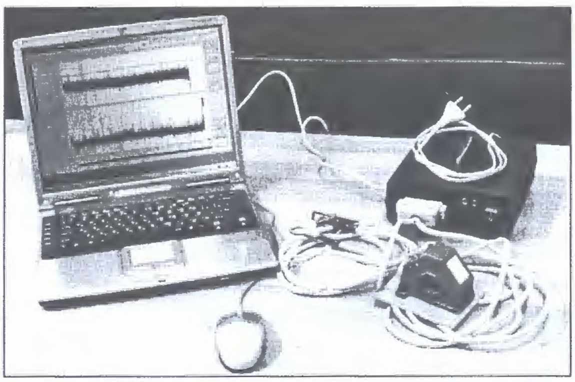

Figure 1. Appearance of IMS

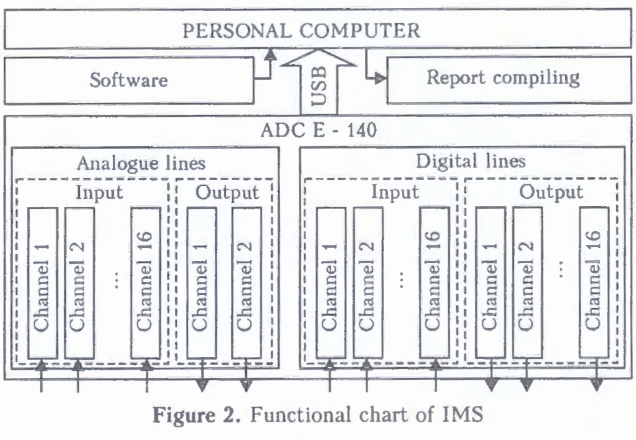

Figure 2. Functional chart of IMS

IMS (Figure 1) consists of personal computer with specialized software «IMS2006», functioning in the environment of operation system Windows Me/2000/XP, external analogue-digital converter (ADC) and a set of gauges. ADC E-140 (L-Card, Russia) provides continuous gathering of analogue data on frequencies of digitization from 0.122 to 100 kHz [1]. In the basic variant, IMS comes complete with current and voltage gauges providing galvanic decoupling of the circuit and measurement of current up to 300 A and voltage up to 500 V. If necessary, the user can make use of gauges with normalized level of output signal up to 10 V of any functional designation. Block-diagram of IMS is presented in Figure 2.

Basic specifications of the developed IMS are the following: quantity of analogue inputs is 16 or 32 (depending on the method of connection to signal source); quantity of analogue outputs is 2; 16 input and 16 output digital TTL-compatible lines. Range of input voltages of analogue input channels is not more than 10 V [1].

By means of IMS software, the digitized signal based on preset parametres is recorded into the file in the format of digital integral two-byte number into the hard disk of personal computer. Data processing is based on statistical analysis of electrical signals received from the gauges (for example, welding cur-

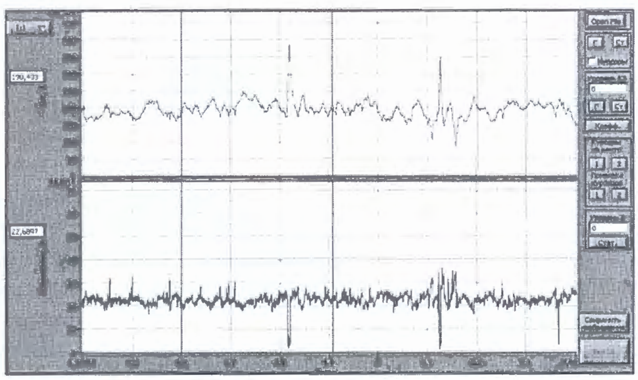

Figure 3. Main window of data processing program

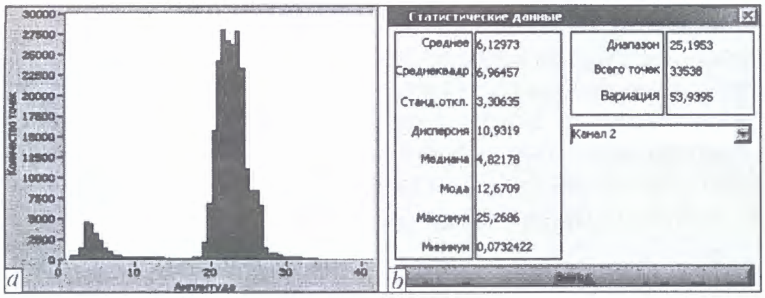

Figure 4. Window of histogram construction (*a*) and window of statistical signal processing (*b*)

rent and arc voltage, wire feed rate and replacement of welding head, consumption of shielding gas, etc.).

While recording the signals, the user can choose the number of data acquisition channel, establish frequency of ADC operation, set amplification factor, specify the file name for recording, and also create the test log. After recording the signals, a binary data file is created on the hard disk. The system allows adding an option of output digital lines control, which enables programming the technological process cycle.

In the main window of data processing program (Figure 3), are displayed oscillograms of the recorded signals, with which the user can carry out the following operations: scaling, definition of instant values, image saving. The main program window also contains buttons for transition to data processing subroutines. With their help the user can pass to calculation of basic statistical characteristics and construction of various histograms. Basic version of the processing program provides for the following modes of calculation of signal parametres.

1. Calculation of statistical characteristics and construction of histograms (Figure 4) for all values of the oscillogram or a chosen section between two cursors (positions of cursors are set by the user manually). The program provides the possibility of calculating for the chosen channel of the recorded data the following characteristics: mean and root mean square values, standard deviation, dispersion, signal mode and median, variation factor, define values of signal minimum, maximum and amplitude, volume of data file chosen for calculations [2]. The user can choose and perform calculation of corresponding parametres, and also save the image of the histogram of peak signal values.

2. Calculation of statistical characteristics and construction of histograms of duration of welding arc short circuits (Figure 5). For processing, the program selects the values which are above (for welding current signal) or below (for arc voltage signal) the level of short circuits set by the user.

The user can obtain characteristics of descriptive statistics, and also the information on mean, minimum and maximum duration of short circuits with their histogram display.

3. Calculation of statistical values and construction of histograms of the times of starting of welding arc (Figure 6). The subroutine operates by an algorithm similar to that described in item 2, with the only difference that for processing are selected the values corresponding to the level of welding arc excitation.

Besides, for the specified version of the program, possibility of calculation of minimum value of open-circuit voltage necessary for reliable welding arc excitation is provided. Such a characteristic is useful in research of new consumables for welding. Calculation was performed using a dependence reported in [3]

$$U_{\mathrm{o.c}}\,(\min) = \frac{\bar{x} + 3\sigma^2}{\sqrt{2}},$$

where $\bar{x}$ is the mean value of arc ignition voltage; σ^2 is the dispersion of values of arc ignition voltage.

4. For visualization, a researcher can obtain volt-ampere characteristic for the specified section of the oscillogram, calculate frequencies by means of Fourier transform, and also rate of current rise for the chosen section.

The described IMS has successfully passed approbation in the research of the process of automatic underwater wet welding [4].

The developed IMS is useful for the researchers in the field of development of welding consumables and

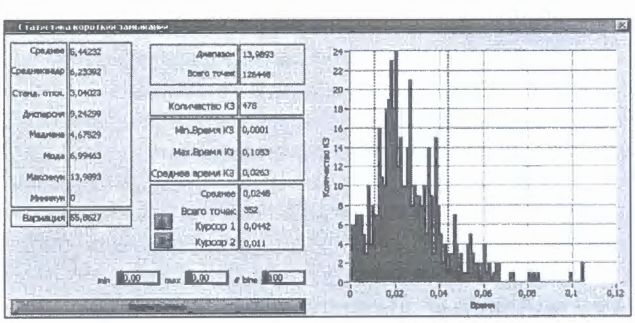

Figure 5. Window of statistical processing of values of welding arc short circuits

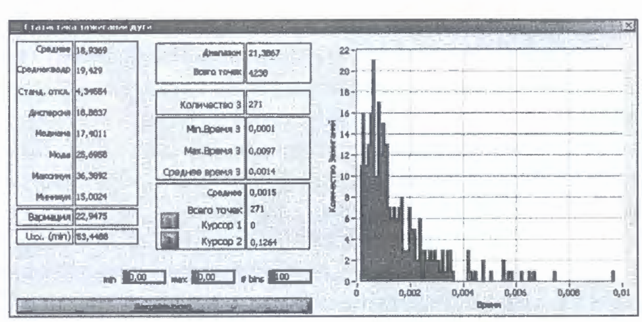

Figure 6. Window of statistical processing of values of welding arc starting

research of technological processes. The system is mobile, which expands the area of its application, is simple in use. Information processing can occur both immediately after the experiment, and at any other time. The obtained information will easily be transformed into plots and tables, which is useful in writing reports and conclusions on the investigated welding consumable or a welding process.

1. Kodorkin, A.V. (2003) *E-140: User's manual*. Moscow: L-Card.
2. Kozlov, B.A., Ushakov, I.A. (1975) *Reference book on calculation of reliability of radioelectronic and automatic equipment*. Moscow: Sov. Radio.
3. Pokhodnya, I.K., Gorpenyuk, V.N., Marchenko, A.E. et al. (1979) Procedure for determination of alternative current arc stability. *Avtomatich. Svarka*, **12**, 16–18.
4. Skachkov, I.O., Pirumov, A.E., Maksimov, S.Yu. et al. (2006) On neural network application for welded joint quality control in underwater welding. *The Paton Welding J.*, **6**, 21–24.

THESES FOR SCIENTIFIC DEGREE

E.O. Paton Electric Welding Institute, NASU, Kiev, Ukraine

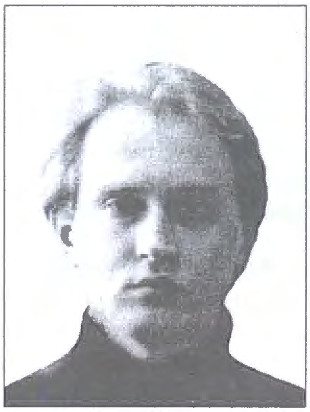

A.V. Lavrenyuk (EWI) defended on 6 June 2007 candidate's thesis «Tree-phase–two-phase direct current power source for CO_2 arc welding».

The dissertation is devoted to further development of theory, design and calculation of traditional power sources (PS) for CO_2 arc welding.

As a result of the conducted analysis of characteristics of two-phase rectification circuits, it was determined that application of circuits with parallel connection of rectifiers in designs of welding PS is irrational, as it leads to considerable narrowing of the range of welding voltage adjustment, which may make up to 25 %.

It was established that optimum variant of two-phase rectifying circuit at development of welding PS, is two-phase circuit with in series connected rectifiers making a two-half-period circuit with a median point.

PS for CO_2 arc welding was developed, based on of two connected in series rectifiers, one controlled, another uncontrolled, their power supply provided from a three-phase–two-phase transformer.

The power circuit of the new welding PS allows providing smooth thyristor adjustment of welding voltage, preventing welding current and voltage dropping to zero within the entire adjustment range, as well as raised initial value of PS voltage due integrated into the circuit diode-condenser voltage multiplier (DCM), thus ensuring high welding properties of such PS. At the same time the developed PS is simple in design and reliable.

The procedure of calculation of combined VAC of the new PS was developed, which yet at the design stage, knowing value of PS VAC slope, allows obtaining corresponding parametres of welding transformer or solving the reverse problem.

New designs of three-phase and tree-phase–two-phase transformers with twisted magnetic circuits, which application enables a 28 % reduction of weight and cost in comparison with existing analogues were developed. Such new designs can be applied both in welding PS with various VAC slopes, and in other electrical devices.

Optimized mathematical models of new transformer designs allowing developing optimum in terms of weight and cost transformers with preset characteristics were created.

Research of the influence of DCM parametres on reliability of establishment of the process of CO_2 arc welding has shown that at multiplier voltage of 110 V and capacity of its condensers of 4500 μF in welding with wires diameter 0.8 and 1.2 mm, permanent reliable starting of the arc from the first touching the workpiece with the wire is ensured. Its application also allows to considerably decrease the open-circuit voltage of welding transformer.

On the basis of the reported and conducted research, dependence of optimum rate of welding current rise at short circuit of the arc gap, on diameter of the electrode wire was obtained, which allows determination of mean optimum value of inductance for various wire diameters, thus making unnecessary labour-consuming experiments.

It was determined that in CO_2 arc welding, for provision of the least spattering (down to 4 %), it is necessary to apply a choke, whose magnetic circuit will not saturate during short circuit period.

The dynamic circuit of physical processes in the system «PS–CO_2 welding arc» was experimentally specified, which allowed determining new criteria for estimation of PS welding properties.

It was proposed to apply complex analysis of dotted dynamic VAC together with oscillograms and histograms of welding current and voltage values distribution, and also with time response of short circuits as criteria in estimation of PS welding properties, which will allow adequate comparison of PS.

As a rèsult of the comparative analysis of welding properties of pre-production model of PS and serially produced rectifiers VS-300B and KIG-401 types it was established that the developed model possesses higher welding properties and has considerably smaller weight and dimensions than those of analogues.

G.S. Pisarenko Institute for Problems of Strength, NASU, Kiev, Ukraine

V.V. Savitsky (EWI) defended on 7 June 2007 candidate's thesis «Definition of residual stresses by electron speckle-interferometry».

The dissertation is devoted to the development of a method of definition of residual stresses in assemblies and elements of structures on the basis of electron speckle-interferometry.

Now there exist various methods of definition of residual stresses. Each of them has its advantages and drawbacks. Most widely accepted in the research of stressed state of structures is a method of electric strain measurement in combination with probing hole technique, which consists in that for elastic unloading of stresses a blind hole is drilled out in the investigated object. In certain points, in the vicinity of the hole, with the help of strain gauges are measured deformations and, using the data of the measurements, values of residual stresses, which existed in the drilling zone, are calculated. It should be noted that at present it is a unique experimental method of definition of residual stresses, which application is regulated by an international standard. However this method has drawbacks connected with the use of strain gauges: it involves also special preparation of the surface of the investigated object, glueing-on strain gauges, complicated mechanical systems of the device positioning for drilling, great measurement base, etc.

The dissertation shows the possibility of determination of residual stresses by means of electronic speckle-interferometry method.

Algorithms of definition of residual stresses according to data of measurements of displacements by electronic speckle-interferometry in the vicinity of the drilled out hole are developed. A compact module allowing determination of stressed state in assemblies and elements of structures in laboratory and shop conditions is developed. Noise-proof algorithms of speckle pattern processing providing unambiguity of determination of residual stresses and excluding the influence of the operator on the results of measurements are proposed.

Mathematical simulation, which allowed raising accuracy of determination of stresses, was carried out. An approach enabling determination of stress tensor normal component in the research of stressed state by probing hole technique is proposed.

Experimental estimation of the accuracy of measurement of displacements and definition of residual stresses by electron speckle-interferometry was carried out. Peculiarities of distribution of residual stresses in elements and assemblies of structures were investigated.

NEWS

PERMANENT IMPROVEMENT OF PRODUCTS

Permanent improvement of products, search for and introduction of advanced technologies, fast reaction to requirements of the market, such are distinctive features of OJSC KZESO activity.

Today engineers of Kakhovka Plant of Welding Equipment offer the customers not only new models of electric welding equipment, but also complete industrial lines in which the best world achievements in this field are embodied.

So, this year KZESO has launched its basic nomenclature of welding equipment of «Elektrik» plant (St.-Petersburg). It is a wide spectrum of resistance spot welding machines, including automated lines for manufacturing high-quality welded wire mesh.

Starting-up and adjustment works have ended, and now is ready for shipment to METRAKS Ltd (Moscow), first such line constructed thanks to cooperation of Russian (NPO «Elektrik Ltd) and Ukrainian (KZESO) designers. It represents a completely new design of the line containing everything the customer needs. Unlike its analogues, it is compact and is convenient in service. Especially for it, the designers have developed a new control system which meets all requirements of today.

«FRONIUS UKRAINE» Ltd OFFERS

Growing requirements of Ukrainian consumers to welding technologies and equipment dictate new requirements to manufacturers of welding materiel.

Following them, «Fronius Ukraine» Ltd has carried out radical technical re-equipment of its production facilities during 2006–2007, along with introduction of management information system KANBAN. Such measures have enabled not only guaranteeing the highest level of manufacturing quality, but also reducing delivery time of finished products to 3–5 days.

Series production of new-generation semiautomatic machines of VARIOSYNERGIC and VARIOSTAR type was another consecutive step in the direction of promotion to the Ukrainian market of inexpensive, hi-tech and easy-to-use MIG/MAG equipment.

Weighted price/technological capabilities trade-off is the main advantage of this series.

New generation of equipment, having retained the best properties of its predecessors (reliability and economy), was created with the aim of improvement

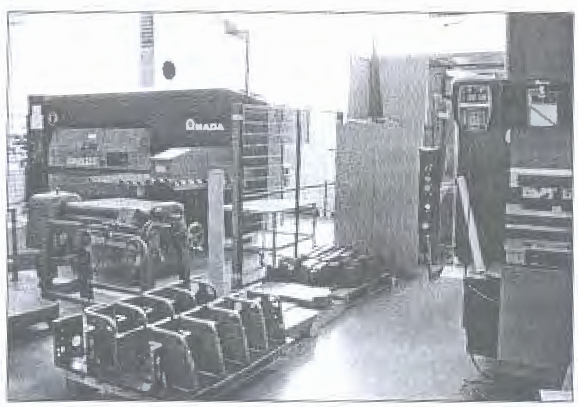

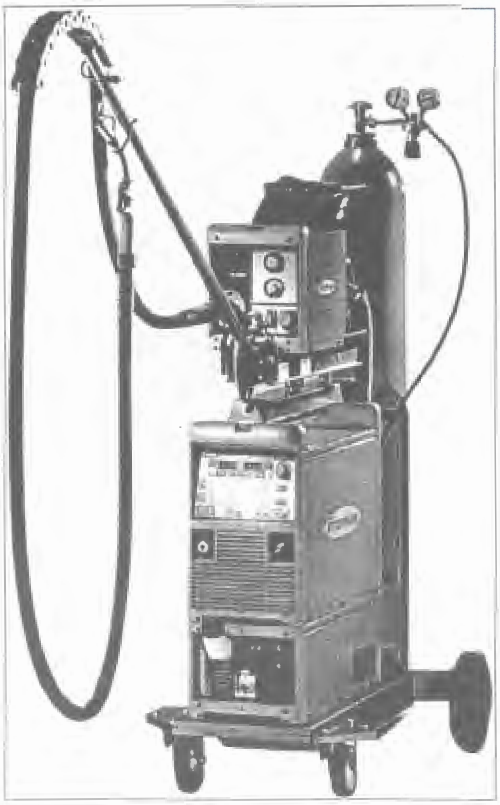

of welding and technological indicators and convenience of use.

Thanks to the integrated assistance in alignment and choke adjustment, welding characteristics in CO_2 arc welding were improved.

Stepping-up with minimum difference of power levels among the models (250A–310A–340A–400A–500A), provides the consumers with considerable economy of investments into their purchase, by selecting the required capacity model.

The built-in «Synergic» mode has for all options of application a corresponding program with pre-selected parametres for welding of low- and high-alloy steels, aluminium alloys, using 0.8, 0.9, 1.0, 1.2, 1.4, 1.6 mm diameter wires, shielding gases CO_2, Ar and their mixtures, and special flux-cored wires.

Thickness of sheet and filler material are preset, the device establishes all other parameters (current, voltage, melting power), as a result, high quality of welding is reached.

The four-roller wire feeder VR 3300 of special enclosed type design, has a light aluminum case (13 kg), and is intended for use in the most severe conditions of operation.

The new design of the case of the feeder protects control elements from mechanical damage. The devices are also delivered complete with open-type feeder VR 3000 providing the possibility of a simpler and faster replacement of wire reels. For work in especially constrained conditions and for stability of feeding of difficult-to-feed to more than 5 m distance Al and CrNi wires, the devices come complete with Pull-MIG torch with built-in wire feeder.

For convenience of work and provision of smooth feeder turning of VR 3000 and VR 3300 type use swing devices.

All devices of VARIOSTAR and VARIOSYNERGIC types can be completed with Human console, which by means of gas cylinder compensates the weight of torch hose unit and thus reduces to the minimum the danger of its damage, and facilitates welder's work.

Isolation of the wire reel prevents its contact with the device case in the use of wire reels with metal frame. Due to smooth adjustment of initial wire feed rate, arc starting process is optimized.

For convenient transposition in the use of up to 30 m hose units, the feeder can be mounted on «Caddie» cart. Intermediate mechanism VR 143 is used for wire feeding to greater distances.

INTERNATIONAL CONFERENCE IN CRIMEA ON PIPELINE TRANSPORT

On May 14–17, in Crimea, the Sixth International Conference «Readiness of OJSC HTZ for manufacturing of pipes for high-strength pipelines» was held. Experts of OJSC HTZ (Khartsyzsk Pipe Plant, Ukraine), VNIIST Ltd (Moscow, Russian Federation), FSUE «I.P. Bardin TsNIIChermet» (Moscow, Russian Federation), OJSCs «Severstal» (Cherepovets, Russian Federation), «MK Azovstal» (Mariupol, Ukraine), «Ilyich MK» (Mariupol, Ukraine), VMZ (Vyksa, Russian Federation), «Uralstal» (Sverdlovsk, Russian Federation), E.O. Paton Electric Welding Institute (Kiev, Ukraine), UkrNIINK Ltd (Kiev, Ukraine), SE NITI (Dnepropetrovsk, Ukraine), NPO «Spetsneftegaz» Ltd (Moscow, Russian Federation), AC «Transneft» (Moscow, Russian Federation), «Quality Program Design» Company (Houston, USA) have taken part in the conference.

With an opening speech addressed the conference participants general director of HTZ A.V. Shishatsky. Technical director of HTZ A.V. Borovikov has made a report on basic achievements of the plant for the last two years in the field of improvement of the technology of manufacturing large-diameter pipes from high-strength low-alloy steels. For production process modernization, improvement and development in 2005 and 2006 more than UAH 180 mln was spent. Anticipated expenses in 2007 make UAH 56 mln. In pipe electric welding shop № 2, construction of the third technological line for manufacture of pipes 406–1420 mm diameter with thickness of wall up to 40 mm from steel of strtength classes X70 and X80 comes to the end.

Works on modernization were carried out also in the shop for applying of insulating coating on pipes. During the past period, the Khartsyzsk Pipe Plant has acquired X-ray inspection apparatuses with X-ray tubes voltage up to 225 kV. AUSC plant of Company «Krautkramer» was purchased and is successfully operated. Now assembly works on new AUSC plant of Company «Karl Deutsch» are under way, and come to an end assembly and adjustment works of AUSC plant for ends of pipes of the Ukrainian Company «Ultrakon» (UkrNIINK Ltd).

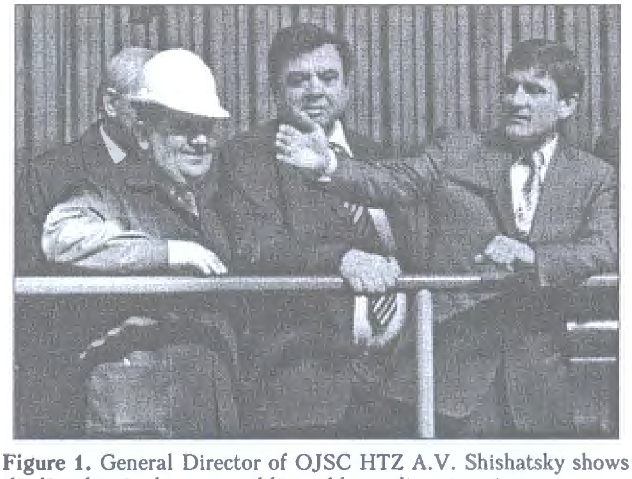

Figure 1. General Director of OJSC HTZ A.V. Shishatsky shows the line for single-seam welding of large-diameter pipes

Production engineering services of the plant continue to work on application of new productive materials. While two years ago, at this plant welding of pipes was performed using agglomerated fluxes only on pilot batches of products, today 70 % of pipes at the plant are welded with these fluxes of companies «Oerlikon», «Lincoln», «Boehler Thyssen», ESAB, and others.

Application of the agglomerated fluxes has allowed meeting increased requirements of the consumers to impact toughness of welds and reduce quantity of internal defects. The performed works have allowed improving the geometry of welds, essentially raise their quality, considerably reduce volume of welding repair of pipes (from 4.5 % in 2005 to 2.2 % during 4 months of 2007), decrease the quantity of pipes transferred into the lower quality category.

The quality management system of the plant is certified by the Canadian quality management institute QMI for conformity with international standards ISO 9001, ISO 14001, QHSAS 18001, and for conformity with standard DSTU ISO 9001 in national system UkrSEPRO.

Now works on certification of the operating Control system for conformity with the Russian standard ROST ISO 9001 in System TRANSERT are coming to an end, and work on certification for conformity with standard ISO 9001–«Gazprom» is starting.

In the report «Development of requirements to steels for new projects of main gas pipelines and problems of guaranteeing performance of heavy-gauge rolled sheets for such pipes», manager of sector of pipe steels of FSUE «I.P. Bardin TsNIIChermet» Yu.D. Morozov has informed that intensive industrialization of developing countries, requires along with structural materials, increased consumption of energy sources, such as oil and gas, and, hence, development of transport systems of their delivery to consumers. From here follow, growth of demand for pipes and construction of new pipelines. Apparently, development of new perspective oil and gas fields and construction of pipelines for their transportation, shift more and more into remote areas of the North, Siberia and the Arctic shelf. So, since 2007 till 2012, «Gazprom» plans implementation of 13 large projects of high pressure gas pipelines construction, their total length of more than 13,000 km (1020–1420 mm diameter). Among them such as:

• North-European gas pipeline: onland section of the pipeline 1420 mm in diameter with working pressure of 9.8 MPa, and underwater section of the pipeline 1219 mm in diameter designed for pressure 22 MPa;

• Bovanenkovo-Ukhta gas pipeline: in diameter 1420 mm, from steel strength class K65 for working pressure 11.8 MPa, and underwater transition through Bajdaratskaya bay — pipes in diameter 1219 mm.

Besides, till 2012, the construction of underwater pipelines of the second line «Blue stream» on the Black sea bottom and gas pipeline from the Shtokmanskoye gas field is planned.

Construction of new gas pipelines requires solution of two problems:

• increasing of volumes of large-diameter pipes production, including heavy-gauge sheets for their manufacturing;

• improving of qualitative characteristics of the metal and pipes, taking into account construction of gas pipelines for pressure 11.8 MPa on land and up to 25 MPa in the sea, application in new projects of pipes from steels of strength K65 and raised thicknesses of their walls taking into account construction and operation of pipelines in severe climatic and geological conditions.

Possibility of manufacturing pipes necessary for the construction of new main pipelines, is to a great extent defined by the presence of modern equipment at the metallurgical and pipe-producing enterprises.

In this respect producers of welded pipes are still ahead of metallurgists. In Russia now, single-seam pipes 1420 mm in diameter, and also thick-sheet pipes (40 mm) 1020–1220 mm in diameter are ready for production at Izhors Pipe Plant (IPP) and Vyksunsky Metallurgical Works (VMP). Total volumes of deliveries of such pipes already makes nearly 1 mln t a year and are based mainly on imported metal. There are projects on construction of similar shops at VPZ companies in Volzhsk, ChTPZ in Chelyabinsk, and one more shop at VMZ. Thus, in 2–3 years, the volume of pipes production for modern main pipelines may make 2.5 mln t a year, which should fully satisfy the needs of «Gazprom» and «Transneft».

Situation with production of skelp, especially for pipes 1420 mm in diameter, is much worse. From among rolling mills in the territory of the CIS, now only «Severstal» runs a rolling mill 5000 with annual volume of skelp production of no more than 600,000 t. Only by 2010 it is expected that rolled stock will start come from the first of the new projected rolling mill 5000 at MMK. The volume of production of rolled stock for pipes 1420 mm in diameter and for thick-walled pipes 1020–1220 mm in diameter, can make up to 1 mln t a year. By 2011, it is possible to expect the beginning of supply from rolling mill 5000, which OMK plans to construct in Vyksa. Therefore, during the next two or three years, there will be a deficiency of thick-wall rolled stock for pipes for new main pipelines. During this time, the metallurgists should solve the problems connected with production of quality steel and continuous-cast slabs with required surface finish, with minimum segregation, minimum harmful impurities and nonmetallic inclusions. As is specified above, much attention is attached to performance of IPG test at rolling of thick sheets. Requisite proportions between thicknesses of sheet rolled stock and strip plate in the finishing mill, partial deformations in the break-down mill for full recrystallization to take place, were established. Such proportions of pipe diameter and length, define necessary parameters of continuously cast slab. Presently only NTMK produces slab meeting listed requirements (section 300 × × 2700 mm). Work in this direction is is still ahead of other integrated iron-and-steel works.

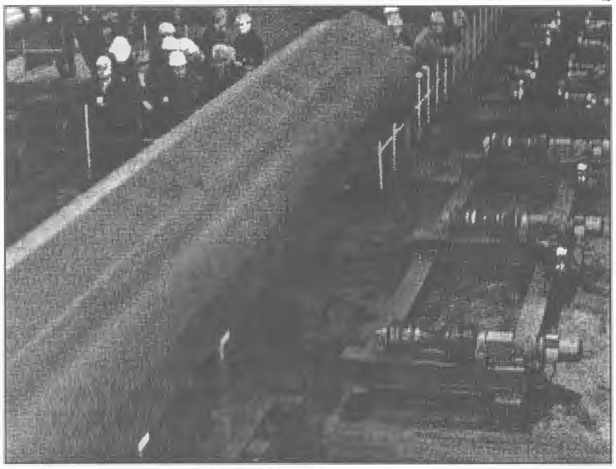

Figure 2. Line for single-seam welding of large-diameter pipes

Representatives of «Azovstal» (I.V. Ganoshenko), «Ilyich MK» (A.V. Murashkin), «Uralstal» (A.M. Stepashin), VMZ (A.A. Shishov) have told to participants of the conference about the complex of works conducted at metallurgical enterprises of Russia and Ukraine, which are directed at improvement of skelp steel quality.

Employees of HTZ company (S.Yu. Lyakh, A.V. Talalaj, A.A. Kravtsov, A.Yu. Loskutov, V.Yu. Kotenzhi, S.A. Basula, E.G. Kononenko), in their reports have taken up the problems of reconstruction, modernization and development of pipe production facilities at HTZ.

Big and substantial report was delivered by president of the company «Quality Program Design», Ch.L. Hallam, who presented the new (44th) edition of Standard API Specification 5L and has informed, that since February 2008 it will be effective as Standard ISO 3183. Then followed the discussion, in which took part both metallurgists-pipe producers and experts in construction and operation of pipelines, it has shown big interest to issues of standardization, certification and validation of the entire complex of technological processes connected with manufacturing of pipes, construction and operation of pipelines.

At the conference reports of employees of the E.O. Paton Electric Welding Institute were presented (A.A. Rybakov, S.E. Semyonov, V.V. Golovko, V.I. Galinich), which reflected the results of cooperation of the institute with companies HTZ, «Zaporozhsteklofluys» and other organizations in the field of introduction of new and advanced types of equipment and welding consumables on technological lines for manufacture of pipes for high-strength pipelines. The reports presented at the conference will be published by HTZ in the collection format.

V.V. Golovko, Dr. Tech. Sci., PWI
V.I. Galinich, Cand. Sci. Tech., PWI

INTERNATIONAL SPECIALIZED TRADE FAIR «WELDING, CUTTING, SURFACING» IN MOSCOW

The world's largest trade fair «Schweissen&Schneiden» taking place once in four years in Essen, for the first time has taken place in Russia. On May 28–31 2007, in Moscow, «Expocenter», hosted International specialized trade fair «Welding, Cutting, Surfacing». Its organizers were Messe Essen GmbH, «Messe Duesseldorf Moscow» Ltd in cooperation with its partners: DVS – German Welding Society, NAKS – National Association of NDT and Welding, «Expocenter» Ltd.

Messe Essen GmbH for 50 years now, each four years, holds the so-called contest of welding technologies – «Schweissen&Schneiden» trade fair. It is a leading trade fair of welding technologies and related processes, representing all aspects of the world market of the industry, and is a venue for meeting of experts and buyers from all countries and continents. With each trade fair, the quantity of participants and exhibitors increases, which defines its permanent success. At the last trade fair in Essen in 2005, more than a thousand exhibitors from 45 countries have presented their innovative developments in pavilions having total area of 89,000 m^3. Trade fairs «Schweissen&Schneiden» held once in two years in China and India also enjoy widespread popularity. Thus trade fair in China, held alternately in Beijing and Shanghai, is recognized as second in its importance after the leading trade fair in Essen.

Dynamic development of the Russian economy, and, first of all, such industries as power, automotive- and aircraft industries, chemical- and general mechanical engineering, has led Messe Essen to a logic decision – holding trade fair in Moscow.

The trade fair topics and themes embraced all aspects of welding production:

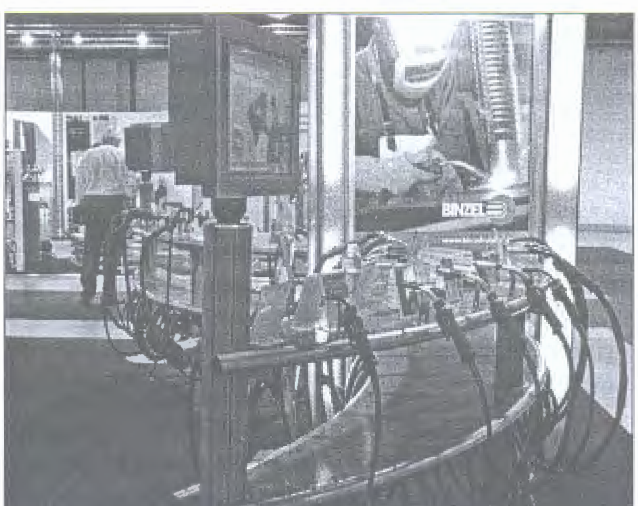

- plants, equipment and technologies for welding of metals and plastics; application of coatings; brazing and soldering; surfacing; thermal spraying; manufacture of filler and consumables;
- methods of deposition;
- plants and equipment for heat treatment;
- joining, cutting and application of coatings from metallic and nonmetallic compounds;
- fully mechanized and automatic plants, industrial robots, data processing, control and monitoring;
- installations for adhesive joining, application of adhesives, metering devices;
- accessories and welding materials;
- application of gases and gas mixtures for welding, cutting and surfacing;
- measuring equipment and testing methods (equipment and/or services);
- health protection and safety (individual protective means), environment protection;
- research, services, information materials, literature.

Now the welding exposition became a constituent part of International forum of innovative technologies represented also by trade fairs: «Pipes of Russia 2007», «Wire of Russia 2007», «Metallurgy–Litmash 2007», «Aluminium/NFM 2007», «Tekhnoforum 2007», «Sanitary ware, heating, air-conditioning 2007», «Leprombiznes 2007», «Electric power industry of Russia 2007».

The purpose of integral trade fair and information space is opening for firms-exhibitors new prospects for products promotion in the Russian market, expansion of business partnership with experts of title and allied industries, raising efficiency of marketing and giving the chance to visitors and exhibitors to obtain first-hand information from leading world manufacturers.

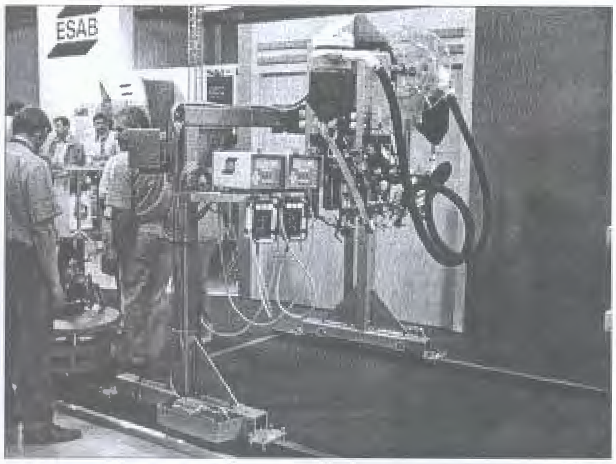

Exhibitors from 15 countries (Hungary, Germany, Denmark, India, Spain, Italy, China, Russia, the USA, Turkey, Ukraine, Finland, France, Czechia, Sweden) have taken part in the trade fair. Predominant part of the exposition was presented by Germany (31), Russia (28) and China (23).

Among well-known world brands are such companies as Alexander Binzel Schweisstechnik, Deloro Stellite, Doima, Carl Cloos Schweisstechnic, KUKA, UTP (Germany), Kemppi (Finland), ESAB (Sweden), Polisoude (France), and others.

Speaking during trade fair opening, President of «Messe Essen» J. Hanneke, general manager of DVS K. Middeldorf, President of NAKS, academician of Russian Academy of Sciences N.P. Alyoshin and others, have expressed confidence of doubtless success of the trade fair, big prospects of its expansion in the future, huge interest to it and wide resonance among scientists and experts of welding industry.

From Ukraine, in the trade fair have taken part E.O. Paton Electric Welding Institute, companies «Trading house Ilnitsky plant MSO», «Artyom-Kontakt», SiMZ, «Donmet».

Exposition of the E.O. Paton Electric Welding Institute was noted for good stand design, availability of publications and a catalogue reflecting developments of the institute for last five years. Of great interest was the collection of scientific articles on the results of performance by the Ukrainian scientists of target complex program of the NAS of Ukraine «Problems of service life and safe operation of constructions, structures and machines».

Basic interest of the stand visitors was connected with the following developments:

- welding and repair in oil-and-gas industry;
- EBW of heat-resistant materials, complex sections;
- resistance butt welding of flanges, tips of drill pipes;
- welding of structures from zink-plated metal;
- welding and surfacing of copper and its alloys by friction stir welding;
- repair and restoration of parts of the metallurgical equipment and dies.

During the work of the trade fair, experts of DVS and GSI have staged the innovative forum of welding technologies, including reports on the following themes: «State-of-the-art quo and trends of recognition of quality requirements in welding according to ISO 3834» (Dr. H.-G. Gross, GSI, Germany), «Clean air at the working place» (B. Kemper, Kemper GmbH, Germany), «Flood welding as a Weld Mold Company Technology for repair of forging dies» (S. Elek, Weld

Mold Company, USA), «Application of manufacturing systems for automobile medium-sized businesses» (Dr. P. Rippel, KUKA GmbH, Germany), «New alloying systems of filler materials for repair and production welding in chemical plant construction» (D. Kalinin, UTP, Germany), «System technology for laser welding/brazing» (Dr. P. Rippel), «New torches for arc welding of company TBI Industries-Germania» (S.B. Vorobiov, Tekhnoterm, Russia), «Advanced flame brazing process control» (J. Vlcek, Themis, Czechia), «State-of-the-art and perspectives of employment of international welding equipment at the Russian market» (N.N. Rubtsova, «Mir Svarki», Russia), «Welding with flux-cored wires of high strength fine grain steels» (Dr. R. Rosert, Drahtzug Stein wire & welding GmbH, Germany), «Application potential for friction and magnetic arc welding outside motive industry» (Dr. P. Rippel). The reports have aroused keen interest of participants and visitors of the trade fair.

Successful should recognized combination of trade fair proper with a quite representative International conference «Welding — outlook in the future» (29–30 May 2007), whose organizers were NAKS, DVS and N.E. Bauman STU. The conference included plenary session and work of four sections: «Certification in welding» (headed by V.F. Lukianov), «Non-destructive testing in welding» (headed by Ya.G. Smorodinsky, G. Doblan), «Personnel training in welding» (headed by V.I. Lysak) and «Modern welding technologies» (headed by V.A. Lopota).

The conference held in the 15th anniversary of NAKS, was opened by its chairman, academician B.E. Paton. He has congratulated its participants and wished fruitful work to all. In B.E. Paton's speech were expounded modern conceptions on the prospects of development of welding and related processes, which are as for today most widely applied manufacturing processes and continue to develop intensively, providing solutions of many most complicated technical problems. B.E. Paton has expressed confidence that the conference will serve the consolidation of scientists-welders of many countries, will promote international cooperation and progress.

At the plenary session also took the floor: representative of State Duma V.A. Yazev, head of «Rostekhnadzor» K.B. Pulikovsky, president of NAKS academician N.P. Alyoshin, vice-president of IIW L. Kvintino, director of DVS K. Middeldorf.

Speeches at the plenary session and subsequent work of sections have attracted big interest of the conference participants.

In summary, it should be noted, that trade fair «Welding, Cutting, Surfacing» was a success. It was promoted by its staging in tandem with large international conference.

V.N. Lipodaev, Dr. Tech. Sci., PWI
N.G. Tretyak, Cand. Tech. Sci., PWI

EQUIPMENT, TECHNOLOGY AND MATERIALS FOR WELDING OF VERTICAL WELDS

possess an experience of application of arc welding with self-shiıng flux-cored wires in construction of tanks for storage of peteum products, ship hulls in yards and vertical joints of span struc-'es of bridges.

ıe weld surface is formed by special devices (slides, backings), hich cool the weld and adjacent zones, preventing the overflowing ıd overheating of the weld pool.

he required mechanical properties of the welded joint are guaranteed vithout additional heat treatment.

Complex for welding vertical joints is designed for welding vertical site welds of steel structures, composed of separate sheets.

Technical characteristics of the complex

Thickness of metal to be welded, mm	8–30
Radius of maintenance at up to 20 m height, m	not less than 40
Diameter of electrode flux-cored wire, mm	2.4; 3.0
Welding speed, m/h	4–12

Delivery set of equipment

Welding head with a control panel	1
Device of a self-contained cooling	1
Mobile operator's cabin	1
Welding electric supply source	1
System of communications	1

Technological documentation and welding consumables

Technological documentation for the technology of welding vertical welds, set	1
Drawings for technological equipment, set	1
Software for calculation of welding conditions in accordance with characteristics of joint being welded, set	1

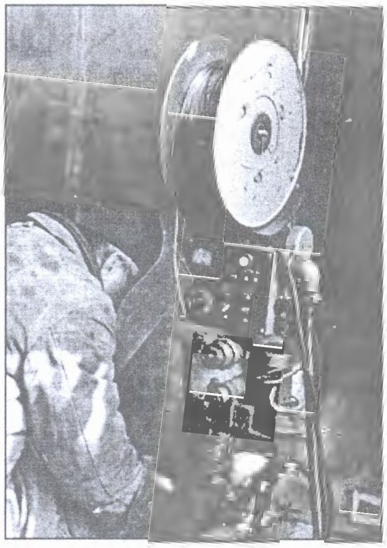

The flux-cored wires (according to standard ANSI/AWS A5.26) provide the ultimate tensile strength from 490 to 650 MPa of weld metal in accordance with a class of steel to be welded and are delivered by the approved specifications.

EQUIPMENT, TECHNOLOGY AND MATERIALS FOR WELDING HORIZONTAL WELDS

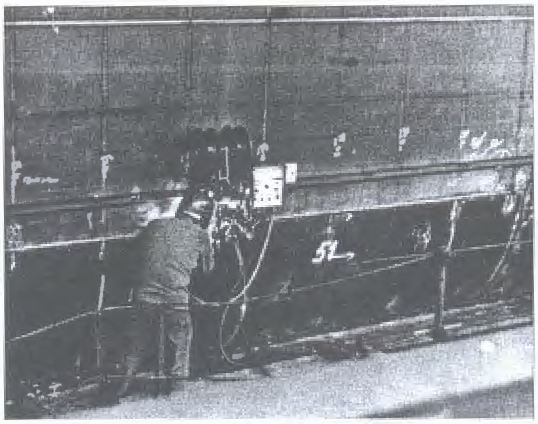

New prospects have been appeared owing to the development of technological procedures of welding using flux-cored wires with a half-forced formation of weld metal of horizontal joints of sheet structures in vertical plane.

Technology provides the optimum combination of quality and productivity at high welding effectiveness and speed of a groove filling by using the method of weld surface formation by a slide of a special design.

An experience has been gained of successful application of welding with flux-cored wires in construction of tanks for storage of petroleum products, ship hulls in yards, structures of blast furnaces and air heaters.

Technical characteristics of the complex

Thickness of metal to be welded, mm	12–60
Minimum radius of curvature, mm	not less than 300
Diameter of electrode flux-cored wire, mm	2.0; 2.4; 3.0
Welding speed, m/h	3–30

Delivery set of equipment

Welding machine with a control cabinet	1
Mobile operator's cabin	1
Welding electric supply source	1
System of communications	1
Gas (flux) equipment	1

Technological documentation and welding consumables

Technological documentation for the technology of welding horizontal welds, set	1
Drawings for technological equipment, set	1
Software for calculation of welding conditions in accordance with characteristics of joint to be welded, set	1

The flux-cored wires (according to standard ANSI/AWS A5.20 or A 5/29) provide the ultimate tensile strength from 490 to 650 MPa of weld metal in accordance with a class of steel to be welded and are delivered by the approved specifications.

TECHNOLOGY, EQUIPMENT AND WELDING CONSUMABLES FOR ELECTRIC ARC POSITION WELDING OF PIPE BUTT JOINTS *COMPLEX «STYK»*

- Optimum combination of quality and productivity
- High efficiency of welding and high speed of a groove filling, prepared for the automatic welding
- Feasibility of welding pipes of steels with a different level of strength
- Simplicity of maintenance in the field conditions
- Use of method of weld surface formation by a slide in all spatial positions
- Pipes of different diameter can be welded by the equipment of a similar type

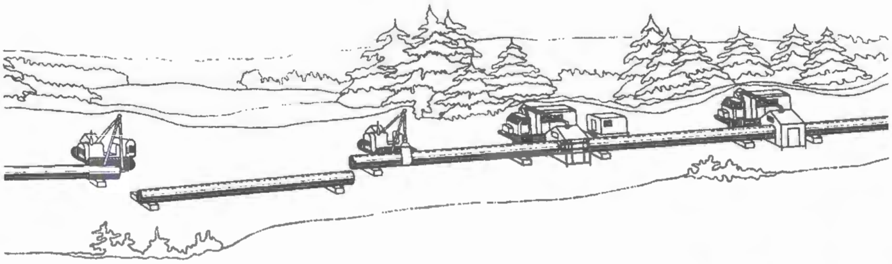

Equipment of complex STYK

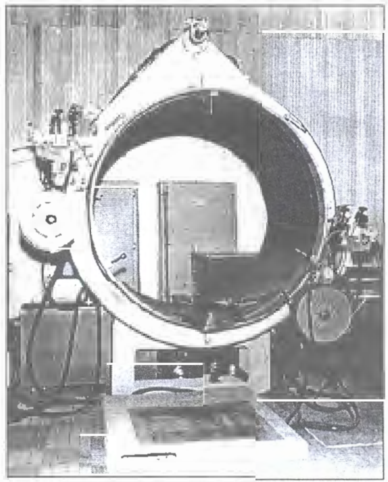

Equipment of complex STYK consists of one, two or three self-propelled welding installations, mobile workshop and internal hydraulic aligning device for straightening pipes being welded. The self-propelled welding installations are equipped with two welding heads for welding pipes simultaneously from two sides upwards. To provide a regular operation of the complex, a pipe laying machine and a bulldozer are also used.

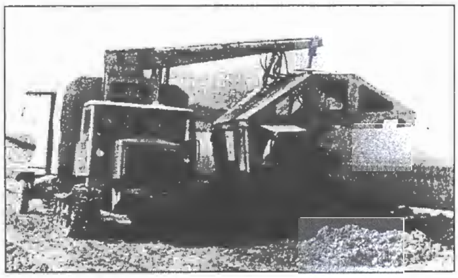

Technology of welding

Technology of welding is based on the principle of weld formation and maintaining of weld pool in all spatial positions using a forming device (slide). For welding with a forced weld formation, the self-shielding flux-cored wires are used. The technology has been developed for welding pipes of wall thickness from 6 to 24 mm for three or four passes by a continuous method.

Technical characteristics of welding installation

Diameter of pipes, mm	530–1420
Efficiency, butt/h	4–8
Capacity of mobile diesel power unit, kW	100
Number of welding heads, pcs	2
Welding current, A	200–500
Arc voltage, V	22–36
Diameter of wires, mm	1.6; 2.0 or 2.4
Dimensions, m	7.2 × 2.7 × 3.5
Mass of welding installation, t	~17

Specification of flux-cored wires and mechanical properties of weld metal

Wire grade	Wire diameter, mm	Ultimate tensile strength, MPa	Elongation, %	Impact toughness *KCV*, J/cm², at temperature, °C	
				+20	−40
PP-AN19S	2.0; 2.4	560	min 22	80	35
PP-AN24S	1.6; 2.0	590	min 22	90	50
PP-AN30M	1.6; 2.0	690	min 20	75	45

Method of welding, equipment, composition of flux-cored wires are protected by patents in the USA, Canada, Germany, Japan, France, Great Britain and other countries.

BOOKS
PROCEEDINGS OF CONFERENCES

(2007) Proceedings of the Third International Conference «Laser Technologies in Welding and Materials Processing» (Katsiveli, Ukraine, 29 May – 1 June, 2007). Ed. by Prof. V.S. Kovalenko. Kiev: PWI, approx. 200 pp. Format 200×290 mm. Softback. $50 (the Book of proceedings will come out of print in October–November 2007).

(2006) Proceedings of Jointly 16th International Conference «Computer Technology in Welding and Manufacturing» & 3rd International Conference «Mathematical Modelling and Information Technologies in Welding and Related Processes» (Kiev, Ukraine, June 6–8, 2006). Ed. by Prof. W. Lucas and Prof. V.I. Makhnenko. Kiev: PWI, 328 p. Format 200×290 mm. Softback. ISBN 966-95847-8-7. $50.

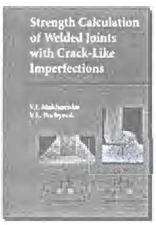

Makhnenko V.I., Pochynok V.E. (2005) Strength Calculation of Welded Joints with Crack-Like Imperfections. Kiev: PWI, 266 pp. Format 165×235 mm. Softback. ISBN 966-8072-02-9. $90.

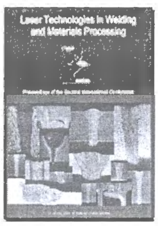

(2005) Proceedings of the Second International Conference «Laser Technologies in Welding and Materials Processing» (Katsiveli, Ukraine, May 23–27, 2005). Ed. by Prof. V.S. Kovalenko. Kiev: PWI, 256 pp. Format 200×290 mm. Softback. ISBN 966-8872-01-0. $50

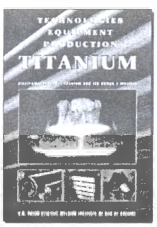

(2005) TITANIUM. Collection of Scientific Papers. Kiev: PWI, 218 pp. Format 200×297 mm. Softback. $38.

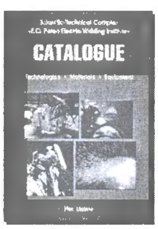

(2005) CATALOGUE. Technologies. Materials. Equipment. Kiev: PWI, 260 pp. Format 200×297 mm. Softback. $50.

(2003) Proceedings of the International Conference «Laser Technologies in Welding and Materials Processing» (Katsiveli, Ukraine, May 19–23, 2003). Ed. by Prof. V.S. Kovalenko. Kiev: PWI, 256 pp. Format 200×290 mm. ISBN 966-95847-3-6. Softback. $50.

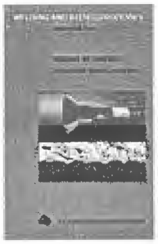

Ryabov V.R., Dobrushin L.D., Jung-Gi Moon (2003) Welding of Bimetals. Kiev: PWI, 130 pp. Format 140×200 mm. ISBN 966-95847-4-4. Softback. $38.

Juettner B., Vasenin Yu.L. (2003) Cathodic Processes of the Metal Vapor Arc. Kiev: PWI, 68 pp. Format 140×200 mm. ISBN 966-95847-6-0. Softback. $38.

Lysak V.I., Kuzmin S.V. (2003) Explosive Welding of Metal Layered Composite Materials. Kiev: PWI, 118 pp. Format 140×200 mm. ISBN 966-95847-5-2. Softback. $38.

More detail information (abstracts and contents) about books please find on site:
http://www.iaw.com.ua/english/books/books-1.html

SUBSCRIPTION
FOR «THE PATON WELDING JOURNAL»

If You are interested in making subscription directly via Editorial Board, fill, please, the coupon and send application by fax or e-mail.

The cost of annual subscription via Editorial Board is $324.

Telephones and faxes of Editorial Board of «The Paton Welding Journal»:
Tel.: (38044) 287 6302, 271 2403, 529 2623
Fax: (38044) 528 3484, 528 0486, 529 2623.

«The Paton Welding Journal» can be also subscribed worldwide from catalogues of subscription agency EBSO.

SUBSCRIPTION COUPON

Address for journal delivery ____________________

Term of subscription since ______ 200 ______ till ______ 200 ______

Name, initials ____________________

Affiliation ____________________

Position ____________________

Tel., Fax, E-mail ____________________

ADVERTISEMENT
IN «THE PATON WELDING JOURNAL»

External cover, fully-colored:
First page of cover (190×190 mm) – $500
Second page of cover (200×290 mm) – $350
Third page of cover (200×290 mm) – $350
Fourth page of cover (200×290 mm) – $400

Internal cover, fully-colored:
First page of cover (200×290 mm) – $350
Second page of cover (200×290 mm) – $350
Third page of cover (200×290 mm) – $350
Fourth page of cover (200×290 mm) – $350

Internal insert:
Fully-colored (200×290 mm) – $300
Fully-colored (double page A3) (400×290 mm) – $500
Fully-colored (200×145 mm) – $150
Black-and-white (170×250 mm) – $80
Black-and-white (170×125 mm) – $50
Black-and-white (80×80 mm) – $15

- Article in the form of advertising is 50 % of the cost of advertising area
- When the sum of advertising contracts exceeds $1000, a flexible system of discounts is envisaged

Technical requirement for the advertising materials:
- Size of journal after cutting is 200×290 mm
- In advertising layouts, the texts, logotypes and other elements should be located 5 mm from the module edge to prevent the loss of a part of information

All files in format IBM PC:
- Corell Draw, version up to 10.0
- Adobe Photoshop, version up to 7.0
- Quark, version up to 5.0
- Representations in format TIFF, color model CMYK, resolution 300 dpi
- Files should be added with a printed copy (makeups in WORD for are not accepted)